A Subclass of Exceptional Parallel Self-similar G_2 Cosmologies

by

Sepehr Rashidi

A thesis
presented to the University of Waterloo
in fulfillment of the
thesis requirement for the degree of
Master of Science
in
Physics

Waterloo, Ontario, Canada, 2019

Author's Declaration

I hereby declare that I am the sole author of this thesis. This is a true copy of the thesis, including any required final revisions, as accepted by my examiners.

I understand that my thesis may be made electronically available to the public.

Abstract

We perform a qualitative and asymptotic analysis of a particular class of cosmological models, namely the exceptional G_2 perfect fluid and vacuum models that are additionally self-similar with the fluid flow lying tangential to the H_3 orbits. We show that for the values of the equation of state parameter in $(1, \frac{3}{2})$, there exist open sets of well-behaved vacuum models that are asymptotically spatially homogeneous, at large spatial distances. For the values of the equation of state parameter in the intervals $(1, \frac{10}{9})$ and $(\frac{4}{3}, \frac{3}{2})$, there exist open sets of well-behaved perfect fluid inhomogeneous cosmological models that are asymptotically spatially homogeneous, at large spatial distances, and we illustrate the spatial structure of their matter-energy density. In addition, the perfect fluid models exhibit only two possible asymptotic behaviours, namely they are well-behaved and asymptotically spatially homogeneous or badly-behaved.

Acknowledgements

I thank my supervisors Professor Hewitt and Professor Charbonneau for their guidance, availability, and revisions to this thesis. This work would not have been close to what it currently is without their suggestions.

I would like to thank and acknowledge University of Waterloo's Department of Physics and Astronomy for providing me with the Graduate Research Scholarships, Marie Curie Awards, and Science Graduate Awards for the past two years to support this work.

I would like to thank Professors John Wainwright and Niayesh Afshordi for being on my advisory committee and asking questions. In addition, I thank Professor Michael Balogh for agreeing to be on my defence committee and asking questions.

I thank both of my supervisors for providing funding via NSERC so that I could give a talk at the Atlantic General Relativity Conference of 2018 in Nova Scotia. I am grateful to both Professors Alan Coley and Robert van den Hoogen for their hospitality at the conference. I also thank Matthew Robbins and Professor Robert Mann for inviting me to their group to give a talk.

Thank you all,

Sepehr.

Dedication

This is dedicated to anyone who is interested in theoretical physics and pure mathematics; and to all people who are curious to see how theories may fit with observations.

Table of Contents

List of Figures

List of Tables

Chapter 1

Introduction

In this chapter, we present some of the mathematical tools used in cosmology. We begin by briefly describing the simplest cosmological models, namely the spatially homogeneous and isotropic FLRW models. We proceed by defining the G_2 cosmologies which possess less symmetry than the FLRW models. In this thesis, we focus on a particular subclass of the G_2 cosmologies, which we refer to as the exceptional G_2 cosmologies.
In Chapter 2, we examine the consequences of using a non-coordinate frame in differential geometry. We use the orthonormal tetrad formalism, as introduced to cosmology by Ellis and MacCallum [9]. We demonstrate how an appropriate choice of alignment of the tetrad allows us to simplify the examination of the models under consideration.
In Chapter 3, we develop the Einstein Field Equations corresponding to the exceptional class of G_2 cosmologies and then convert our variables to expansion normalized variables. The Einstein Field Equations take the form of a system of quasi-linear PDEs

$$\partial_0 \mathbf{W} = \mathbf{M}(\mathbf{W})\ \partial_1 \mathbf{W} + \mathbf{G}(\mathbf{W}). \tag{1.1}$$

We impose the restriction $\partial_0 \mathbf{W} = \mathbf{0}$ on the PDEs, and demonstrate that the cosmological models do not lose their evolutionary nature. We show that under this condition, the cosmological models reduce to a one parameter, three dimensional, system of ODEs. This system describes the inhomogeneous spatial structure of these models.

In Chapter 4, we commence a qualitative analysis of the ODEs. We interpret the solution curves by providing details of the corresponding cosmological models, both in the perfect fluid and the vacuum cases. The incomplete and partial analysis of Van den Bergh in [41] and Wills in [48] is completed by proving the existence of open sets of well behaved

perfect fluid and vacuum models. We proceed by explaining how the existence of a monotone function, for the values of the equation of state parameter in the interval $(1, \frac{6}{5}) \cup (\frac{4}{3}, \frac{3}{2})$ allows us to conclude that the perfect fluid models exhibit only two types of behaviours at large spatial distance, namely they are well-behaved and asymptotically spatially homogeneous or badly behaved. Compared to the works of Van den Bergh and Wills, the proof for the existence of an open set of these well-behaved models, as well as the spatial structure of their matter-energy density, and their only possible asymptotic behaviours, is solely found in this thesis.

In Chapter 5, we examine the ODE when $\gamma = \frac{10}{9}$. In this case, the ODE admits a first integral and phase space is foliated by a one parameter family of two dimensional invariant sets. We give the physical properties of cosmological models by describing the spatial structure of their energy density, shear, and asymptotic behaviour. We show the existence of well behaved cosmological models that have not been discovered before.

In Chapter 6, we perform some asymptotic analysis. We prove that the perfect fluid models which tend to infinity in the phase space correspond to models that are badly behaved by showing that they have divergent physical variables.

1.1 Theoretical Cosmology & The Cosmological Fluid

The goal of theoretical cosmology is to construct a mathematical model that describes the large scale structure of the universe. For the underlying model, we use a four-dimensional smooth manifold $\mathcal{M}$, with a Lorentzian metric g. The pair $(\mathcal{M}, g)$ is called a spacetime. We use the convention that the Greek indices run from 1 to 3 and the Latin indices run from 0 to 3.

Assumption A1: *We assume that the geometry of this manifold (captured in its Ricci tensor R_{ab} Ricci scalar R, and metric tensor g_{ab}) and the matter content in the universe (described by stress-energy tensor T_{ab}) are related by the Einstein Field Equations (EFEs)*

$$R_{ab} - \frac{1}{2} R g_{ab} = T_{ab}. \tag{1.2}$$

We use geometrized units with $c = 1$, $8\pi G = 1$

In order to make progress in calculations with the EFEs, we make certain simplifying assumptions. The assumptions related to the geometric properties of the spacetime manifold are introduced in Section 2.3. In this section, we introduce the assumptions related to the matter content in the universe.
We model the matter content in the universe by a fluid, called the *cosmological fluid*, whose particles may be considered to represent galaxies or galactic clusters. The motion of the fluid is indicated by a time-like normalized vector field $\mathbf{u}$ (with $u^a u_a = -1$). The integral curves of the vector field $\mathbf{u}$ indicate the world lines of the particles in spacetime, and may be interpreted as the world lines of *fundamental observers*, who are co-moving with the the fluid [16, p.1]. Spacetime, together with the vector field $\mathbf{u}$, is referred to as a cosmological model, and denoted by $(\mathcal{M}, \mathbf{g}, \mathbf{u})$.

We define the projection tensor, h_{ab}, by

$$h_{ab} = g_{ab} + u_a u_b. \tag{1.3}$$

This tensor projects a vector, $\mathbf{w}$, into the three space orthogonal to $\mathbf{u}$, that is

$$(h_{ab} w^a) u^b = 0. \tag{1.4}$$

Any symmetric two index tensor, S_{ab}, can be uniquely decomposed using h_{ab} as

$$S_{ab} = \mu u_a u_b + p h_{ab} + \pi_{ab} + 2 q_{(a}\ u_{b)} \tag{1.5}$$

with π_{ab} being a traceless and symmetric object such that $\pi_{ab} u^b = 0$, and q_a is defined by

$$q_a = S^{cd} h_{ca} u_d, \tag{1.6}$$

and satisfies $q_a u^a = 0$. For the stress-energy tensor corresponding to the cosmological fluid, these objects have physical meanings [17]. We call μ the relativistic energy density, q_a the relativistic momentum density, p the isotropic pressure, and π_{ab} the trace-free anisotropic pressure or stress [8, p.8].
A *perfect fluid* is defined by having zero momentum density and zero anisotropic pressure:

$$q_a = 0, \tag{1.7}$$
$$\pi_{ab} = 0. \tag{1.8}$$

That is, the stress energy tensor of matter in a universe behaving as a perfect fluid with pressure p, density μ, and the co-moving normalized 4-velocity of the fluid $\mathbf{u}$ has the form

$$T_{ab} = u_a u_b (\mu + p) + p g_{ab}. \tag{1.9}$$

Assumption A2: *We assume that the EFEs admit a perfect fluid source, with a linear equation of state*

$$p = (\gamma - 1)\mu, \tag{1.10}$$

where γ is the equation of state parameter, also referred to as the adiabatic constant.

An equation of state defines the relationship between the pressure and the density. The value of the equation of state parameter is important because it is related to the physical properties of the fluid. In fact,

- matter is attractive when $\gamma > \frac{2}{3}$,
- matter is repulsive when $\gamma < \frac{2}{3}$,
- matter is dust with zero pressure when $\gamma = 1$,
- matter is called radiation fluid when $\gamma = \frac{4}{3}$, and
- matter is called stiff fluid when $\gamma = 2$.

It follows from the EFEs that the stress energy tensor has zero divergence, that is

$$T^{ab}{}_{;b} = 0. \tag{1.11}$$

Physically, this corresponds to conservation law of energy and momentum. We can show (see Appendix C for a short proof) that a consequence of this is the conservation equation

$$\dot{\mu} = -u^{a}{}_{;a}\gamma\mu. \tag{1.12}$$

1.2 The FLRW Models

One of the simplest cosmological models is the FLRW models, developed in the works of [12, 13, 37, 38, 39, 47]. Robertson and Walker are credited with the line element

in Eq.(1.13), and Friedmann and Lemaître were two of the earliest cosmologist to make use of this line-element, so the models are typically denoted by FLRW. These models are *isotropic*(the universe looks the same in all directions) and *homogeneous*(the universe looks the same to observers, at the same time, regardless of their position or location). Their matter content is described by a perfect fluid with the linear equation of state $p = (\gamma - 1)\mu$. The line element of these models maybe written as

$$ds^2 = -dt^2 + l(t)^2\Big[\frac{dr^2}{1-kr^2} + r^2(d\theta^2 + \sin^2\theta d\phi^2)\Big], \tag{1.13}$$

where $l(t)$ is called the *length scale function*, and satisfies the equations Eq.(1.17)-(1.18) below. The surfaces $t = t_0$ are three-spaces of constant curvature, and are distinguished by the sign of k. These correspond to different types of FLRW universes as given in Table 1.1.

Table 1.1: The table of FLRW universes distinguished by the sign of k

k	Name
positive	closed
0	flat
negative	open

The coordinate t measures proper time along the world line of the fundamental observer with $\mathbf{u} = \frac{\partial}{\partial t}$. The Hubble parameter H is defined by

$$H := \frac{\dot{l}}{l}, \tag{1.14}$$

and the deceleration parameter q is defined by

$$q := -\frac{\ddot{l}l}{\dot{l}^2}. \tag{1.15}$$

The dimensionless energy density is defined by

$$\Omega := \frac{\mu}{3H^2}. \tag{1.16}$$

For these models, $u^a_{;a} = 3\frac{\dot{l}}{l}$ so the conservation equation, Eq.(1.12), becomes

$$\dot{\mu} = -3\frac{\dot{l}}{l}\gamma\mu. \tag{1.17}$$

The EFEs reduce to the Raychaudhuri equation, and the Friedmann equation, that is

$$\frac{\ddot{l}}{l} = -\frac{1}{6}(3\gamma - 2)\mu l, \tag{1.18}$$

and

$$3\frac{\dot{l}^2}{l^2} = \mu - \frac{3k}{l^2}, \tag{1.19}$$

respectively. If the equation of state parameter γ satisfies $\gamma > \frac{2}{3}$, then it follows from Eq.(1.18) that $\ddot{l} < 0$, so $l(t)$ is concave down. In addition, if for some instant of time t_c, $\dot{l}(t_c) > 0$, then there exists a time t_b in the past such that $l(t_b) = 0$, meaning that the length scale has shrunk to zero. Integration of Eq.(1.17) gives

$$\mu(t) = C_1 l^{-3\gamma}, \tag{1.20}$$

where C_1 is the constant of integration, and so

$$\lim_{t \to t_{b^+}} \mu(t) = \infty. \tag{1.21}$$

That is, the energy density diverges as $t \to t_{b^+}$. We refer to the surface $t = t_b$ as a singularity. Since the energy density diverges as $t \to t_{b^+}$, we refer to $t = t_b$ as the time of the big bang, and the singularity is often called a big bang singularity [16, p.5].

1.3 Expansion, CMB, & Isotropy

The notion of an expanding universe was introduced by Friedmann [12, 13] and Lemaitre [32]. This idea gained major attention by the physics community, particularly by cosmologists, after Hubble observed [26] that the electromagnetic radiation emitted from the majority of the observed galaxies is redshifted with respect to the Earth, meaning that these galaxies are moving away from Earth. This provided evidence that the universe must be expanding. In addition, the redshifts of galaxies increase with distance, implying that the further they are from the Earth, the faster they are moving away.

The FLRW model of the universe has a big bang singularity. As the universe approaches this phase of the past, it gets denser and hotter. In the early 1960s, Dicke and Peebles [5, 6] began to consider the observational consequences of the hot dense phase of the universe for the modern cosmologists. They proposed that the universe must have had produced

radiation, the remnants of which ought to be detectable. In 1966, Penzias and Wilson accidentally observed an electromagnetic signal which had a peak in the microwave part of the spectrum [35]. This remnant radiation is known as the *Cosmic Microwave Background* (CMB), and it has been examined by sophisticated detections since [15]. When an electromagnetic detector is aimed in an arbitrary direction from the earth towards outer space, it will receive signals from localized sources, which can be filtered out, together with a spurious signal which has a peak intensity at a wavelength of approximately 609 nm [11, p.919]. The spurious signal is the CMB. In classical physics we often consider an idealized perfect radiator, called a *Black Body Radiator*. This radiator emits electromagnetic waves with a certain temperature dependent wavelength spectrum. Information about the measurements of the CMB are often translated into temperature measurements, which assumes that the source was a black body. As of 2009, the spectrum corresponds to a black body radiator with a temperature of approximately 2.7 K [11, p.920]. Note that when this radiation was created, the wavelength would have been approximately 966 nm corresponding to a temperature of approximately 3000 K [1]. The results of these measurements are displayed on a two dimensional map. This map is highly uniform, and so astronomers state that the CMB is highly isotropic. The most common interpretation is that the radiation was created at a time when the universe was isotropic on large enough scales, and that this radiation has traveled to us through a universe which is isotropic. The detection of the CMB provides strong evidence that the universe had a hot dense phase.

1.4 Motivation

The primary goal of theoretical cosmology is to find the simplest cosmological models that fit with our observations of the universe. However, the secondary goal of theoretical cosmology is to construct more complicated models that yield consequences which may be compared, fitted, and tested against the current observations in the universe.

The commonly accepted model of the present day universe, called the *standard model*, is based on the FLRW models and they describe a universe which is perfectly *isotropic* and *homogeneous*. However, FLRW models also have their limitations. We briefly show a couple of references below and state that FLRW models have their observational challenges.

The idea that we are not in a special place in the universe is referred to as the *Copernican principle*. This is compatible with homogeneity. The idea that, on large enough scales, the universe is homogeneous and isotropic is referred to as the *Cosmological Principle*. In a more realistic case, there are subtleties involved with these principles and the standard model [2, p.3]. Considering the separation between galaxies, homogeneity and isotropy are

not valid for scales below 200 Mpc [14, p.465]. In 2012, a paper summarizing the facts about the Copernican principle has discussed in detail that this principle has yet to be rigorously shown and there are several ways of testing homogeneity [2]. For example, the measurement of the energy density due to curvature, Ω_k, via the area distance and the Hubble parameter as a function of redshifts only [7, p.14] has been extended by [3, p.2] to a consistency relation that can serve as a test for spatial homogeneity.

In addition, we are motivated by the conjecture that the specific models obtained in this thesis prove to be useful for further generalizations of the EFEs. The cosmological properties of the solutions in this thesis, such as the variation of the energy density in one spatial direction etc, may possibly appear in a more general solution: a solution with even less symmetry.

1.5 Classifying Cosmology By Isometry Groups

The complexity of a cosmological model may be classified by the geometric properties of the spacetime manifold. We state several definitions to describe these geometric properties. A vector field $\mathbf{v}$ is called a Killing Vector Fields (KVF) if

$$\mathcal{L}_{\mathbf{v}}\mathbf{g} = 0. \tag{1.22}$$

A vector field $\mathbf{H}$ is called a Homothetic Vector Field (HVF) if there exists a k such that

$$\mathcal{L}_{\mathbf{H}}\mathbf{g} = 2k\mathbf{g}. \tag{1.23}$$

A KVF is a trivial HVF.
A vector field $\mathbf{X}$ is called *hypersurface orthogonal* (HO) if $X_{[\rho}X_{\mu;\nu]} = 0$. This condition is equivalent to $\mathbf{w} \wedge d\mathbf{w} = 0$ for the one form $\mathbf{w}$ defined by $\mathbf{w}(\mathbf{v}) = g(X, \mathbf{v})$.

An isometry of a manifold $(\mathcal{M}, \mathbf{g})$ is a mapping from $\mathcal{M}$ to $\mathcal{M}$ that preserves distance. The set of all isometries of a manifold form a Lie Group. We write G_n to denote any subgroup of dimension n of the isometry group. For any G_n, there are n linearly independent KVFs, and these KVFs generate the G_n. The orbit of any point $p \in \mathbf{M}$ under the action of the group G_n is $\mathrm{Orb(p)}_{G_n} := \{\psi(p) | \psi \in G_n\}$. The KVFs are tangent to the orbits.
Let dim[$Orb_{G_n}(p)$] $= d$. If $d = n$, we say that the group acts *simply transitively*. In this particular case, the KVFs evaluated at p are linearly independent. If $d < n$, then we say that the isometry group acts *multiply transitively* on the orbit. In this latter case, there

exists $n-d$ linearly dependent generators at any point $p \in \mathcal{M}$. These generators form the so called *isotropy group* and we say that $\mathcal{M}$ has, some, isotropy. For example, the FLRW models admit a G_6. The group orbits are three dimensional and so the G_6 acts multiply transitively. At each point there is a three dimensional isotropy group. Geometrically, the isotropy group indicates that the models look the same in all spatial directions at any point. We say that the models are spatially homogeneous to indicate that any point p in the spacetime is equivalent to any other point on the three dimensional spacelike orbits at p. The so called *Bianchi* cosmological models are less symmetric, admitting, in general a G_3 acting on three dimensional spacelike orbits. The models maintain the spatial homogeneity of the FLRW models but, in general, are not isotropic: the observer can distinguish between some different spatial directions. Each of these classes of models are subdivided based on how the 4-velocity of the fluid is oriented with respect to the group orbits. For example, Orthogonal Bianchi cosmologies are cosmological models in which spacetime admits a G_3, a three parameter isometry group whose space-like orbits are hypersurfaces orthogonal to the 4-velocity of the cosmological fluid [45, 21, 18, 19]; in this thesis, we make an analogous assumption.

We go one step further and relax the condition of spatial homogeneity. The model $(\mathcal{M}, \mathbf{g}, \mathbf{u})$ is a G_2 *cosmological model*, or simply a G_2 *cosmology*, if it admits an Abelian group G_2 of isometries whose orbits are spacelike 2-surfaces. For these models, the cosmological variables may change in one spatial direction, as well as evolve in time. One may claim that these are the simplest cosmological models in which we can examine inhomogeneities. We say that G_2 acts *orthogonally transitively* on the orbits if the 2-spaces orthogonal to the orbits are surface-forming.

G_2 cosmologies were first classified by Wainwright, by the nature of the action of the G_2, in 1979 and 1981, [43] [44, p.1134], and the four mutually exclusive classes of spacetimes in this classification are:

A(i): non-orthogonally transitive G_2 with no HO KVFs.

A(ii): non-orthogonally transitive G_2, with only one HO KVF.

B(i): orthogonally transitive G_2, with no HO KVF.

B(ii): orthogonally transitive G_2, with two mutually orthogonal HO KVFs.

We illustrate these classes in the Venn Diagram below.

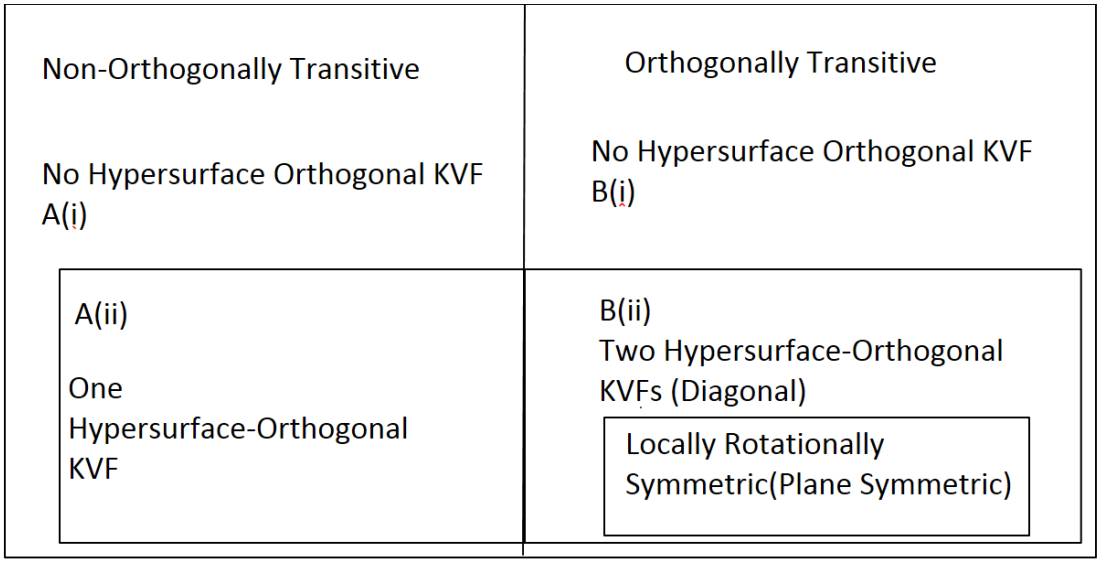

To the best of the author's knowledge, class A(i) and B(i) have not been thoroughly investigated as of the present day. Class B(ii) has been thoroughly investigated by many authors [30, p.264-267]. In this thesis, we examine class A(ii) models. We refer to these models as the *exceptional* G_2 *cosmologies*, extending the terminology used for the orthogonal Bianchi models in, for example [19].

Three papers have investigated the exceptional G_2 cosmologies in some detail. In [41] and [42], Van den Bergh examined vacuum and stiff fluid models of this class, respectively. The paper in [41] assumes a metric ansatz,

$$ds^2 = -e^{2k}dt^2 + e^{2h}dx^2 + r[f\ dy^2 + f^{-1}(dz + \ wdx)^2], \tag{1.24}$$

with k, h, n, f depending only on x and t and being separable. The case $w \neq 0$ corresponds to class A(ii), while $w = 0$ corresponds to class B(ii).
In [41, p.168], Van den Bergh admits that even though separability is discussed in terms of this preferred coordinate system, a more invariant approach to separability is preferred. It has been stated in the paper that, for class A(ii), it has not been possible to obtain the general separable vacuum solution in explicit form. Many of the vacuum solutions considered in [41] are self-similar. The EFEs are written as a system of ODEs which is not fully analyzed. One of the results of this thesis is to extend this work. We show that there is an open set of well-behaved models within this class.

Wills [48] started to analyze perfect fluid models of class A(ii) by writing the metric in

Eq.(1.24) as

$$ds^2 = -e^{2(K+k)}dt^2 + e^{2(K+k)}dx^2 + e^{2(S+s+F+f)}dy^2 + e^{2(S+s-F-f)}(dz+2wdx)^2,$$

where w is still dependent on x, t and the function K, F, and S depend on t only and k, f, and s depend on x only. The Einstein Field Equations are obtained using this metric ansatz and solutions are found by assuming that a particular combination of the components of the metric tensor are solely space or time dependent. This combination is derived from the components of the Ricci tensor and is written as

$$V^2 = \exp\Big[2(F+K-3S+f+k-3s)\Big] = f^{''} + 2f^{'}s^{'} - \ddot{F} - 2\dot{F}\dot{S}. \tag{1.25}$$

If V^2 is time independent then the solutions are possible only for the stiff fluid case, meaning $\gamma = 2$, or $\gamma = \frac{6\alpha}{(5\alpha+2)}$, where the constant α is defined by equations

$$\dot{K} = \alpha\dot{F}, \tag{1.26}$$

$$\dot{S} = \frac{1}{3}(\alpha+1)\dot{F}, \tag{1.27}$$

$$f^{'} = \frac{1}{3}(\alpha+1)k^{'} + \frac{1}{3}(2\alpha-1)s^{'}. \tag{1.28}$$

However, for the range $1 < \gamma < \frac{3}{2}$, there is no explicit solution corresponding to a well-behaved cosmological model. Also, when the equation of state parameter is $\frac{10}{9}$, Wills gives a metric in [48, p.372] and shows that the metric admits an extra KVF (so a G_3) and corresponds to the Wainwright solution listed in the paper by Wainwright and Hsu [25]. In Chapter 5, we show that there are open sets of well-behaved, perfect fluid, self-similar exceptional G_2 cosmologies when the equation of state parameter is $\frac{10}{9}$, and we show that these solutions are not the Wainwright solutions of [25], but asymptotically tend to them.

These papers tackled this class of models by using a metric ansatz and assuming that the functions in the metric tensor are separable. In this thesis, we do not rely on these assumptions. Even though our main focus is on class A(ii), we also pick up some of the models in B(ii) on the boundary of our phase space.

Chapter 2

Coordinate And Orthonormal Tetrads

2.1 Orthonormal Tetrad Formalism

In this section, we introduce the orthonormal tetrad formalism. The use of this formalism has proven to be extremely convenient in cosmology [33, 10] and one of the leading papers that demonstrated the convenience of this formalism in the analysis of a set of homogeneous models is [9].
We begin by introducing the formulation of its mathematical foundation. We continue by writing down the identities, physical variables, commutation functions, and the EFEs in this formalism. We conclude by making certain choices and assumptions in Section 2.3 that reduce the number of variables in the EFEs for the models under consideration.

Let TM be the tangent bundle of the manifold M and g be a Lorentzian metric. Four vector fields $\mathbf{v}_0, ..., \mathbf{v}_3$ (smooth local sections of TM) form a *frame* if for all p, $\mathbf{v}_0(p), \mathbf{v}_1(p), \mathbf{v}_2(p), \mathbf{v}_3(p)$ is a basis of T_pM.
Consider two different frames $\mathbf{v}_0, ..., \mathbf{v}_3$ and $\mathbf{w}_0, ..., \mathbf{w}_3$, and the corresponding metric tensors $g_{ab} := g(\mathbf{v}_a, \mathbf{v}_b)$ and $\tilde{g}_{ij} := g(\mathbf{w}_i, \mathbf{w}_j)$. For some functions v^i_a, we have

$$\mathbf{v}_a = v^i_a \mathbf{w}_i.$$

Then

$$g_{ab} = g(\mathbf{v}_a, \mathbf{v}_b) = g(v^i_a \mathbf{w}_i, v^j_b \mathbf{w}_j) = v^i_a v^j_b g(\mathbf{w}_i, \mathbf{w}_j) = v^i_a v^j_b \tilde{g}_{ij}.$$

Thus, one may write components of the first metric tensor in terms of the second.
Given coordinates $x_0, ..., x_3$, we have tangent vector fields $\frac{\partial}{\partial x_0}, ..., \frac{\partial}{\partial x_3}$. These vector fields span the tangent space of every point in the coordinate neighborhood. Hence, $\frac{\partial}{\partial x_0}, ..., \frac{\partial}{\partial x_3}$ is a frame, called a *coordinate frame* or *coordinate tetrad*. The main property of such a frame is its commutativity:

$$\Big[\frac{\partial}{\partial x_i}, \frac{\partial}{\partial x_j}\Big] = 0. \tag{2.1}$$

An orthonormal frame is a frame $\mathbf{e}_0, ..., \mathbf{e}_3$ with

$$g(\mathbf{e}_i, \mathbf{e}_j) = \eta_{ij} = \text{diag}(-1, +1, +1, +1). \tag{2.2}$$

It is always possible to locally find such a frame; see Appendix B.
Thus, the metric tensor takes a very simple form for an orthonormal tetrad. This simplicity comes at a cost: the frame is not commutative. There exists functions $\gamma^c{}_{ab}$ for which

$$[\mathbf{e}_a, \mathbf{e}_b] = \gamma^c{}_{ab}\mathbf{e}_c. \tag{2.3}$$

The $\gamma^c{}_{ab}$ are called the *commutation functions*.

We choose an orthonormal frame. Then, for all C^2 vector fields $\mathbf{X}, \mathbf{Y}, \mathbf{Z}$, we derive a set of identities for the commutation functions $\gamma^c{}_{ab}$ by using the *Jacobi Identity*

$$[[\mathbf{X}, \mathbf{Y}], \mathbf{Z}] + [[\mathbf{Z}, \mathbf{X}], \mathbf{Y}] + [[\mathbf{Y}, \mathbf{Z}], \mathbf{X}] = \mathbf{0}. \tag{2.4}$$

By applying the Jacobi identity to the orthonormal frame vectors $\mathbf{e}_0, \mathbf{e}_1, \mathbf{e}_2, \mathbf{e}_3$, one obtains 16 distinct identities of the type

$$\begin{aligned} 0 &= [[\mathbf{e}_a, \mathbf{e}_b], \mathbf{e}_c] + [[\mathbf{e}_c, \mathbf{e}_a], \mathbf{e}_b] + [[\mathbf{e}_b, \mathbf{e}_c], \mathbf{e}_a] \\ &= [\gamma^d{}_{ab}\mathbf{e}_d, \mathbf{e}_c] + [\gamma^d{}_{ca}\mathbf{e}_d, \mathbf{e}_b] + [\gamma^d{}_{bc}\mathbf{e}_d, \mathbf{e}_a] \\ &= \gamma^d{}_{ab}\mathbf{e}_d\mathbf{e}_c - \mathbf{e}_c(\gamma^d{}_{ab})\mathbf{e}_d - \gamma^d{}_{ab}\mathbf{e}_c\mathbf{e}_d + \gamma^d{}_{ca}\mathbf{e}_d\mathbf{e}_b \\ &\quad - \mathbf{e}_b(\gamma^d{}_{ca})\mathbf{e}_d - \gamma^d{}_{ca}\mathbf{e}_b\mathbf{e}_d + \gamma^d{}_{bc}\mathbf{e}_d\mathbf{e}_a - \mathbf{e}_a\gamma^d{}_{bc}\mathbf{e}_d - \gamma^d{}_{bc}\mathbf{e}_a\mathbf{e}_d. \end{aligned} \tag{2.5}$$

Any version of Eq.(2.5) where at least two of the a, b, c are equal provide no information since $[\mathbf{e}_a, \mathbf{e}_b] = -[\mathbf{e}_b, \mathbf{e}_a]$. Thus, there are $\binom{4}{3}$ different meaningful versions of Eq.(2.5), yielding 16 ($\binom{4}{3} \times 4$) different scalar equations.
The symbol $\varepsilon_{\alpha\beta\nu}$ is a tensor of rank three, which takes on the values

$$\varepsilon_{\alpha\beta\nu} = \begin{cases} 0, & \text{if any two labels are the same,} \\ 1, & \text{if } (\alpha, \beta, \nu) \in \{(1,2,3), (2,3,1), (3,1,2)\}, \\ -1, & \text{if } (\alpha, \beta, \nu) \in \{(1,3,2), (2,1,3), (3,2,1)\}. \end{cases} \tag{2.6}$$

In this formalism, the spatial components of the commutation functions are decomposed into a 2-index symmetric object $n_{\alpha\beta}$ and a 1-index object a_α by the following formula [46, p.32]

$$\gamma^{\mu}{}_{\alpha\beta} = \varepsilon_{\alpha\beta\nu} n^{\mu\nu} + a_\alpha \delta^{\mu}{}_{\beta} - a_\beta \delta^{\mu}{}_{\alpha}. \tag{2.7}$$

The objects a_α and $n^{\mu\nu}$ are curvature quantities. They are computed in terms of the structure constants by

$$n^{\beta\tau} = \frac{1}{2}\gamma^{(\beta}{}_{\nu\sigma}\ \varepsilon^{\tau)\nu\sigma},$$
$$a_\beta = \frac{1}{2}\gamma^{\alpha}{}_{\beta\alpha}.$$

We decompose $u_{a;b}$ using the projection tensor as follows

$$\begin{aligned} u_{a;b} &= u_{c;d} h^c_a h^d_b - \dot{u}_a u_b \\ &= V_{ab} - \dot{u}_a u_b, \end{aligned}$$

Note that $V_{ab}V^a = V_{ba}u^a = 0$ and

$$V_{ab} = V_{[ab]} + V_{(ab)}. \tag{2.8}$$

We define the expansion tensor θ_{ab} by

$$\theta_{ab} = V_{(ab)}, \tag{2.9}$$

and we decompose this into its trace, the expansion scalar θ, and the trace-free shear tensor σ_{ab} [46, p.19]

$$\theta = \theta^a{}_a,$$
$$\sigma_{ab} = \theta_{ab} + \frac{1}{3}\theta h_{ab}. \tag{2.10}$$

The shear scalar is defined by

$$\sigma^2 = \frac{1}{2}\sigma_{ab}\sigma^{ab}. \tag{2.11}$$

The antisymmetric part of V_{ab} is used to define the vorticity tensor, vector, and scalar, ω_{ab} ω_a and ω respectively by

$$\omega_{ab} = u_{a;b} - u_{b;a} + \dot{u}_a u_b - \dot{u}_b u_a, \tag{2.12}$$
$$\omega^a = \frac{1}{2}\varepsilon^{abcd} u_b \omega_{cd}, \tag{2.13}$$
$$\omega^2 = \frac{1}{2}\omega_{ab}\ \omega^{ab}. \tag{2.14}$$

Note that $\omega_{ab} = 0$ iff $\omega_a = 0$ iff $\omega = 0$.
We then write

$$\begin{aligned} u_{a;b} &= \theta_{ab} + \omega_{ab} - \dot{u}_a u_b \\ &= (\sigma_{ab} + \frac{1}{3}\theta h_{ab}) + \omega_{ab} - \dot{u}_a u_b. \end{aligned}$$

The variables $\dot{u}_a, \theta_{ab}, \sigma_{ab}, \omega_a$ are called the *basic physical variables*. These are related to the Christoffel symbols through

$$u^a{}_{;b} = u^a{}_{,b} + \Gamma^a{}_{bc} u^c. \tag{2.15}$$

and also to the commutation functions since (see Appendix A)

$$\Gamma_{abc} = \frac{1}{2}(\gamma_{abc} + \gamma_{cab} - \gamma_{bca}). \tag{2.16}$$

By using the decompositions in Eq.(2.15), Eq.(2.7), and the Christoffel symbols in Eq.(2.16), we write the commutation functions in terms of the physical variables and the spatial curvature variables.
We have 24 independent commutation functions. So far we have defined the objects $n_{\mu\nu}$, a_μ, θ, $\sigma_{\mu\nu}$, $\omega_{\mu\nu}$, and $\dot{u}_\mu$ which give 21 unique components (taking the symmetries of these objects into account). The remaining information is in the so called local angular velocity. If $\mathbf{e}_0 = \mathbf{u}$ then the local angular velocity in the rest frame of an observer with the 4-velocity $\mathbf{u}$ of a set of Fermi-propagated axis with respect to $\mathbf{e}_1, \mathbf{e}_2, \mathbf{e}_3$ [9, p.111] is

$$\Omega^\alpha := \frac{1}{2}\varepsilon^{\alpha\mu\nu}(\mathbf{e}_\mu)^i(\mathbf{e}_\nu)_{i;j}u^j. \tag{2.17}$$

It follows that the commutation relations between the frame vectors is expressed [43, p.2026] by

$$[\mathbf{e}_0, \mathbf{e}_1] = \dot{u}^1\mathbf{e}_0 - \theta_{11}\mathbf{e}_1 - (\sigma_{12} - \omega_3 - \Omega_3)\mathbf{e}_2 - (\sigma_{13} + \omega_2 + \Omega_2)\mathbf{e}_3, \tag{2.18}$$
$$[\mathbf{e}_0, \mathbf{e}_2] = \dot{u}^2\mathbf{e}_0 - (\sigma_{12} + \omega_3 + \Omega_3)\mathbf{e}_1 - \theta_{22}\mathbf{e}_2 - (\sigma_{23} - \omega_1 - \Omega_1)\mathbf{e}_3, \tag{2.19}$$
$$[\mathbf{e}_0, \mathbf{e}_3] = \dot{u}^3\mathbf{e}_0 - (\sigma_{13} - \omega_2 - \Omega_2)\mathbf{e}_1 - (\sigma_{23} + \omega_1 + \Omega_1)\mathbf{e}_2 - \theta_{33}\mathbf{e}_3, \tag{2.20}$$
$$[\mathbf{e}_1, \mathbf{e}_2] = -2\omega_3\mathbf{e}_0 + (n_{13} - a_2)\mathbf{e}_1 + (n_{23} + a_1)\mathbf{e}_2 + n_{33}\mathbf{e}_3, \tag{2.21}$$
$$[\mathbf{e}_2, \mathbf{e}_3] = -2\omega_1\mathbf{e}_0 + n_{11}\mathbf{e}_1 + (n_{12} - a_3)\mathbf{e}_2 + (n_{13} + a_2)\mathbf{e}_3, \tag{2.22}$$
$$[\mathbf{e}_3, \mathbf{e}_1] = -2\omega_2\mathbf{e}_0 + (n_{12} + a_3)\mathbf{e}_1 + n_{22}\mathbf{e}_2 + (n_{23} - a_1)\mathbf{e}_3. \tag{2.23}$$

When we substitute the the kinematical quantities and the curvature quantities into the Jacobi identity Eq.(2.5), and get [43, p.2027]

$$\mathbf{e}_\mu n^{\mu\alpha} + \varepsilon^{\alpha\mu\nu}\mathbf{e}_\mu a_\nu - 2\theta^\alpha_\beta\omega^\beta - 2n^\alpha_\beta a^\beta - 2\varepsilon^{\alpha\mu\nu}\omega_\mu\Omega_\nu = 0. \tag{2.24}$$

2.2 The Einstein Field Equations, Jacobi Identities, & Contracted Bianchi Identities In The Orthonormal Tetrad Formalism

We may write the EFEs in terms of the Ricci tensor as

$$R_{ab} = T_{ab} - \frac{1}{2}T_r^r g_{ab}. \tag{2.25}$$

By using the form of T_{ab} in Eq.(1.5), we can derive the EFEs in this formalism by expressing the Ricci tensor in terms of the commutation functions and the Jacobi identities represented in Eq.(2.24).

The first form of the EFEs which is written down below is done so for a general fluid ($\pi_{\alpha\beta} \neq 0,\ q_\alpha \neq 0$). We require the perfect fluid condition in the next chapter.

The most general form of the EFEs written in this formalism has been given by a number of authors [9, 10, 46]. We follow the convention of Wainwright and Ellis in [46]. With $H = \frac{1}{3}\theta$, the EFEs are written such that $\mathbf{e}_0$ is acting on the physical quantities, and hence we obtain a set of evolution equations for H, $\sigma_{\alpha\beta}$, as well as equations for the energy density μ, and q_α. Let

$$b_{\alpha\beta} := 2n^\mu_\alpha n_{\mu\beta} - n^\mu_\mu n_{\alpha\beta}, \tag{2.26}$$

$$\begin{aligned} S_{\alpha\beta} := {} & \frac{1}{2}\Big(\mathbf{e}_\alpha(a_\beta) + \mathbf{e}_\beta(a_\alpha)\Big) \\ & - \frac{1}{3}\mathbf{e}_\mu(a^\mu)\delta_{\alpha\beta} - (\mathbf{e}_\mu - 2a_\mu)\frac{1}{2}\Big(n_{\nu\alpha}\varepsilon_\beta{}^{\mu\nu} + n_{\nu\beta}\varepsilon_\alpha{}^{\mu\nu}\Big) + b_{\alpha\beta} - \frac{1}{3}b^\mu_\mu\delta_{\alpha\beta}. \end{aligned} \tag{2.27}$$

The curvature scalar of the 3-spaces of the manifold whose tangent space at every point is spanned by the vector fields $\mathbf{e}_1, \mathbf{e}_2, \mathbf{e}_3$ is

$${}^3R = 4\ \mathbf{e}_\mu(a^\mu) - 6\ a_\mu a^\mu - \frac{1}{2}b^\mu{}_\mu. \tag{2.28}$$

We refer to the following equations as the EFEs

$$\mathbf{e}_0 H = -H^2 - \frac{2}{3}\sigma^2 + \frac{2}{3}\omega^2 + \frac{1}{3}(\mathbf{e}_\alpha + \dot{u}_\alpha - 2a_\alpha)\dot{u}^\alpha - \frac{1}{6}(\mu + 3p), \tag{2.29}$$

$$\begin{aligned}\mathbf{e}_0\sigma_{\alpha\beta} = &-3H\sigma_{\alpha\beta} + \varepsilon^{\mu\nu}{}_\alpha\sigma_{\beta\mu}\Omega_\nu + \varepsilon^{\mu\nu}{}_\beta\sigma_{\alpha\mu}\Omega_\nu - \omega_\alpha\Omega_\beta - \omega_\beta\Omega_\alpha + \frac{2}{3}\omega^\mu\Omega_\mu\delta_{\alpha\beta}\\ &+ \frac{1}{2}(\mathbf{e}_\alpha + \dot{u}_\alpha + a_\alpha)\dot{u}_\beta + \frac{1}{2}(\mathbf{e}_\beta + \dot{u}_\beta + a_\beta)\dot{u}_\alpha - \frac{1}{3}(\mathbf{e}^\mu + \dot{u}^\mu + a^\mu)\dot{u}_\mu\delta_{\alpha\beta}\\ &- \frac{1}{2}\varepsilon^{\mu\nu}{}_\alpha n_{\beta\mu}\dot{u}_\nu - \frac{1}{2}\varepsilon^{\mu\nu}{}_\beta n_{\alpha\mu}\dot{u}_\nu - S_{\alpha\beta} + \pi_{\alpha\beta},\end{aligned} \tag{2.30}$$

$$\mu = 3H^2 - \sigma^2 + \omega^2 - 2\ \omega_\alpha\Omega^\alpha + \frac{1}{2}R, \tag{2.31}$$

$$q_\alpha = 2\mathbf{e}_\alpha(H) - (\mathbf{e}_\beta - 3a_\beta)\sigma^\beta_\alpha - \varepsilon_\alpha{}^{\mu\nu}\sigma^\beta_\mu n_{\beta\nu} + \varepsilon_\alpha{}^{\mu\nu}(\mathbf{e}_\mu + 2\dot{u}_\mu - a_\mu)\omega_\nu - n^\beta_\alpha\omega_\beta. \tag{2.32}$$

The Jacobi Identities are written as

$$\begin{aligned}\mathbf{e}_0 n_{\alpha\beta} = &-Hn_{\alpha\beta} + \sigma^\mu_\alpha n_{\beta\mu} + \sigma^\mu_\beta n_{\alpha\mu} + [\varepsilon^{\mu\nu}{}_\alpha n_{\beta\mu} + \varepsilon^{\mu\nu}{}_\beta n_{\alpha\mu}](\omega_\nu + \Omega_\nu)\\ &- \frac{1}{2}(\mathbf{e}_\alpha + \dot{u}_\alpha)(\omega_\beta + \Omega_\beta) - \frac{1}{2}(\mathbf{e}_\beta + \dot{u}_\beta)(\omega_\alpha + \Omega_\alpha)\\ &- \frac{1}{2}(\mathbf{e}_\mu + \dot{u}_\mu)[\sigma_{\nu\alpha}\varepsilon_\beta{}^{\mu\nu} + \sigma_{\nu\beta}\varepsilon_\alpha{}^{\mu\nu} - 2(\omega^\mu + \Omega^\mu)\delta_{\alpha\beta}],\end{aligned} \tag{2.33}$$

$$\begin{aligned}\mathbf{e}_0 a_\alpha = &-Ha_\alpha - \sigma^\beta_\alpha a_\beta - (\mathbf{e}_\alpha + \dot{u}_\alpha)H + \frac{1}{2}(\mathbf{e}_\beta + \dot{u}_\beta)\sigma^\beta_\alpha\\ &- \frac{1}{2}\varepsilon_\alpha{}^{\mu\nu}(\mathbf{e}_\mu + \dot{u}_\mu - 2a_\mu)(\omega_\nu + \Omega_\nu),\end{aligned} \tag{2.34}$$

$$\mathbf{e}_0\omega_\alpha = -2H\omega_\alpha + \sigma^\beta_\alpha\omega_\beta + \varepsilon_\alpha{}^{\mu\nu}\omega_\mu\Omega_\nu - \frac{1}{2}\varepsilon_\alpha{}^{\mu\nu}(\mathbf{e}_\mu - a_\mu)\dot{u}_\nu + \frac{1}{2}n^\beta_\alpha\dot{u}_\beta, \tag{2.35}$$

$$0 = (\mathbf{e}_\beta - 2a_\beta)n^\beta_\alpha + \varepsilon_\alpha{}^{\mu\nu}\mathbf{e}_\mu a_\nu - 2H\omega_\alpha - 2\sigma^\beta_\alpha\omega_\beta - 2\varepsilon_\alpha{}^{\mu\nu}\omega_\mu\Omega_\nu, \tag{2.36}$$

$$0 = (\mathbf{e}_\alpha - \dot{u}_\alpha - 2a_\alpha)\omega^\alpha. \tag{2.37}$$

And the contracted Bianchi identities are

$$\mathbf{e}_0\mu = -3H(\mu + p) - \sigma^\beta_\alpha\pi^\alpha_\beta - (\mathbf{e}_\alpha + 2\dot{u}_\alpha - 2a_\alpha)q^\alpha, \tag{2.38}$$

$$\begin{aligned}\mathbf{e}_0 q_\alpha = &-4Hq_\alpha - \sigma^\beta_\alpha q_\beta + \varepsilon_\alpha{}^{\mu\nu}(\omega_\mu - \Omega_\mu)q_\nu - \mathbf{e}_\alpha p - (\mu + p)\dot{u}_\alpha\\ &- (\mathbf{e}_\beta + \dot{u}_\beta - 3a_\beta)\pi^\beta_\alpha + \varepsilon_\alpha{}^{\mu\nu}n^\beta_\mu\pi_{\beta\nu}.\end{aligned} \tag{2.39}$$

2.3 Assumptions & Choices

In this section, we show how many of the basic physical variables are forced to be zero due to our assumptions and choices. We show a step by step proof of some results that are not new and have already been proven by Wainwright in [43]; to help the reader, we show them in this section.

Assumption A3: *We assume that spacetime admits an Abelian G_2 acting on two-dimensional spacelike orbits.*

Assumption A4: *We assume that the fluid flow vector* $\mathbf{u}$ *is orthogonal to the orbits.*

Since we have a perfect fluid, we have that $\mathbf{u}$ is invariant under the isometry group, and from [44, p.1134] we have that $\mathbf{u}$ is hypersurface orthogonal.

Let $\boldsymbol{\xi}$ and $\boldsymbol{\eta}$ be two linearly independent KVFs that generate the abelian G_2.

Lemma 2.3.1. *There exists a class of invariant tetrads with frame vectors* $\mathbf{e}_0, \mathbf{e}_1, \mathbf{e}_2, \mathbf{e}_3$ *for which* $\mathbf{e}_2$ *and* $\mathbf{e}_3$ *are orbit aligned and* $\mathbf{e}_0$ *is aligned with* $\mathbf{u}$*. That is, there exits* $A, B, C, D \in C^2$ *such that*

$$\mathbf{e}_2 = A\boldsymbol{\xi} + B\boldsymbol{\eta}, \qquad (2.40)$$

$$(\textit{orbit aligned})$$

$$\mathbf{e}_3 = C\boldsymbol{\xi} + D\boldsymbol{\eta}, \qquad (2.41)$$

and

$$[\boldsymbol{\xi}, \mathbf{e}_a] = [\boldsymbol{\eta}, \mathbf{e}_a] = \mathbf{0}. \qquad (\textit{invariant})$$

Any two tetrads in this class are related by rotating $\mathbf{e}_2$ *and* $\mathbf{e}_3$ *in the orbits. This freedom of rotation is expressed by*

$$\tilde{\mathbf{e}}_2 = \cos(\phi)\mathbf{e}_2 + \sin(\phi)\mathbf{e}_3,$$
$$\tilde{\mathbf{e}}_3 = \sin(\phi)\mathbf{e}_2 + \cos(\phi)\mathbf{e}_3.$$

with $\boldsymbol{\eta}(\phi) = \boldsymbol{\xi}(\phi) = 0$.

This result is contained in the proof of Theorem 3.1 in [43].

Choice C1: *We choose an orbit aligned, group invariant frame with* $\mathbf{e}_0$ *aligned with* $\mathbf{u}$.

Since $\mathbf{u}$ is hypersurface orthogonal then $\mathbf{e}_0$ is hypersurface orthogonal and we have

$$\gamma^0{}_{\alpha\beta} = 0. \tag{2.42}$$

Due to this choice, the physical variables are the kinematical quantities of the fluid. And since $\mathbf{e}_0$ is hypersurface orthogonal, the fluid is irrotational; meaning $\omega_\mu = 0$.

Consequences of orbit aligned

Lemma 2.3.2. *For any frame* $\mathbf{e}_0, ..., \mathbf{e}_3$ *whose existence is generated by lemma 2.3.1, then* $\mathbf{e}_1$ *is hypersurface orthogonal.*

Proof. We invert Eq.(2.40)-(2.41) to get

$$\boldsymbol{\xi} = E\mathbf{e}_2 + F\mathbf{e}_3, \tag{2.43}$$
$$\boldsymbol{\eta} = G\mathbf{e}_2 + H\mathbf{e}_3, \tag{2.44}$$

for some $E, F, G, H \in C^2$. Using the above and Eq.(2.40)-(2.41), we have

$$\begin{aligned}
[\mathbf{e}_0, \mathbf{e}_2] &= [\mathbf{e}_0, A\boldsymbol{\xi} + B\boldsymbol{\eta}] \\
&= \mathbf{e}_0(A)\boldsymbol{\xi} + A[\mathbf{e}_0, \boldsymbol{\xi}] + \mathbf{e}_0(B)\boldsymbol{\eta} + B[\mathbf{e}_0, \boldsymbol{\eta}] \\
&= \mathbf{e}_0(A)\boldsymbol{\xi} + \mathbf{e}_0(B)\boldsymbol{\eta} \\
&= \Big(\mathbf{e}_0(A)E + \mathbf{e}_0(B)G\Big)\mathbf{e}_2 + \Big(\mathbf{e}_0(A)F + \mathbf{e}_0(B)H\Big)\mathbf{e}_3.
\end{aligned} \tag{2.45}$$

and we conclude that $\gamma^1{}_{02} = 0$. Similarly,

$$[\mathbf{e}_0, \mathbf{e}_3] = \gamma^2{}_{03}\mathbf{e}_2 + \gamma^3{}_{03}\mathbf{e}_3, \text{ and } \gamma^1{}_{03} = 0, \tag{2.46}$$
$$[\mathbf{e}_1, \mathbf{e}_2] = \gamma^2{}_{12}\mathbf{e}_2 + \gamma^3{}_{12}\mathbf{e}_3, \text{ and } \gamma^1{}_{12} = 0, \tag{2.47}$$
$$[\mathbf{e}_1, \mathbf{e}_3] = \gamma^2{}_{13}\mathbf{e}_2 + \gamma^3{}_{13}\mathbf{e}_3, \text{ and } \gamma^1{}_{13} = 0, \tag{2.48}$$
$$[\mathbf{e}_2, \mathbf{e}_3] = \gamma^2{}_{13}\mathbf{e}_2 + \gamma^3{}_{13}\mathbf{e}_3, \text{ and } \gamma^1{}_{23} = 0. \tag{2.49}$$

Since we already know that $\gamma^1{}_{QK} = 0$ for $Q, K \in \{0, 2, 3\}$, then $\mathbf{e}_1$ is also hypersurface orthogonal. □

Consequences of group invariance

$$\begin{aligned}\mathbf{0} = [\boldsymbol{\xi}, \mathbf{e}_2] &= [\boldsymbol{\xi}, A\boldsymbol{\xi} + B\boldsymbol{\eta}] \\ &= \boldsymbol{\xi}(A)\boldsymbol{\xi} + \boldsymbol{\xi}(B)\boldsymbol{\eta} - B[\boldsymbol{\eta}, \boldsymbol{\xi}] \\ &= \boldsymbol{\xi}(A)\boldsymbol{\xi} + \boldsymbol{\xi}(B)\boldsymbol{\eta}. \end{aligned} \tag{2.50}$$

Thus,

$$\boldsymbol{\xi}(A),\ \boldsymbol{\xi}(B) = 0.$$

Similarly,

$$\boldsymbol{\xi}(C),\ \boldsymbol{\xi}(D) = 0.$$

Also, $[\boldsymbol{\eta}, \mathbf{e}_2] = [\boldsymbol{\eta}, \mathbf{e}_3] = 0$, so

$$\boldsymbol{\eta}(A) = 0,\ \boldsymbol{\eta}(B) = 0, \boldsymbol{\eta}(C) = 0,\ \boldsymbol{\eta}(D) = 0.$$

It follows that

$$\begin{aligned}[\mathbf{e}_2, \mathbf{e}_3] &= [A\boldsymbol{\xi} + B\boldsymbol{\eta}, C\boldsymbol{\xi} + D\boldsymbol{\eta}] \\ &= (AD - BC)[\boldsymbol{\xi}, \boldsymbol{\eta}] + \Big(A\boldsymbol{\xi}(A) - C\boldsymbol{\xi}(B)\Big)\boldsymbol{\eta} + \Big(B\boldsymbol{\eta}(C) + D\boldsymbol{\eta}(A)\Big)\boldsymbol{\xi} \\ &= 0,\end{aligned}$$

that is the two frame vectors $\mathbf{e}_2$ and $\mathbf{e}_3$ commute.

Assumption A5: *We assume that one of the KVFs, $\boldsymbol{\xi}$, is hypersurface orthogonal.*

Choice C2: *We align $\mathbf{e}_2$ with $\boldsymbol{\xi}$.*

It follows that $\mathbf{e}_2$ is also hypersurface orthogonal and so we have

$$\gamma^2{}_{QK} = 0, \quad \text{Q, K} \in \{0, 1, 3\}. \tag{2.51}$$

Finally, we have the following, potentially, nonzero commutation functions

$$\gamma^0_{01},\ \gamma^1_{01},\ \gamma^3_{01},\ \gamma^2_{02},\ \gamma^3_{03},\ \gamma^2_{12},\ \gamma^3_{31},$$

corresponding to the nonzero physical variables

$$\theta, \dot{u}_1,\ a_1,\ n_{23},\ \sigma_{11},\ \sigma_{22},\ \sigma_{33},\ \sigma_{13} = \theta_{13} = \Omega_2. \tag{2.52}$$

There is no remaining frame freedom.

Chapter 3

A Class of Exceptional H_3 Cosmological Models: Reduction Of The EFEs To A System of ODEs

In this chapter we write the EFEs for the models under consideration as a system of first order PDEs in terms of dimensionless variables. This is achieved in two stages. In Section 3.1, we develop a system of PDEs in terms of the basic physical variables, and in Section 3.2 we rewrite the system via converting the variables to dimensionless variables. In Section 3.3, we change variables to aid with the comparison of a paper that qualitatively analyzed models of class B(ii). We continue in Section 3.4 by compactifying the phase space. We conclude by giving the invariant sets and explaining their importance.

3.1 The Reduction Of The EFEs

In this section, we describe how the EFEs reduce to the system of PDEs that govern changes of the kinematical quantities of the cosmological fluid.
We define the state vector $\mathbf{w}$ by

$$\mathbf{w} = [\theta,\ \sigma_{11},\ \sigma_{22},\ \sigma_{33},\ \sigma_{13},\ n_{23},\ a_1,\ \dot{u}_1]^T. \tag{3.1}$$

Due to the choices and assumptions in Chapter 2, we have $\mathbf{e}_2(\mathbf{w}) = \mathbf{0}, \mathbf{e}_3(\mathbf{w}) = \mathbf{0}$. The general EFEs in Eq.(2.29)-(2.32) reduce to a system of PDEs in terms of the differential

operators $\mathbf{e}_0$ and $\mathbf{e}_1$. This system takes the form

$$\mathbf{e}_0\mathbf{w} = \mathbf{B}(\mathbf{w})\ \mathbf{e}_1\mathbf{w} + \mathbf{C}(\mathbf{w}) \tag{3.2}$$

with $\mathbf{C}(\mathbf{w}) \in \mathbb{R}^8$, $\mathbf{B}(\mathbf{w}) \in \mathbb{M}_{8\times 8}(\mathbb{R})$. We note that $\sigma_{\alpha\alpha}$ are not independent as $\sigma^{\alpha}{}_{\alpha} = 0$. The operator $\mathbf{e}_0$ is a differential operator along the direction of the fluid 4-velocity, and $\mathbf{e}_1$ is a spatial differential operator. The evolution equation for $\dot{u}_1$ is obtained by applying the commutator $[\mathbf{e}_0, \mathbf{e}_1]$ to μ and using the auxiliary equations Eq.(3.14)-(3.15), when $\mu \neq 0$. Appendix D provides greater details about the reduction of EFEs to the system of PDEs. The EFEs reduce to the evolution equations

$$\begin{aligned}
\mathbf{e}_0\theta &= \mathbf{e}_1\dot{u}_1 - \frac{1}{3}\theta^2 - \Big((\sigma_{11})^2 + (\sigma_{22})^2 + (\sigma_{33})^2 + 2(\sigma_{13})^2\Big) \\
&\quad + (\dot{u}_1 - 2a_1)\dot{u}_1 - \frac{(3\gamma-2)}{2}\mu, && (3.3)\\
\mathbf{e}_0\sigma_{11} &= \frac{2}{3}\mathbf{e}_1\dot{u}_1 - \frac{2}{3}\mathbf{e}_1 a_1 - \theta\sigma_{11} - 2(\sigma_{13})^2 + \frac{2}{3}\dot{u}_1(\dot{u}_1 + a_1) + \frac{4}{3}(n_{23})^2, && (3.4)\\
\mathbf{e}_0\sigma_{22} &= -\mathbf{e}_1 n_{32} - \frac{1}{3}\mathbf{e}_1\dot{u}_1 + \frac{1}{3}\mathbf{e}_1 a_1 - \theta\sigma_{22} - \frac{1}{3}\dot{u}_1(\dot{u}_1 + a_1 + 3n_{23}) \\
&\quad + n_{32}(2a_1 - \frac{2}{3}n_{23}), && (3.5)\\
\mathbf{e}_0\sigma_{33} &= \mathbf{e}_1 n_{23} - \frac{1}{3}\mathbf{e}_1\dot{u}_1 + \frac{1}{3}\mathbf{e}_1 a_1 - \theta\sigma_{33} + 2(\sigma_{13})^2 - \frac{1}{3}\dot{u}_1(\dot{u}_1 + a_1) \\
&\quad + n_{23}(\dot{u}_1 - 2a_1 - \frac{2}{3}n_{23}), && (3.6)\\
\mathbf{e}_0\sigma_{13} &= (-\theta - \sigma_{33} + \sigma_{11})\sigma_{13}, && (3.7)\\
\mathbf{e}_0 n_{23} &= -\frac{1}{2}\mathbf{e}_1\sigma_{22} + \frac{1}{2}\mathbf{e}_1\sigma_{33} - n_{23}(\frac{1}{3}\theta - \sigma_{22} - \sigma_{33}) - \frac{1}{2}\dot{u}_1(\ \sigma_{22} - \sigma_{33}\ ), && (3.8)\\
\mathbf{e}_0 a_1 &= -\frac{1}{3}\mathbf{e}_1\theta + \frac{1}{2}\mathbf{e}_1\sigma_{11} - a_1(\frac{1}{3}\theta + \sigma_{11}) - \frac{1}{3}\dot{u}_1\theta, && (3.9)\\
\mathbf{e}_0\dot{u}_1 &= (\gamma-1)\mathbf{e}_1\theta - \dot{u}_1\Big(\sigma_{11} - (\gamma-1)\theta + \frac{1}{3}\theta\Big) \quad (\mu \neq 0). && (3.10)
\end{aligned}$$

The constraint equations are

$$\begin{aligned}
0 = q_1 &= \frac{2}{3}\mathbf{e}_1\theta - \mathbf{e}_1\sigma_{11} + 3a_1\sigma_{11} + n_{23}(\sigma_{33} - \sigma_{22}), && (3.11)\\
0 = q_3 &= -\mathbf{e}_1\sigma_{13} + \sigma_{13}(3a_1 - n_{23}), && (3.12)
\end{aligned}$$

and the defining equation for μ is

$$\mu = \frac{1}{3}\theta^2 - \frac{1}{2}\Big((\sigma_{11})^2 + (\sigma_{22})^2 + (\sigma_{33})^2 + 2(\sigma_{13})^2\Big) + 2\mathbf{e}_1(a_1) - 3\ (a_1)^2 - \ (n_{23})^2. \tag{3.13}$$

And finally, there are equations that contain certain information about the energy density, which the system of PDEs possesses. These equations are not independent of the system. However, since this information does not manifest itself explicitly in the form that the PDEs are written, we refer to these equations as auxiliary equations. These are

$$\mathbf{e}_0\mu = -\gamma\mu\theta, \tag{3.14}$$

$$\mathbf{e}_1\mu = -\frac{\gamma\mu\dot{u}_1}{(\gamma-1)}. \tag{3.15}$$

We reduce the number of variables of the PDEs in Eq.(3.3)-(3.10) by using the relationship between the expansion tensor and the shear tensor. We introduce the shear variables σ_+ and σ_- defined by

$$\sigma_+ := \frac{3}{2}(\sigma_{22} + \sigma_{33}), \tag{3.16}$$

$$\sigma_- := \frac{1}{2}(\sigma_{22} - \sigma_{33}). \tag{3.17}$$

Equivalently

$$\sigma_{22} = \sigma_- + \frac{1}{3}\sigma_+, \tag{3.18}$$

$$\sigma_{33} = \frac{1}{3}\sigma_+ - \sigma_-. \tag{3.19}$$

Since $\sigma_{\alpha\beta}$ is trace free, we have

$$\sigma_{11} = -\frac{2}{3}\sigma_+. \tag{3.20}$$

We let $\tilde{\mathbf{w}}$ be a state vector in $\mathbb{R}^7$ defined by

$$\tilde{\mathbf{w}} = [\theta,\ \sigma_+,\ \sigma_-,\ \sigma_{13},\ n_{23},\ a_1, \dot{u}_1]^T, \tag{3.21}$$

the PDEs are

$$\mathbf{e}_0\theta = \mathbf{e}_1\dot{u}_1 - \frac{1}{3}\theta^2 - 2\Big(\frac{1}{3}(\sigma_+)^2 + (\sigma_-)^2 + (\sigma_{13})^2\Big) + \dot{u}_1(\dot{u}_1 - 2a_1) - \frac{3\gamma - 2}{2}\mu, \tag{3.22}$$

$$\mathbf{e}_0(\sigma_+) = -\mathbf{e}_1\dot{u}_1 + \mathbf{e}_1 a_1 - \sigma_+\theta + 3(\sigma_{13})^2 - \dot{u}_1(\dot{u}_1 + a_1) - 2(n_{23})^2, \tag{3.23}$$

$$\mathbf{e}_0(\sigma_-) = -\mathbf{e}_1 n_{23} - \theta\sigma_- - (\sigma_{13})^2 - n_{23}(\dot{u}_1 - 2a_1), \tag{3.24}$$

$$\mathbf{e}_0\sigma_{13} = \sigma_{13}\ (\sigma_- - \sigma_+ - \theta), \tag{3.25}$$

$$\mathbf{e}_0 n_{23} = -\mathbf{e}_1\sigma_- + \frac{1}{3}n_{23}(-\theta + 2\sigma_+) - \sigma_-\dot{u}_1, \tag{3.26}$$

$$\mathbf{e}_0 a_1 = -\frac{1}{3}\mathbf{e}_1\sigma_+ - \frac{1}{3}\mathbf{e}_1\theta - \frac{1}{3}\theta(a_1 + \dot{u}_1) + \frac{1}{3}\sigma_+(2a_1 - \dot{u}_1), \tag{3.27}$$

$$\mathbf{e}_0\dot{u}_1 = (\gamma - 1)\mathbf{e}_1\theta + \frac{1}{3}(2\sigma_+ - \theta)\dot{u}_1 + (\gamma - 1)\theta\dot{u}_1. \tag{3.28}$$

The constraint equations are

$$0 = \frac{1}{3}\mathbf{e}_1(\theta) + \frac{1}{3}\mathbf{e}_1(\sigma_+) - a_1(\sigma_+) - (\sigma_-)n_{23}, \tag{3.29}$$

$$0 = -\mathbf{e}_1(\sigma_{13}) + \sigma_{13}(3a_1 - n_{23}), \tag{3.30}$$

and the defining equation for μ is

$$\mu = \frac{1}{3}\theta^2 - \Big(\frac{1}{3}(\sigma_+)^2 + (\sigma_-)^2 + (\sigma_{13})^2\Big) + 2\mathbf{e}_1(a_1) - 3(a_1)^2 - (n_{23})^2. \tag{3.31}$$

The auxiliary equations, Eq.(3.14)-(3.15) remain the same.

3.2 Dimensionless Variables & The Master PDEs

The variables of the system of PDEs in Eq.(3.22)-(3.28) are the basic physical variables of the cosmological fluid described in Chapter 1. These variables typically diverge near the initial singularity. They might also tend to zero at later times [20]. In order to avoid these issues, *expansion normalized* variables [25, p.1409] are used. These dimensionless variables are obtained by dividing the actual physical variable by an appropriate power of the expansion θ. An additional reason to use these variables is that they are often used for experimental observations [34, p.773]. For example, the variable Ω defined below, is measured by astronomers [4, 28, 36]. The expansion normalized variables are defined as

follows. The shear variables are

$$\Sigma_+ := \frac{\sigma_+}{\theta}, \tag{3.32}$$

$$\Sigma_- := \frac{\sigma_-}{\theta}, \tag{3.33}$$

$$\Sigma_{13} := \frac{\sigma_{13}}{\theta},$$

the acceleration variable is

$$\dot{U} := \frac{\dot{u}_1}{\theta}, \tag{3.34}$$

the spatial curvature variables are

$$A := \frac{3a_1}{\theta}, \tag{3.35}$$

$$N_\times := \frac{n_{23}}{\theta}, \tag{3.36}$$

and the dimensionless energy density is

$$\Omega := \frac{3\mu}{\theta^2}. \tag{3.37}$$

In addition, we use the dimensionless operators $\boldsymbol{\partial} i$ defined as

$$\boldsymbol{\partial}_i := \frac{3}{\theta}\mathbf{e}_i. \tag{3.38}$$

The quantities $\mathbf{e}_0\theta$ and $\mathbf{e}_1\theta$ appear in the PDEs and we replace them by introducing the dimensionless scalars q and r defined[1] by

$$\mathbf{e}_0\theta = -\frac{1}{3}(1+q)\theta^2, \tag{3.39}$$

$$\mathbf{e}_1\theta = -\frac{1}{3}r\theta^2. \tag{3.40}$$

We illustrate the development of the PDEs in terms of the dimensionless variables by considering $\Sigma_+ = \frac{\sigma_+}{\theta}$. We know that

$$\boldsymbol{\partial}_0(\Sigma_+) = \frac{3}{\theta}\mathbf{e}_0(\frac{\sigma_+}{\theta}) = -\frac{3}{\theta^3}\mathbf{e}_0(\theta)(\sigma_+) + \mathbf{e}_0(\sigma_+)\frac{3}{\theta^2}. \tag{3.41}$$

[1]From Chapter 1, the quantity θ is the average expansion of the fluid and in the FLRW models, θ is defined in terms of the length scale l by $\theta = 3\frac{\dot{l}}{l}$. The scalar q is the deceleration parameter defined in the FLRW models by $q = -\frac{\ddot{l}l}{\dot{l}^2}$.

We use Eq.(3.39) and Eq.(3.40) to obtain

$$\boldsymbol{\partial}_0(\Sigma_+) = \frac{3}{\theta}\mathbf{e}_0(\frac{\sigma_+}{\theta}) = -\frac{3}{\theta}\Big(-\frac{1}{3}(1+q)\Big)\sigma_+ + \mathbf{e}_0(\sigma_+)\frac{3}{\theta^2}. \tag{3.42}$$

By substituting $\mathbf{e}_0(\sigma_+)$ from the above into Eq.(3.23) we get

$$\begin{aligned}\boldsymbol{\partial}_0(\Sigma_+) - (1+q)\Sigma_+ = &-\frac{3}{\theta^2}\mathbf{e}_1(\dot{u}_1) + \frac{3}{\theta^2}\mathbf{e}_1(a_1) - 3\Sigma_+ + 9(\Sigma_{13})^2 \\ &- 3\dot{U}(\dot{U} + \frac{A}{3}) - 6(N_\times)^2.\end{aligned} \tag{3.43}$$

Since

$$\boldsymbol{\partial}_1\dot{U} = \frac{3}{\theta}\mathbf{e}_1(\frac{\dot{u}_1}{\theta}) = \frac{3}{\theta}\Big(-\frac{1}{\theta^2}(-\frac{1}{3}r\theta^2)\dot{u}_1 + \frac{1}{\theta}\mathbf{e}_1(\dot{u}_1)\Big), \tag{3.44}$$

we have

$$\frac{3}{\theta^2}\mathbf{e}_1(\dot{u}_1) = \boldsymbol{\partial}_1(\dot{U}) - r\dot{U}, \tag{3.45}$$

and similarly

$$\frac{3}{\theta^2}\mathbf{e}_1(a_1) = \frac{1}{3}\boldsymbol{\partial}_1 A - \frac{1}{3}Ar. \tag{3.46}$$

We substitute Eq.(3.45) and Eq.(3.46) into Eq.(3.43) to get

$$\boldsymbol{\partial}_0(\Sigma_+) = -\boldsymbol{\partial}_1(\dot{U}) + \frac{1}{3}\boldsymbol{\partial}_1(A) + \Sigma_+(q-2) + 9(\Sigma_{13})^2 - A\dot{U} - \frac{1}{3}rA - 3\dot{U}^2 + r\dot{U} - 6(N_\times)^2.$$

The same procedure is applied to the other variables. The new six dimensional state vector is

$$\mathbf{W} = [\Sigma_+, \Sigma_-, \Sigma_{13}, N_\times, A, \dot{U}]^T, \tag{3.47}$$

and the resulting system of PDEs are the **Master PDEs**

$$\begin{aligned}\boldsymbol{\partial}_0(\Sigma_+) = &-\boldsymbol{\partial}_1(\dot{U}) + \frac{1}{3}\boldsymbol{\partial}_1(A) + \Sigma_+(q-2) \\ &+ 9(\Sigma_{13})^2 - A\dot{U} - \frac{1}{3}rA - 3\dot{U}^2 + r\dot{U} - 6(N_\times)^2,\end{aligned} \tag{3.48}$$

$$\boldsymbol{\partial}_0(\Sigma_-) = -\boldsymbol{\partial}_1(N_\times) + (\Sigma_-)(q-2) - 3(\Sigma_{13})^2 - N_\times(3\dot{U} - r - 2A), \tag{3.49}$$

$$\boldsymbol{\partial}_0(\Sigma_{13}) = \Sigma_{13}(-2 + q + 3\Sigma_- - 3\Sigma_+), \tag{3.50}$$

$$\boldsymbol{\partial}_0(N_\times) = -\boldsymbol{\partial}_1(\Sigma_-) + N_\times(q + 2\Sigma_+) + r\Sigma_- - 3(\Sigma_-)\dot{U}, \tag{3.51}$$

$$\boldsymbol{\partial}_0(A) = -\boldsymbol{\partial}_1(\Sigma_+) + A(q + 2\Sigma_+) + (1 + \Sigma_+)(r - 3\dot{U}), \tag{3.52}$$

$$\boldsymbol{\partial}_0\dot{U} = (q + 2\Sigma_+)\dot{U} + (\gamma - 1)(3\dot{U} - r) \quad (\Omega \neq 0). \tag{3.53}$$

The defining equations for r, q, and Ω are

$$0 = \boldsymbol{\partial}_1(\Sigma_+) - r(1+\Sigma_+) - 3A(\Sigma_+) - 9(\Sigma_-)N_\times, \tag{3.54}$$

$$q = 2(\Sigma_+)^2 + 6(\Sigma_-)^2 - \boldsymbol{\partial}_1(\dot{U}) + \dot{U}(r - 3\dot{U} + 2A) + \frac{1}{2}\Omega(3\gamma - 2) + 6\Sigma_{13}, \tag{3.55}$$

$$\Omega = 1 - (\Sigma_+)^2 - 3(\Sigma_-)^2 - 3(\Sigma_{13})^2 + \frac{2}{3}\,\boldsymbol{\partial}_1(A) - A(\frac{2}{3}r + A) - 3(N_\times)^2. \tag{3.56}$$

The constraint equations is

$$0 = -\boldsymbol{\partial}_1(\Sigma_{13}) + \Sigma_{13}(r + 3A - 3N_\times). \tag{3.57}$$

We also have the auxiliary equations

$$\boldsymbol{\partial}_0 r - \boldsymbol{\partial}_1 q = (3\dot{U} - r)(1+q) + (q + 2\Sigma_+)r, \tag{3.58}$$

$$\boldsymbol{\partial}_0(\Omega) = \Omega\Big(2q - (3\gamma - 2)\Big), \tag{3.59}$$

$$\boldsymbol{\partial}_1(\Omega) = \Omega\Big(2r + \frac{3\gamma\dot{U}}{1-\gamma}\Big), \tag{3.60}$$

where the first equation is obtained by applying the commutator $[\mathbf{e}_0, \mathbf{e}_1]$ to θ. From Eq.(3.39) and Eq,(3.40), we have the decoupled equations

$$\boldsymbol{\partial}_0\theta = -(1+q)\theta, \tag{3.61}$$

$$\boldsymbol{\partial}_1\theta = -r\theta. \tag{3.62}$$

Another important piece of information is the commutator relation between the scaled basis vectors $\frac{3}{\theta}\mathbf{e}_0$ and $\frac{3}{\theta}\mathbf{e}_1$.

$$\begin{aligned}[\boldsymbol{\partial}_0, \boldsymbol{\partial}_1] &= \frac{9}{\theta^2}[\mathbf{e}_0, \mathbf{e}_1] + \frac{9}{\theta}\mathbf{e}_0(\frac{1}{\theta})\mathbf{e}_1 - \frac{9}{\theta}\mathbf{e}_1(\frac{1}{\theta})\mathbf{e}_0 \\ &= (1+q)\boldsymbol{\partial}_1 - r\boldsymbol{\partial}_0 + \frac{9}{\theta^2}[\mathbf{e}_0, \mathbf{e}_1].\end{aligned} \tag{3.63}$$

Therefore, from the commutation relations in Eq.(2.18), we get a dimensionless form of the commutation relation, namely

$$[\boldsymbol{\partial}_0, \boldsymbol{\partial}_1] = \Big(q + 2\Sigma_+\Big)\boldsymbol{\partial}_1 + \Big(3\dot{U} - r\Big)\boldsymbol{\partial}_0 - 6\Sigma_{13}\boldsymbol{\partial}_3. \tag{3.64}$$

The dimensionless PDEs of Eq.(3.48)-(3.53) along with Eq.(3.64) and the auxiliary equations give us enough information to analyze the cosmological models.

3.3 A Class of Exceptional H_3 Cosmological Models

In this section, we set a restriction on the PDEs in Eq.(3.48)-(3.60). This restriction yields a subcase of the problem that we address by using the qualitative theory of differential equations. This subcase is a 1-parameter, three dimensional system of ODEs.

Let $\mathbf{M} = \mathbf{M}(\mathbf{W}) \in \mathbb{M}_{6\times 6}(\mathbb{R})$, and $\mathbf{G}(\mathbf{W}) \in \mathbb{R}^6$. The EFEs in Eq.(3.48)-(3.53) are written as system of quasi-linear PDEs of the form

$$\boldsymbol{\partial}_0\mathbf{W} = \mathbf{M}\,\boldsymbol{\partial}_1\mathbf{W} + \mathbf{G}(\mathbf{W}). \tag{3.65}$$

Models that admit

$$\boldsymbol{\partial}_0\mathbf{W} = \mathbf{0}, \tag{3.66}$$

are the *dynamical equilibrium states* of the exceptional G_2 cosmologies.
Using Eq.(3.54)-(3.57), we can show that if $\gamma \neq \frac{2}{3}$, $\Sigma_+ \neq -1$, $\mathbf{M}$ is invertible so

$$\boldsymbol{\partial}_1(\mathbf{W}) = \mathbf{F}(\mathbf{W}). \tag{3.67}$$

By the chain rule

$$\boldsymbol{\partial}_0\boldsymbol{\partial}_1(\mathbf{W}) = \boldsymbol{\partial}_0(\mathbf{F}(\mathbf{W})) = \mathbf{0}. \tag{3.68}$$

From Eq.(3.58)-(3.60), we have

$$\boldsymbol{\partial}_0 r = 0, \quad \boldsymbol{\partial}_0\Omega = 0, \quad \boldsymbol{\partial}_0 q = 0. \tag{3.69}$$

Applying $[\boldsymbol{\partial}_0, \boldsymbol{\partial}_1]$ to $\mathbf{W}$ yields

$$[\boldsymbol{\partial}_0, \boldsymbol{\partial}_1]\mathbf{W} = \boldsymbol{\partial}_0\boldsymbol{\partial}_1\mathbf{W} - \boldsymbol{\partial}_1\boldsymbol{\partial}_0\mathbf{W} = \mathbf{0}. \tag{3.70}$$

From the above and the commutator relation in Eq.(3.64), we have

$$0 = [\boldsymbol{\partial}_0, \boldsymbol{\partial}_1]\mathbf{W} = \Big[q + 2\Sigma_+\Big]\boldsymbol{\partial}_1\mathbf{W}. \tag{3.71}$$

There are two possibilities:

$$\boldsymbol{\partial}_1\mathbf{W} \neq \mathbf{0}, \qquad q + 2\Sigma_+ = 0 \tag{3.72}$$

or

$$\boldsymbol{\partial}_1 \mathbf{W} = \mathbf{0}. \tag{3.73}$$

We define *spatially inhomogeneous dynamical equilibrium states*, similar to the work in [20, p.2297], to be the models that satisfy Eq.(3.72). In this thesis, we consider these models.

Models that also satisfy Eq.(3.73) are transitively self-similar, i.e. they admit a H_4 acting transitively on spacetime. The corresponding models appear as the equilibrium points of the three dimensional ODE considered later.

We recall from Chapter 2 that $\mathbf{e}_1$ is hypersurface orthogonal. We label the family of timelike hypersurfaces to which $\mathbf{e}_1$ is orthogonal by $\mathcal{H}(x)$. The tangent spaces to $\mathcal{H}(x)$ are spanned by $\{\mathbf{e}_0, \mathbf{e}_2, \mathbf{e}_3\}$ or equivalently by $\{\boldsymbol{\xi}, \boldsymbol{\eta}, \mathbf{u}\}$. Since we have $\boldsymbol{\partial}_0(\mathbf{W}) = \boldsymbol{\partial}_2(\mathbf{W}) = \boldsymbol{\partial}_3(\mathbf{W}) = \mathbf{0}$, it follows that the dimensionless variables do not change on these hypersurfaces $\mathcal{H}(x)$, that is $\mathbf{W} = \mathbf{W}(x)$. In Proposition 1, we characterize the spatially inhomogeneous dynamical equilibrium states as self-similar spacetimes for which the hypersurfaces $\mathcal{H}$ are the orbits of a similarity group H_3. In the proposition below, by maximal we mean that there does not exist an H_n with $n \geq 4$.

Proposition 1. *A G_2 cosmology is a spatially inhomogeneous dynamical equilibrium state if and only if the spacetime is self-similar, admitting a maximal H_3 acting on the hypersurfaces generated by the KVFs and the fluid 4-velocity.*

The proof of the result is identical to the proof in [20, p. 2307] for orthogonally transitive G_2 models that admit a maximal H_3 similarity group.

Since the fluid is tangential to the H_3 orbits, we refer to these models as the *Parallel Self-Similar Cosmologies*. In this thesis, we examine the *Exceptional Parallel Self-Similar* cosmologies by which we mean cosmological models which admit a H_3 acting on timelike hypersurfaces to which the fluid flow is tangential and there is an Abelian G_2 subgroup consisting of one HO KVF.

Let us now review a possible scenario where the H_3 can degenerate into a G_3. In the proof of proposition 1 in [20, p.2307], a variable t is defined as $t = \frac{1}{\theta}$. It may be shown that the H_3 can degenerate into a G_3 if and only if t is functionally dependent on x [20, p. 2306]. This implies that $\theta = \theta(x)$, and as a consequence $\mathbf{e}_0(\theta) = 0$. This means that the physical variables are constant in the G_3 orbits. So θ does not change in the direction of the fluid 4-velocity and hence the model does not possess evolution. Thus, such models

are not cosmological models. From the proof of proposition 1, [20, p. 2307], we also have $q = -1$ and $r = 0$. However, if $q = -1$, from Eq.(3.59) and $\boldsymbol{\partial}_0\Omega = 0$, we have that $\gamma = 0$, which implies that the cosmological fluid has negative pressure (for positive energy density). We do not consider such models in this thesis.

The condition $\boldsymbol{\partial}_0\mathbf{W} = 0$ reduces the system of PDEs to a 1-parameter, three dimensional, system of ODEs as we now develop. From the evolution of $\dot{U}$ in Eq.(3.53), we have

$$3\dot{U} - r = 0. \tag{3.74}$$

For models with positive energy density, it follows from Eq.(3.59) that

$$q = \frac{1}{2}(3\gamma - 2). \tag{3.75}$$

From Eq.(3.72), Σ_+ is

$$\Sigma_+ = -\frac{1}{4}(3\gamma - 2). \tag{3.76}$$

From Eq.(3.50), we have that

$$q = 2 - 3(\Sigma_-) + 3(\Sigma_+). \tag{3.77}$$

Therefore, Σ_- is

$$\Sigma_- = -\frac{1}{4}(5\gamma - 6). \tag{3.78}$$

From Eq.(3.54) we have

$$r = \frac{A(3\gamma - 2) - 3(6 - 5\gamma)N_\times}{2 - \gamma}. \tag{3.79}$$

And from Eq.(3.74) we have

$$\dot{U} = \frac{A(3\gamma - 2) - 3(6 - 5\gamma)N_\times}{3(2 - \gamma)}. \tag{3.80}$$

From Eq.(3.49), Eq.(3.74), Eq.(3.76), and Eq.(3.78), we have

$$\boldsymbol{\partial}_1 N_\times = -\frac{3}{8}(6 - 5\gamma)(2 - \gamma) - 3(\Sigma_{13})^2 + 2AN_\times.$$

From Eq.(3.74) and Eq.(3.57), we obtain

$$\boldsymbol{\partial}_1(\Sigma_{13}) = 3(A + \dot{U} - N_\times)\Sigma_{13}.$$

And finally, using Eq.(3.48), Eq.(3.55), and Eq.(3.56) we get

$$\boldsymbol{\partial}_1 A = 2A^2 - \frac{9(2-\gamma)^2}{8} + \frac{3}{2}(2-\gamma)\Omega + 9(\Sigma_{13})^2.$$

We then have the following 1-parameter, three dimensional, system of ODEs in dimensionless form:

$$\boldsymbol{\partial}_1 A = 2A^2 - \frac{9(2-\gamma)^2}{8} + \frac{3}{2}(2-\gamma)\Omega + 9(\Sigma_{13})^2, \tag{3.81}$$

$$\boldsymbol{\partial}_1(N_\times) = 2AN_\times - 3\Sigma_{13}^2 - \frac{3}{8}(2-\gamma)(6-5\gamma), \tag{3.82}$$

$$\boldsymbol{\partial}_1(\Sigma_{13}) = 3\Big(A + \dot{U} - N_\times\Big)\Sigma_{13}, \tag{3.83}$$

The defining equation for Ω is

$$\Omega = \frac{1}{3(\gamma-1)}\Big[9(\Sigma_{13})^2 + 9(3-2\gamma)(\gamma-1) - 9(N_\times)^2 + \frac{(6-7\gamma)}{(2-\gamma)}A^2 + \frac{6(6-5\gamma)}{(2-\gamma)}AN_\times\Big], \tag{3.84}$$

while the auxiliary equation is

$$\boldsymbol{\partial}_1(\Omega) = 3\Omega\dot{U}\Big(\frac{2-\gamma}{1-\gamma}\Big). \tag{3.85}$$

Note that the dimensionless shear Σ defined by $\Sigma = 3\frac{\sigma^2}{\theta^2}$ is equal to

$$\Sigma_+^2 + 3\Sigma_-^2 + 3\Sigma_{13}^2, \tag{3.86}$$

and for these models we have

$$\Sigma = \frac{1}{4}(21\gamma^2 - 48\gamma + 28) + 3\Sigma_{13}^2. \tag{3.87}$$

Σ takes its minimum value of $\frac{1}{7} \approx 0.1428$ when $\gamma = \frac{8}{7}$ and $\Sigma_{13} = 0$.

3.4 Compactification, Symmetries & Invariant Sets

The ODEs in Eq.(3.81)-(3.84) govern the cosmological models with self-similar spacetimes that admit an abelian G_2 subgroup with at least one HO KVF. In the papers of Hewitt, Wainwright, and Goode [23] and Hewitt, Wainwright, and Glaum [22], the models with two HO KVFs were examined. To aid with the comparison of these models with those in the work of Hewitt, Wainwright, and Goode (HWG) [23], we introduce the intermediate variables

$$T := \frac{4}{\sqrt{2-\gamma}}\Sigma_{13}, \quad U := \frac{4}{3(2-\gamma)}A, \quad V := -4N_{\times} + \frac{4(6-5\gamma)}{3(2-\gamma)}A. \tag{3.88}$$

If we set $T = 0$ then we recover some of the models in (HWG) [23]. We also define the differential operator

$$\frac{d}{dX} := \frac{8(\gamma-1)}{3}\boldsymbol{\partial}_1. \tag{3.89}$$

The EFEs in Eq.(3.81)-(3.83) then reduce to

$$\frac{dU}{dX} = 4(10-7\gamma)(\gamma-1)(1-U^2) - V^2 + \gamma T^2, \tag{3.90}$$

$$\frac{dV}{dX} = (6-5\gamma)\Big(16(\gamma-1)(3-2\gamma)(1-U^2) - V^2\Big) + 4(\gamma-1)(2-\gamma)UV + (12\gamma - 4 - 7\gamma^2)T^2, \tag{3.91}$$

$$\frac{dT}{dX} = \frac{4(\gamma-1)}{(2-\gamma)}\Big(\ (-20+36\gamma-15\gamma^2)U + (4-3\gamma)V\ \Big)\ T. \tag{3.92}$$

The defining equation for Ω takes the form

$$\Omega = \frac{3}{16(\gamma-1)}\Big[16(3-2\gamma)(\gamma-1)[1-U^2] - V^2 + (2-\gamma)T^2\Big], \tag{3.93}$$

while the auxiliary equation becomes

$$\frac{d\Omega}{dX} = 2\Omega\Big[(5\gamma-6)V + 4(7\gamma-10)(\gamma-1)U\Big]. \tag{3.94}$$

The ODEs satisfy the discrete symmetries

$$(X, U, V, T) \mapsto (X, U, V, -T), \tag{3.95}$$

$$(X, U, V, T) \mapsto (-X, -U, -V, T). \tag{3.96}$$

As a consequence of the first symmetry, it suffices to consider the region of phase space where $T \geq 0$.

We have two invariant sets

- $T = 0$, the models admitting two hypersurface orthogonal KVFs studied previously in (HWG), and

- $\Omega = 0$, the vacuum boundary.

Due to Eq.(3.50) in the PDEs and Eq.(3.72), we have

$$0 = \Sigma_{13}\Big[\Sigma_- + \frac{1}{4}(5\gamma - 6)\Big]. \tag{3.97}$$

In this thesis, Σ_{13} is nonzero. so $\Sigma_- = -\frac{1}{4}(5\gamma - 6)$.
If we set $T = 0$, we have $\Sigma_{13} = 0$, and we obtain a subset of models analyzed in HWG [23] and [22]. In [23, 22], there are two free parameters γ and r(not the same r defined in this thesis). Let $s^2 = (2-\gamma)(3\gamma - 2)$, the variable Σ_- in [23] is

$$\Sigma_- = \frac{rs}{4}. \tag{3.98}$$

The models considered in [23] have the restriction $0 \leq r^2 < \frac{(7\gamma-6)}{(3\gamma-2)}$[23, p.1320], for our models this restriction becomes $16(\gamma-1)(3-2\gamma) > 0$. Thus, we only consider $1 < \gamma < \frac{3}{2}$. The models in [22] are already restricted by $rs = (3\gamma - 2)$, and since we do not consider models with $\gamma = 1$ or $\gamma = 2$, we do not obtain any of the models in [22].

The vacuum boundary, or the set in the phase space corresponding to $\Omega = 0$, is given by

$$1 = \frac{16(3-2\gamma)(\gamma-1)U^2}{(2-\gamma)T^2 + 16(3-2\gamma)(\gamma-1)} + \frac{V^2}{(2-\gamma)T^2 + 16(3-2\gamma)(\gamma-1)}.$$

The diagram in Fig 3.1 represents the phase space with the vacuum boundary. As the diagram illustrates, the vacuum boundary is not bounded when we use the variables U, V, and T. Hence the dimensionless variables have no bounds and it is difficult to identify cosmological models that do not have divergent dimensionless variables in this phase space.

Figure 3.1: Phase space with the hyperboloid vacuum boundary

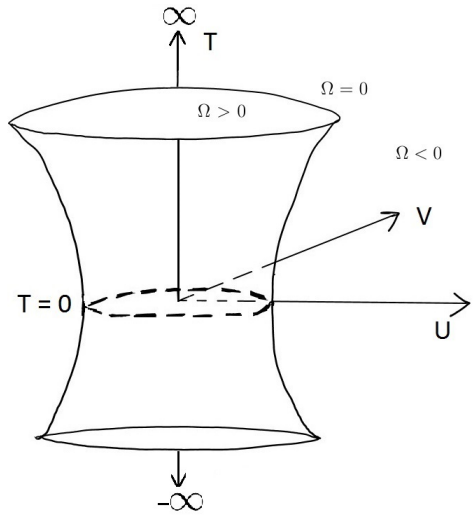

To facilitate our work, we introduce another change of variables to compactify the phase space.
Prior to introducing the variables, let

$$D := 1 + \frac{2-\gamma}{16(\gamma-1)(3-2\gamma)}T^2. \tag{3.99}$$

From Eq.(3.93), note that we obtain

$$D = \frac{1}{16(\gamma-1)(3-2\gamma)}\Big[\frac{16(\gamma-1)}{3}\Omega + V^2 + 16(\gamma-1)(3-2\gamma)U^2\Big], \tag{3.100}$$

with $D \geq 1$ in the physical region of phase space. Let

$$S := \frac{1}{\sqrt{D}}, \quad \frac{d}{d\chi} := S\frac{d}{dX}. \tag{3.101}$$

The coordinate transformations that compactify the vacuum boundary, as well as the physical region of phase space, are

$$Y_1 := US,\ Y_2 := VS,\ Y_3 := TS,\ Y_4 := \Omega S^2. \tag{3.102}$$

The transformed ODEs of Eq.(3.90), Eq.(3.91), and Eq.(3.92) are:

$$\frac{dY_1}{d\chi} = \frac{4(1-S^2)(\gamma-1)}{(2-\gamma)}[4\gamma(3-2\gamma) - Y_1 L] + 4(10-7\gamma)(\gamma-1)\ (S^2 - Y_1^2) - Y_2^2, \quad (3.103)$$

$$\frac{dY_2}{d\chi} = \frac{4(1-S^2)(\gamma-1)}{(2-\gamma)}\ [4(12\gamma - 4 - 7\gamma^2)(3-2\gamma) - Y_2 L] + 4(\gamma-1)(2-\gamma)Y_1 Y_2 + (6-5\gamma)\ [16(\gamma-1)(3-2\gamma)(S^2 - Y_1^2) - Y_2^2], \quad (3.104)$$

$$\frac{dS}{d\chi} = -\frac{4S(1-S^2)(\gamma-1)L}{(2-\gamma)}. \quad (3.105)$$

where $L = (-20 + 36\gamma - 15\gamma^2)Y_1 + (4-3\gamma)Y_2$. In addition, the equation for the scaled energy density Y_4 and the auxiliary equation, respectively, are

$$Y_4 = \frac{3}{16(\gamma-1)}\Big[(3-2\gamma)(\gamma-1)(1-Y_1^2) - Y_2^2\Big], \quad (3.106)$$

$$\frac{dY_4}{d\chi} = 2Y_4\Big[(5\gamma-6)Y_2 + 4(7\gamma-10)(\gamma-1)Y_1 - \frac{4(1-S^2)(\gamma-1)L}{(2-\gamma)}\Big]. \quad (3.107)$$

Note that an equation for Y_3 is not required since the variable S has replaced the information in Σ_{13} and T. The system possesses the discrete symmetries

$$\begin{aligned}(\chi, Y_1, Y_2, S) &\mapsto (\chi, Y_1, Y_2, -S),\\ (\chi, Y_1, Y_2, S) &\mapsto (-\chi, -Y_1, -Y_2, S).\end{aligned} \quad (3.108)$$

Due to these symmetries, we consider the physical region of phase space where $S \geq 0$. Since, from Eq.(3.102), $Y_4 = 0 \Leftrightarrow \Omega = 0$, the equation for the vacuum boundary in this coordinate system is

$$1 = Y_1^2 + \frac{Y_2^2}{16(\gamma-1)(3-2\gamma)}. \quad (3.109)$$

Fig 3.2 illustrates the phase space. From the coordinate transformations in Eq.(3.102), it is evident that as $T \to \infty,\ S \to 0$.
If $\Sigma_{13} = 0$, then $T = 0$, which implies $S = 1$. Thus when $S = 1$, the three dimensional system of ODEs turn into a two dimensional system corresponding to the case where there exists two HO KVFs [23]. The vacuum boundary is now compact and the bottom of the elliptical cylinder, $S = 0$, corresponds to infinities in the previous phase space.
We conclude that we have three invariant sets

Figure 3.2: Compactified Phase Space

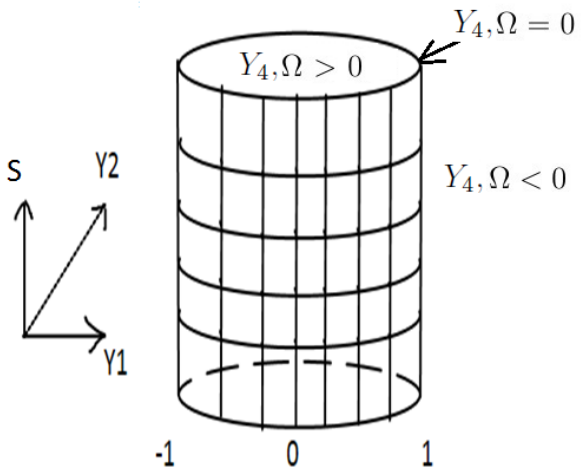

- $S = 1$ models admitting two hypersurface orthogonal KVFs [23],
- $Y_4 = 0$ the vacuum boundary, and
- $S = 0$ infinities.

The solutions that tend to the plane $S = 0$ have dimensionless variables that tend to infinity. In Chapter 6, we show that the basic physical variables also tend to infinity for the solutions with $\Omega > 0$ or $Y_4 > 0$. So, the models with $Y_4 > 0$ (perfect fluid models) that tend to $S = 0$ are called *badly-behaved cosmological models* and the models that do not are called *well-behaved cosmological models*.
Since our aim is to look for well-behaved cosmological models, we seek solution curves that do not approach the bottom of the elliptical cylinder.

Chapter 4

Qualitative Analysis

In this chapter, we commence a qualitative analysis of the 1-parameter, three dimensional system of ODEs in Eq.(3.103)-(3.105). We show that there exist open sets of well-behaved models for certain ranges of the equation state parameter γ. We also analyze the asymptotic behaviour of such solutions.

4.1 Equilibrium Points & The Eigenvalues of The Linearization Matrix

The equilibrium points are found by using Eq.(3.103)-(3.105) and Eq.(3.107). These equations are solved in cases and illustrated in Table 4.1. The case $S = 0$, $Y_4 < 0$ (negative energy density) is not included in the table.

The equilibrium points are transitively self-similar cosmological models. They admit a H_4, which possess a H_3 subgroup. The H_3 has an abelian G_2 subgroup and the fluid is tangential to the H_3 orbits.
Let

$$
\begin{aligned}
Q_1(\gamma) &:= -63\gamma^2 + 156\gamma - 92, \\
Q_2(\gamma) &:= -15\gamma^2 + 36\gamma - 20, \\
Q_3(\gamma) &:= -193\,\gamma^2 + 412\,\gamma - 196, \\
Q_4(\gamma) &:= -171\gamma^2 + 408\gamma - 224.
\end{aligned}
$$

Figure 4.1: The three dimensional phase space for $\gamma = 1.09$. The equilibrium points $\mathrm{RT}^{\pm}$, $\mathrm{LK}^{\pm}$, and $\mathrm{INF}^{\pm}$ are on the boundary (vacuum). The Collins equilibrium points are located in the interior of the top of the cylinder.

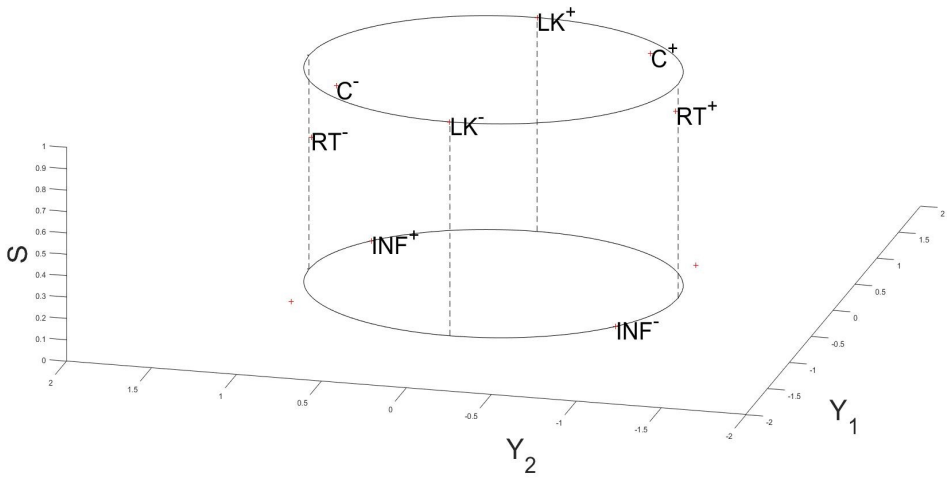

For $\gamma \in (1, \frac{3}{2})$, all the quadratics above are positive except for Q_3 which has a root $r_t = \frac{206}{193} + \frac{48\sqrt{2}}{193} \approx 1.42$, Q_3 is positive for $\gamma \in [1, r_t)$ and it is negative for $\gamma \in (r_t, \frac{3}{2})$.

Table 4.1: The table of equilibrium points for the three dimensional system

Equilibrium Point (label)	S^2	Y_1^2	Y_2	Y_4
Unphysical (INF)	0	$\frac{4(3-2\gamma)(\gamma-1)}{(\gamma-2)^2}$	$2(4-3\gamma)Y_1$	$Y_4 = 0$
Collins VI_h (C)	1	$\frac{(6-5\gamma)^2}{(3\gamma-2)(2-\gamma)}$	$-4\frac{(10-7\gamma)(\gamma-1)}{(6-5\gamma)}Y_1$	$\frac{3(10-7\gamma)(\gamma-1)}{(3\gamma-2)}$
Plane Waves (LK)	1	1	0	0
Robinson–Trautman (RT)	$\frac{24(\gamma-1)(3-2\gamma)}{Q_1(\gamma)}$	$\frac{16(\gamma-1)(4-3\gamma)^2(3-2\gamma)}{Q_1(\gamma)(2-\gamma)^2}$	$-\frac{Q_2(\gamma)}{(4-3\gamma)}Y_1$	0
Wainwright ($\gamma = \frac{10}{9}$) (W)	$\frac{7}{3} - 8Y_1^2$	$\frac{1}{6} \leq Y_1^2 \leq \frac{7}{32}$	$-\frac{20}{9}Y_1$	$\frac{7}{3} - \frac{32}{3}Y_1^2$

As it is seen from Table 4.1 one of the equilibrium points is unphysical since it has $S = 0$. The equilibrium points labeled as Wainwright only occur when $\gamma = \frac{10}{9}$ and are analyzed separately in Chapter 5. The LK equilibrium points have fixed coordinates. The other equilibrium points vary with γ. Fig 4.1 illustrates the phase space with equilibrium points in the range $1 < \gamma < \frac{10}{9}$.

In order to reveal the stability of each equilibrium point, the eigenvalues of the linearization matrix computed at the equilibrium point is obtained. The sign of the eigenvalues indicate the local stability of the equilibrium point. Table 4.2 summarizes the eigenvalues of the linearization matrix for each equilibrium point. Note that $\sqrt{-Q_3(\gamma)}$ in the eigenvalue of C equilibrium points is imaginary in the interval $(1, r_t)$, so it does not contribute to $\Re(\lambda_2)$ and $\Re(\lambda_3)$; otherwise for $(r_t, \frac{3}{2})$ the eigenvalues are real.

Equilibrium Point	The eigenvalues of the linearization matrix
$\mathrm{INF}^{\pm}$	$\lambda_1 = \mp 24\,(\gamma-1)^{\frac{3}{2}}\sqrt{3-2\,\gamma}$ $\lambda_2 = \mp(16)(\gamma-1)^{\frac{3}{2}}\sqrt{3-2\gamma}$ $\lambda_3 = \mp 8(5\gamma-4)\sqrt{(\gamma-1)(3-2\gamma)}$
$\mathrm{C}^{\pm}$	$\lambda_1 = \pm\frac{8\sqrt{2-\gamma}(\gamma-1)(10-9\gamma)}{\sqrt{3\,\gamma-2}}$ $\lambda_2 = \pm 2\,\frac{\sqrt{(2-\gamma)}(\gamma-1)\left(6-5\,\gamma+\sqrt{-Q_3(\gamma)}\right)}{\sqrt{3\,\gamma-2}}$ $\lambda_3 = \pm 2\,\frac{\sqrt{(2-\gamma)}(\gamma-1)\left(6-5\,\gamma-\sqrt{-Q_3(\gamma)}\right)}{\sqrt{3\,\gamma-2}}$
$\mathrm{LK}^{\pm}$	$\lambda_1 = \pm 8\,(\gamma-1)(7\,\gamma-10)$ $\lambda_2 = \pm 4\,(\gamma-1)(2-\gamma)$ $\lambda_3 = \pm 8\,\frac{(\gamma-1)Q_2(\gamma)}{(2-\gamma)}$
$\mathrm{RT}^{\pm}$	$\lambda_1 = \pm\frac{8(2-\gamma)\sqrt{\gamma-1}\sqrt{3-2\gamma}(10-9\gamma)}{\sqrt{Q_1(\gamma)}}$ $\lambda_2 = \pm\frac{8(\gamma-1)^{\frac{3}{2}}\sqrt{3-2\gamma}\left(4-3\gamma-\sqrt{Q_4(\gamma)}\right)}{\sqrt{Q_1(\gamma)}}$ $\lambda_3 = \pm\frac{8(\gamma-1)^{\frac{3}{2}}\sqrt{3-2\gamma}\left(4-3\gamma+\sqrt{Q_4(\gamma)}\right)}{\sqrt{Q_1(\gamma)}}$
Wainwright $(\gamma = \frac{10}{9})$	$\lambda_1 = 0$ $\lambda_2 = \frac{16}{81}\,Y_1 \mp \frac{16}{81}\sqrt{533Y_1^2-112}$ $\lambda_3 = \frac{16}{81}\,Y_1 \pm \frac{16}{81}\sqrt{533Y_1^2-112}$

Table 4.2: The table of eigenvalues of the linearization matrix when $\mathrm{Sign}(Y_1) = \pm 1$.

From Table 4.2, we deduce that the following regimes for γ must be analyzed

$$1<\gamma<\frac{10}{9},\quad \frac{10}{9}<\gamma<\frac{6}{5},\quad \frac{6}{5}<\gamma<\frac{10}{7},\quad \frac{10}{7}<\gamma<\frac{3}{2}. \tag{4.1}$$

The list of the signs of the eigenvalues for each equilibrium point in the corresponding regions is presented in Table 4.3.

Table 4.3: Signs of the real parts of the eigenvalues.

Equilibrium Point	$1<\gamma<\frac{10}{9}$	$\frac{10}{9}<\gamma<\frac{6}{5}$	$\frac{6}{5}<\gamma<\frac{10}{7}$	$\frac{10}{7}<\gamma<\frac{3}{2}$
$\mathrm{INF}^{\pm}$	$\mp\mp\mp$			
$\mathrm{C}^{\pm}$	$\pm\pm\pm$	$\mp\pm\pm$	$\mp\mp\mp$	$Y_4<0$ (Unphysical)
$\mathrm{LK}^{\pm}$	$\mp\pm\pm$			$\pm\pm\pm$
$\mathrm{RT}^{\pm}$	$\pm\pm\mp$	$\mp\pm\mp$		

4.2 The Invariant Sets & Analysis of The Vacuum Models

From Chapter 3, we know that the invariant set $S=1$ corresponds to the work of HWG in [23], where the models admit at least two HO KVFs. Due to the fact that we refer to the phase portraits on this two dimensional invariant set to prove the existence of an open set of exceptional models with at least 1 HO KVF, in three dimensions, we advise the reader to keep in mind the phase portraits given in [23, p.1320-1321].

On the invariant set $S=0$, there exists only two equilibrium points; namely INF^{+} and INF^{-}. The phase portraits in this case are given in Fig 5.9.

We now analyze the vacuum boundary. Remark that the solutions on the vacuum boundary are restricted by $Y_4=0$ ($\Omega=0$), which is an invariant set. We analyze the vacuum boundary by unfolding it according to Fig 4.2. The solution curves confined to

Figure 4.2: Unfolding the Vacuum Boundary ($1 = Y_1^2 + \frac{Y_2^2}{16(\gamma-1)(3-2\gamma)}$, on S vs. Y_1)

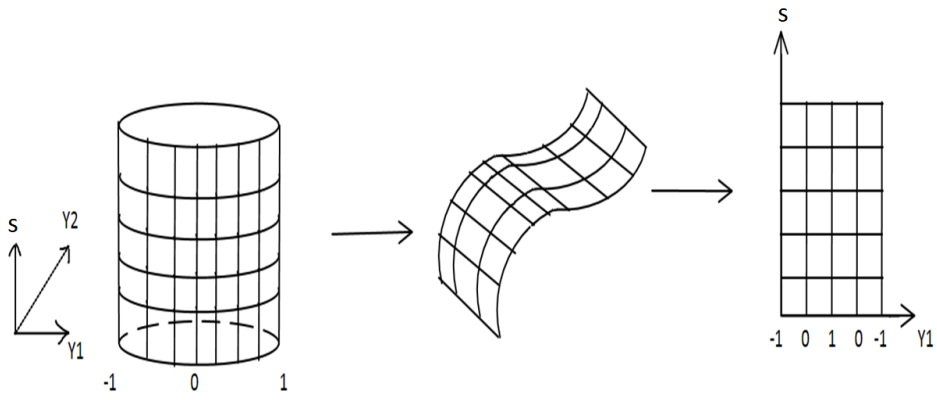

the unfolded two dimensional vacuum boundary must satisfy

$$\frac{dY_1}{d\chi} = \frac{4(S^2-1)(\gamma-1)}{(2-\gamma)}\left[Y_1 L - 4\gamma(3-2\gamma)\right] + 4(10-7\gamma)(\gamma-1)\,(S^2-Y_1^2) - Y_2^2, \tag{4.2}$$

$$\frac{dS}{d\chi} = \frac{4S(S^2-1)(\gamma-1)L}{(2-\gamma)}, \tag{4.3}$$

$$1 = Y_1^2 + \frac{Y_2^2}{16(\gamma-1)(3-2\gamma)}. \tag{4.4}$$

The eigenvalue λ_1 of each equilibrium point reveals the stability of that equilibrium point relative to the fluid. The other two eigenvalues, λ_2 and λ_3, reveal the stability of these equilibrium points in the vacuum boundary.

The equilibrium points are listed in Table 4.4.

Table 4.4: Equilibrium points on the vacuum boundary

Type of Solution	S^2	Y_1
$\text{INF}^{\pm}$	0	$\pm\frac{\sqrt{4(3-2\gamma)(\gamma-1)}}{(\gamma-2)}$
$\text{LK}^{\pm}$	1	± 1
$\text{RT}^{\pm}$	$24\frac{(\gamma-1)(3-2\gamma)}{Q_1(\gamma)}$	$\pm\frac{(4-3\gamma)}{(2-\gamma)}\sqrt{\frac{16(\gamma-1)(3-2\gamma)}{Q_1(\gamma)}}$

Table 4.5: Signs of the eigenvalues for the vacuum boundary

Equilibrium Point	$1 < \gamma < \frac{3}{2}$
$\text{INF}^{\pm}$	$\mp\mp$
$\text{LK}^{\pm}$	$\pm\pm$
$\text{RT}^{\pm}$	$\mp\pm$

We now explain how to obtain the equations for the isoclines corresponding to $\frac{dS}{d\chi} = 0$ and $\frac{dY_1}{d\chi} = 0$ in the vacuum boundary. In the direction of the flow, the sign of Eq.(3.105), which we restate below,

$$\frac{dS}{d\chi} = \frac{4S(S^2-1)(\gamma-1)L}{(2-\gamma)}, \tag{4.5}$$

indicates how the solution curves increase or decrease in the variable S. We know that the range for γ is $1 < \gamma < \frac{3}{2}$. So

$$\frac{(\gamma-1)}{(2-\gamma)} > 0. \tag{4.6}$$

In addition, we know that $0 \leq S \leq 1$, so

$$\frac{4S(S^2-1)(\gamma-1)}{(2-\gamma)} \leq 0. \tag{4.7}$$

Therefore, the change in the sign of $\frac{dS}{d\chi}$ depends on the change in the sign of L. Recall that

$$L = (-20 + 36\gamma - 15\gamma^2)Y_1 + (4 - 3\gamma)Y_2, \tag{4.8}$$

so L changes sign when the solution curves pass though the plane

$$Y_1 = \frac{3\gamma - 4}{Q_2} Y_2. \tag{4.9}$$

On the vacuum boundary,

$$Y_2 = \pm\sqrt{16(\gamma-1)(3-2\gamma)(1-Y_1^2)}. \tag{4.10}$$

The plane at which the change of sign of $\frac{dS}{d\chi}$ occurs is a line in the unfolded vacuum boundary. By substituting Eq.(4.10) into Eq.(4.9), and solving for Y_1, we get that the isocline corresponding to $\frac{dS}{d\chi} = 0$ has the equation

$$Y_1 = \pm \frac{4\sqrt{(\gamma-1)(3-2\gamma)}(3\gamma-4)}{\sqrt{Q_2 + 16(\gamma-1)(3-2\gamma)(3\gamma-4)^2}}. \tag{4.11}$$

Similarly, we get that the isocline corresponding to $\frac{dY_1}{d\chi} = 0$ has the equation

$$S^2 = \frac{-8(4-3\gamma)|Y_1|\sqrt{(1-Y_1^2)(\gamma-1)(3-2\gamma)} - 16(Y_1^2-1)(\gamma-1)(3-2\gamma)}{8(3\gamma-4)|Y_1|\sqrt{(Y_1^2-1)(1-\gamma)(3-2\gamma)} + 2(Y_1^2-1)Q_2(\gamma)}, \tag{4.12}$$

and we illustrate this isocline by the curved dashed line in Fig 4.3.

From Table 4.5, we know that the local stability of each equilibrium point does not change in ranges of γ. We know the solutions that tend to $S = 0$ have dimensionless variables that tend to infinity. By using the information about the isoclines, separatrices, and the invariant set $S = 1$, we illustrate the well-behaved numerical solutions in Fig 4.3. Each solution curve represents a cosmological model (a solution to the EFEs).

We state a theorem below which is sometimes referred to as *the approximation property of orbits* [46, p.104]

Theorem 4.2.1. *Let ϕ_t be a flow on $\mathbb{R}^n$. For all $\mathbf{x}_1 \in \mathbb{R}^n$, for all $T > 0$ and for all $\varepsilon > 0$, there exists a $\delta > 0$ such that for all $\mathbf{x}_2$ and $t \in \mathbb{R}$,*

$$-T \geq t \geq T \quad \textit{and} \quad ||\mathbf{x}_1 - \mathbf{x}_2|| < \delta \quad \Longrightarrow \quad ||\phi_t(\mathbf{x}_1) - \phi_t(\mathbf{x}_2)|| < \varepsilon.$$

Proof. See [40, p.11]. □

Theorem 4.2.2. *For $1 < \gamma < \frac{3}{2}$, there exists an open set of well-behaved vacuum cosmological models that tend to LK^+ as $\chi \longrightarrow -\infty$ and to LK^- as $\chi \longrightarrow \infty$.*

Proof. Throughout this proof, the statements holds for $1 < \gamma < \frac{3}{2}$. From the work of HWG in [23, p.1321], we know that there exist vacuum models that are asymptotic to the $\mathrm{LK}^{\pm}$ equilibrium points; these models are in the invariant set $S = 1$. By the approximation property of orbits or Theorem 4.2.1, there exists an open set of well-behaved vacuum cosmological models that asymptotically tend to LK^+ as $\chi \longrightarrow -\infty$ and to LK^- as $\chi \longrightarrow \infty$. □

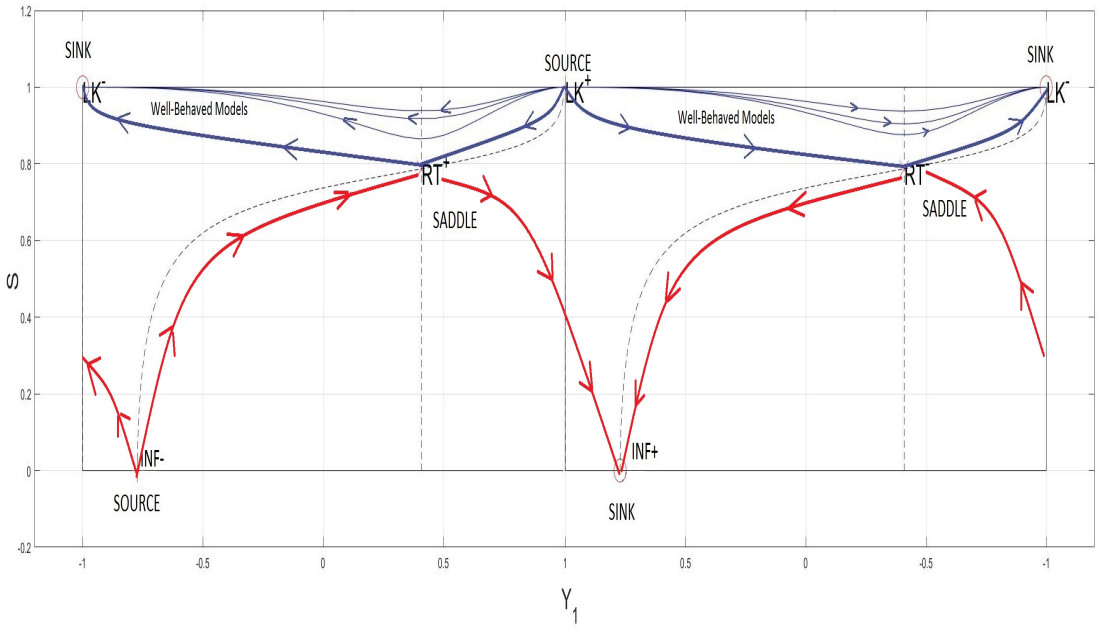

Figure 4.3: Solutions on the vacuum boundary for $\gamma = 1.45$.
The dashed curve represents the isocline $\frac{dY_1}{d\chi} = 0$ and the straight dashed line represents the isocline $\frac{dS}{d\chi} = 0$. The narrow lines with arrows show the solution curves and the direction of the flow. The thicker lines in blue show the well-behaved separatrices and the red lines show separatrices that correspond to solutions that have divergent dimensionless variables at large spatial distance.

We note here that we do not exclude the possibility of an intermediate asymptotic behaviour of the models near the RT equilibrium points. This theorem ultimately implies that there is a non-zero measure for the set made up from the part of the phase space where an initial condition for a well-behaved model is chosen. This is important because if the models are to be created by a random initial condition then there is a nonzero probability that they are well-behaved.

4.3 Analysis of Perfect Fluid Models & The Monotone Function

The existence of an open set of well-behaved perfect fluid models is proven via the existence of solutions in the two invariant sets $Y_4 = 0$ and $S = 1$.

Theorem 4.3.1. *For $1 < \gamma < \frac{10}{9}$, there exists an open set of well-behaved perfect fluid cosmological models that tend to C^+ as $\chi \longrightarrow -\infty$ and to C^- as $\chi \longrightarrow \infty$. And for $\frac{6}{5} < \gamma < \frac{10}{7}$, there exists an open set of well-behaved perfect fluid cosmological models that tend to C^- as $\chi \longrightarrow -\infty$ and to C^+ as $\chi \longrightarrow \infty$.*

Proof. We know that there exist perfect fluid solutions on the invariant set $S = 1$, and that these solutions asymptotically tend to C^+ and C^- as proven by HWG in [23, p.1321]. For $1 < \gamma < \frac{10}{9}$, C^+ is a source and C^- is a sink in three dimensions. By Theorem 4.2.1, there exist an open set of well-behaved perfect fluid solutions that asymptotically tend from C^+ to C^-. The proof is similar for the range $\frac{6}{5} < \gamma < \frac{10}{7}$, since in that case C^- is a source and C^+ is sink in three dimensions. □

Figure 4.4: Three dimensional phase portraits, C^+ to C^-.

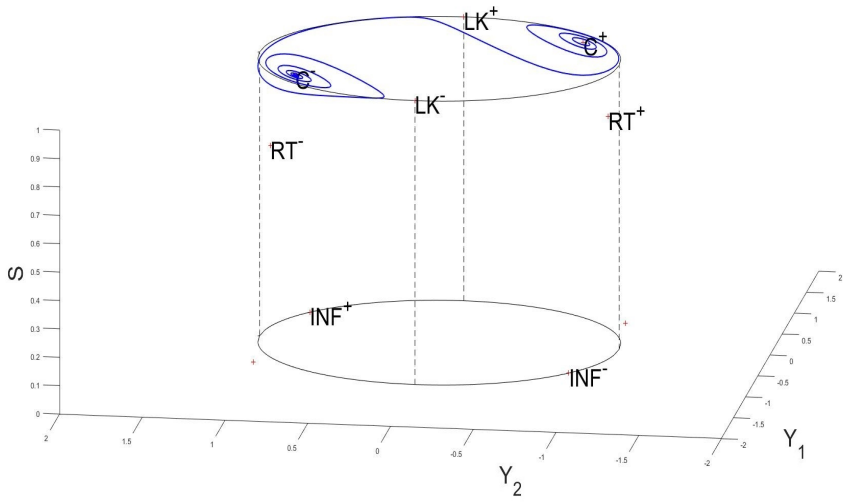

Figure 4.5: Three dimensional phase portraits (top view), C^+ to C^-.

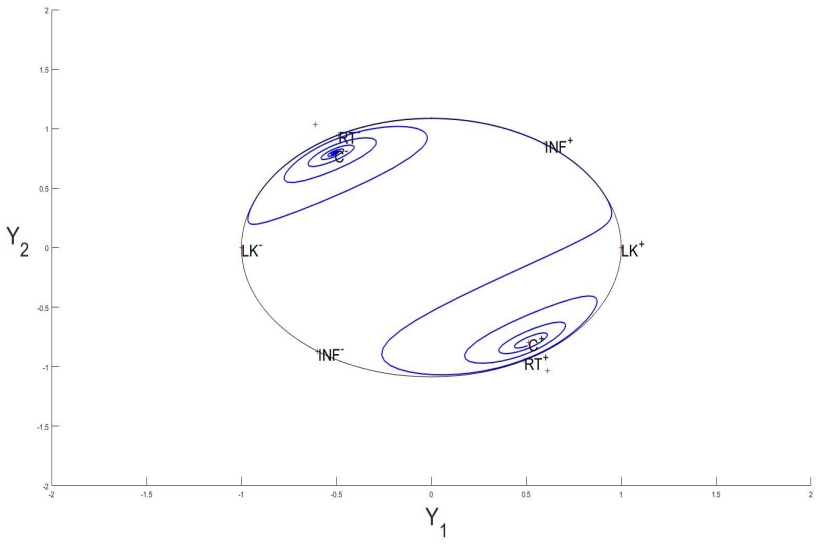

Figure 4.6: Three dimensional phase portraits (side view), C^+ to C^-.

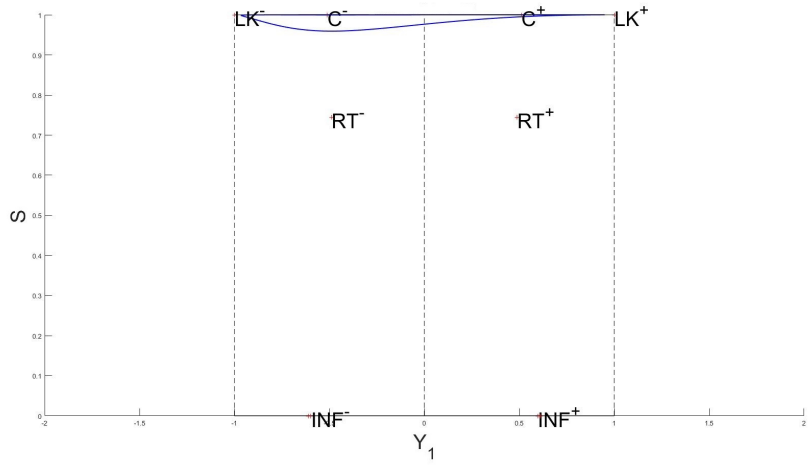

A typical solution of this type is given in Fig 4.4. The behaviour of the dimensionless energy density Ω in terms of the spatial parameter χ is of our interest. Given a numerical

Figure 4.7: Ω vs. χ for the solution in Fig 4.4.

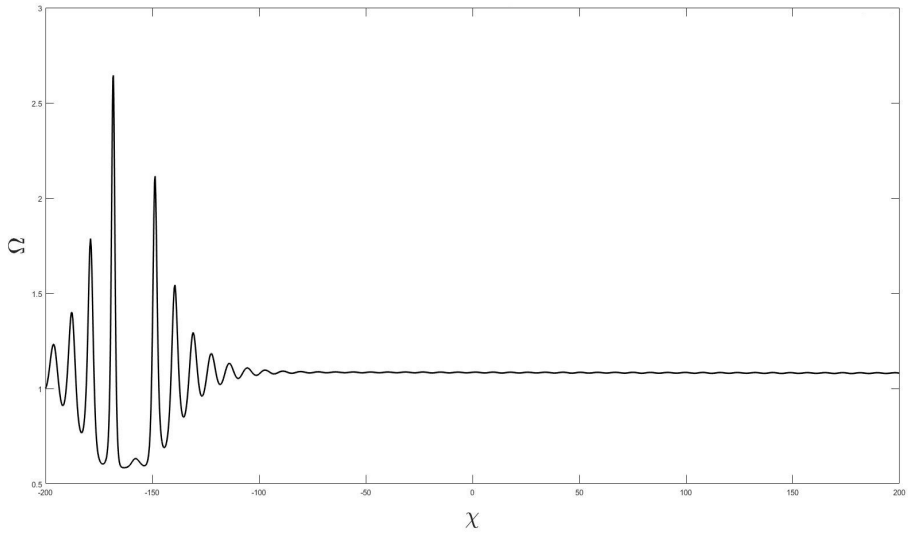

solution with coordinates (Y_1, Y_2, S, Y_4), we use Eq.(3.102) to get

$$\Omega(\chi) = \frac{Y_4(\chi)}{S^2(\chi)}. \tag{4.13}$$

Fig 4.7 illustrates $\Omega(\chi)$ for the solution in Fig 4.4.

Theorem 4.3.2. *For $\frac{10}{7} < \gamma < \frac{3}{2}$, there exists an open set of well-behaved perfect fluid cosmological models that tend to* LK^+ *as $\chi \longrightarrow -\infty$ and to* LK^- *as $\chi \longrightarrow \infty$.*

Proof. By Theorem 4.2.2, we have that, for $1 < \gamma < \frac{3}{2}$, there exists an open set of solutions in two dimensions (the vacuum boundary) that tend to LK^+ as $\chi \longrightarrow -\infty$ and to LK^- as $\chi \longrightarrow \infty$. For $\frac{10}{7} < \gamma < \frac{3}{2}$, the equilibrium point LK^+ is a source and LK^- is a sink in three dimensions. By Theorem 4.2.1, there exists an open set of well-behaved perfect fluid solutions that asymptotically tend to LK^+ as $\chi \longrightarrow -\infty$ and to LK^- as $\longrightarrow \infty$. □

A typical solution of this type is given in Fig 4.8. The dimensionless energy density, $\Omega(\chi)$, of the solution in Fig 4.8 is given in Fig 4.9.
Fig 4.6 represents a side view image of the solution curve in Fig 4.4, illustrating that the

Figure 4.8: Three dimensional phase portraits, LK^+ to LK^-.

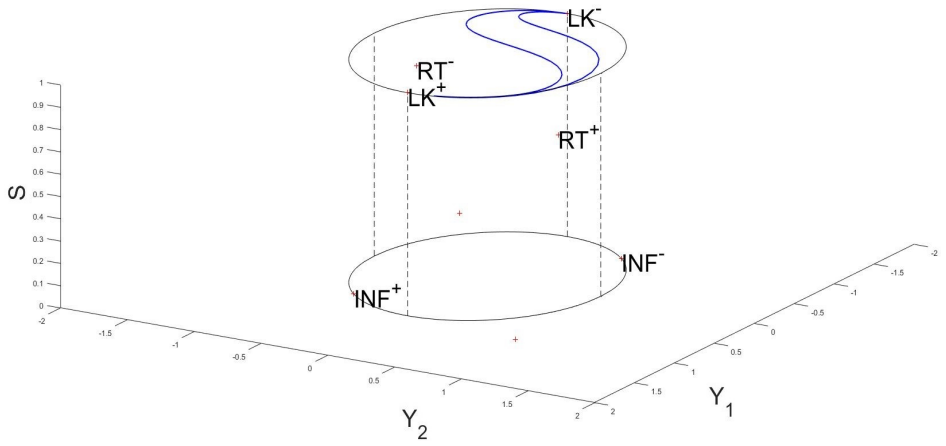

solution curve is not just confined to the top of the elliptical cylinder.
Fig 4.5 represents the top view of Fig 4.4, where the trajectories are mimicking the behaviour of solution curves corresponding to the models with two HO KVFs in the paper by HWG [23, p.1321, Fig 2].

The Monotone Function

Consider the function defined as

$$G := \frac{Y_4^{\frac{81}{40}Q_2(\gamma)}(1-S^2)^{\frac{81}{40}(2-\gamma)(10-7\gamma)}}{S^{\frac{81}{5}\gamma(3-2\gamma)}}. \tag{4.14}$$

The function has been scaled so that the exponents take integer values when $\gamma = \frac{10}{9}$. Note that $Q_2 > 0$ for $1 < \gamma < \frac{3}{2}$, and

$$\frac{dG}{d\chi} = -\frac{81}{20}(10-9\gamma)(2-\gamma)^2 Y_2 G. \tag{4.15}$$

Let β be a positive constant. For any value of γ in $(1, \frac{3}{2})$, the 2-space $G = \beta$ has level curves ($S = constant$) which are ellipses. Fig 4.10 illustrates a representation of these surfaces. Moreover, we define the invariant sets

Figure 4.9: Ω vs. χ, LK^+ to LK^-.

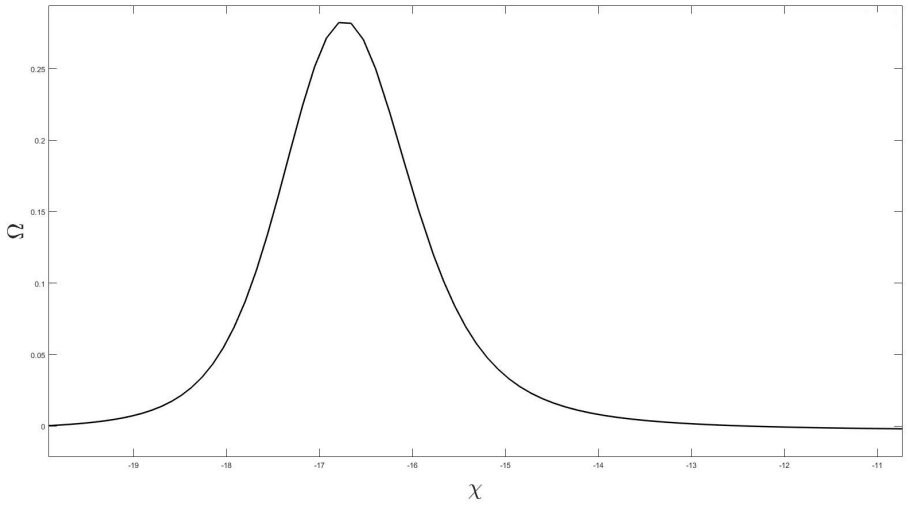

Figure 4.10: The surfaces given by $G = \beta$. The blue surface with plaid pattern describes a larger value of β compared to the gray surfaces.

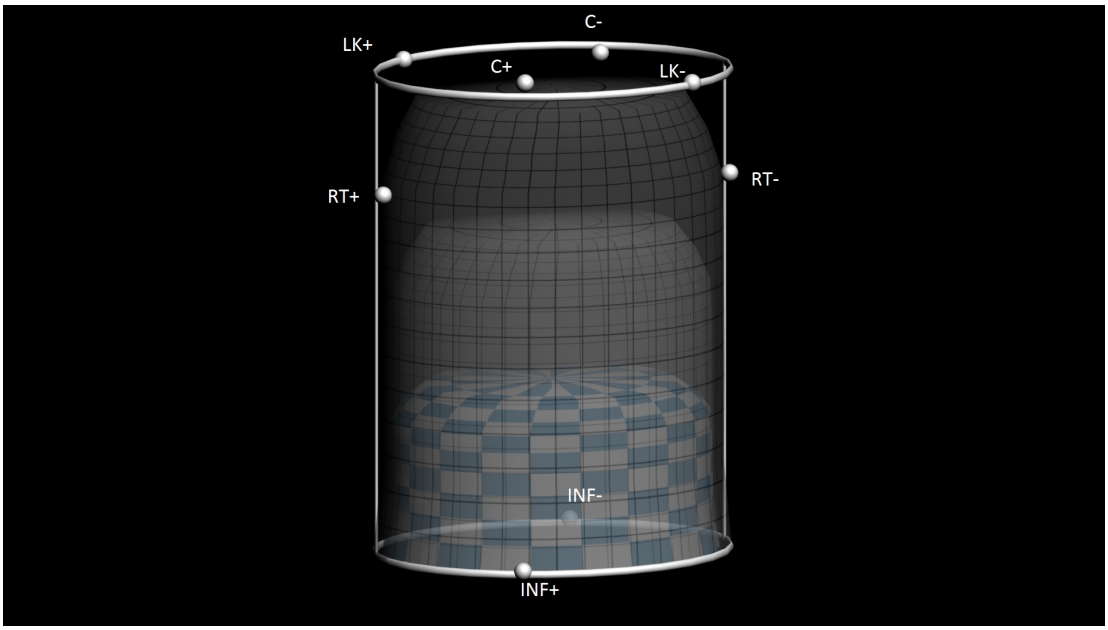

$$Z_+ := \{Y_2, S, Y_4 \in \mathbb{R} \mid 0 < Y_2 < 4\sqrt{(\gamma-1)(3-2\gamma)},\ 0 < S < 1,\ Y_4 > 0\},$$
$$Z_- := \{Y_2, S, Y_4 \in \mathbb{R} \mid 0 > Y_2 > -4\sqrt{(\gamma-1)(3-2\gamma)},\ 0 < S < 1,\ Y_4 > 0\}.$$

these are open sets that consist of the half of the interior of the cylinder when $Y_2 > 0$ (Z_+) and the other half where $Y_2 < 0$ (Z_-). For $1 < \gamma < \frac{6}{5}$, by using Eq.(3.104), we have that the derivative of Y_2, in the direction of the flow, computed at $Y_2 = 0$ is positive. So if $1 < \gamma < \frac{6}{5}$, we have $\frac{dY_2}{d\chi}|_{Y_2=0} > 0$ and Z_+ is a positive invariant set and Z_- is a negative invariant set.
For $\frac{4}{3} < \gamma < \frac{3}{2}$, we have $\frac{dY_2}{d\chi}|_{Y_2=0} < 0$, which means Z_+ is a negative invariant set and Z_- is a positive invariant set for this range. The function $G : Z_+ \longrightarrow \mathbb{R}$ is a C^1 function with range $(0, \infty)$, and for $1 < \gamma < \frac{10}{9}$, G is decreasing in Z_+. Also, the function $G : Z_- \longrightarrow \mathbb{R}$ is a C^1 function with range $(0, \infty)$, and for $\frac{4}{3} < \gamma < \frac{3}{2}$, G is decreasing in Z_-. We use these in what follows. We state the definitions of α and ω-limit sets below.

Let ϕ_t be a flow on $\mathbb{R}^n$, and let $\mathbf{a} \in \mathbb{R}^n$. A point $\mathbf{x} \in \mathbb{R}^n$ is an $\omega-$limit point of $\mathbf{y}$ means there exist a sequence $t_n \longrightarrow +\infty$ such that $\lim_{n\to+\infty} \phi_{t_n}(\mathbf{y}) = \mathbf{x}$. The set of all $\omega-$limit points of $\mathbf{y}$ is called $\omega-$limit set of $\mathbf{y}$ denoted $\omega(\mathbf{y})$. Similarly, the $\alpha-$limit set $\alpha(\mathbf{y})$ is defined using $t_n \longrightarrow -\infty$.

We state the theorem below which is an extended version of what is known as the *Monotonicity Principle* [46, p.103]; the difference is that we consider a positive or negative invariant set.

Theorem 4.3.3. *Let ϕ_t be a flow on $\mathbb{R}^n$ with S be a positive invariant set. Let $G : S \longrightarrow \mathbb{R}$ be a C^1 function whose range is the interval (a,b), where $a \in \mathbb{R} \cup \{-\infty\}$, $b \in \mathbb{R} \cup \{\infty\}$ and $a < b$. If G is increasing on the orbits in S, then for all $\mathbf{x} \in S$*

$$\omega(\mathbf{x}) \subseteq \{\mathbf{s} \in \overline{S} \setminus S | \lim_{\mathbf{y}\to\mathbf{s}} G(\mathbf{y}) \neq a\}.$$

And if S is a negative invariant set and G is decreasing on the orbits in S, then

$$\alpha(\mathbf{x}) \subseteq \{\mathbf{s} \in \overline{S} \setminus S | \lim_{\mathbf{y}\to\mathbf{s}} G(\mathbf{y}) \neq b\}.$$

Proof. See Proposition A1 in [31, p.536]. □

Similar result holds for negative invariant set and $\omega(\mathbf{x}_0)$. We also use the corollary below which follows from Theorem 4.3.3.

Corollary 4.3.3.1. *Let $\{\phi_t\}$ be a flow on $\mathbb{R}^n$. Let S be an open positive invariant set in $\mathbb{R}^n$. Let G be C^1 on S with $\frac{dG}{dt} > 0$ on S. Let $\mathbf{x}_0 \in S$. If $p \in \alpha(\mathbf{x}_0)$ then $p \notin S$.*

Proof. Proof is identical to the proof of Proposition A1 in [31, p.536]. □

By using the results above, as well as the extension to the Poincaré–Bendixon theorem in [18, p.709], we prove the theorems that follow.

Theorem 4.3.4. *For $1 < \gamma < \frac{10}{9}$ and $\frac{4}{3} < \gamma < \frac{10}{7}$, the perfect fluid models exhibit only the following possible asymptotic behaviours:*
For $1 < \gamma < \frac{10}{9}$, they tend to C^+ or INF^- as $\chi \longrightarrow -\infty$ and to C^- or INF^+ as $\chi \longrightarrow \infty$.
For $\frac{4}{3} < \gamma < \frac{10}{7}$, they tend to C^- or INF^- as $\chi \longrightarrow -\infty$ and to C^+ or INF^+ as $\chi \longrightarrow \infty$.

Proof. For $1 < \gamma < \frac{10}{9}$, consider an initial condition in the invariant set Z_+. The function G is decreasing in Z_+ as $\chi \longrightarrow \infty$. By using Theorem 4.3.3 (extension to the Monotonicity Principle) we conclude that the solutions must tend to the boundary of Z_+ as $\chi \longrightarrow \infty$, that is the solutions must tend to $\bar{Z}_+ \setminus Z_+$. By the extension to the Poincaré–Bendixon theorem in [18, p.709], we have that solutions must either tend to C^- or INF^+ as $\chi \longrightarrow \infty$.

As $\chi \longrightarrow -\infty$, by using Corollary 4.3.3.1, the solutions either tend to the boundary of Z_+ or $\bar{Z}_+^c$. Since there are no source equilibrium points on the boundary of Z_+ the solutions must then tend to $\bar{Z}_+^c$. So since the solutions are in Z_-, by using Theorem 4.3.3 (extension to the Monotonicity Principle) and the extension to the Poincaré–Bendixon theorem in [18, p.709], they must tend to INF^- or C^+. And there are no other possibilities. The proof is identical for the case where $\frac{4}{3} < \gamma < \frac{10}{7}$. □

Theorem 4.3.5. *For $\frac{10}{7} < \gamma < \frac{3}{2}$, the perfect fluid models exhibit only the following possible asymptotic behaviours: they tend to LK^+ or INF^- as $\chi \longrightarrow -\infty$ and they tend to LK^- or INF^+ as $\chi \longrightarrow \infty$.*

Proof. For $\frac{10}{7} < \gamma < \frac{3}{2}$, consider an initial condition in the invariant set Z_+, the function G is decreasing in Z_+ as $\chi \longrightarrow -\infty$. We conclude from Theorem 4.3.3 (extension to the Monotonicity Principle) that the solutions must tend to the boundary of Z_+ as $\chi \longrightarrow -\infty$, that is the solutions must tend to $\bar{Z}_+ \setminus Z_+$. By the extension to the Poincaré–Bendixon theorem in [18, p.709], we have that solutions must tend to LK^+ or INF^- as $\chi \longrightarrow -\infty$.

As $\chi \longrightarrow \infty$, by using Corollary 4.3.3.1, the solutions either tend to the boundary of Z_+ or $\bar{Z}_+^c$. Since there are no sink equilibrium points on the boundary of Z_+ the solutions must then tend to $\bar{Z}_+^c$. So since the solutions are in Z_-, by using Theorem 4.3.3 (extension

to the Monotonicity Principle) and the extension to the Poincaré–Bendixon theorem in [18, p.709], they must tend to INF^+ or LK^-. And there are no other possibilities. □

For the case $\gamma = \frac{6}{5}$, the trajectories on the invariant set $S = 1$ form closed curves and two cycle graphs as shown in HWG [23, p. 1320]. In this case we have that

$$\frac{dG}{d\chi} = \frac{1296}{625} Y_2 G. \tag{4.16}$$

Considering the domain of the function restricted to the invariant set Z_+, we have that $G : Z_+ \longrightarrow \mathbb{R}$ is a C^1 function with range $(0, \infty)$ and is increasing as $\chi \longrightarrow \infty$. Similarly, considering the domain of the function restricted to the invariant set Z_-, $G : Z_- \longrightarrow \mathbb{R}$ is increasing as $\chi \longrightarrow -\infty$.
Fig 4.11 illustrates the surfaces described by $G = \beta$ when $\gamma = \frac{6}{5}$.

Lemma 4.3.6. *For $\gamma = \frac{6}{5}$, the perfect fluid models tend*

- *to* INF^+ *or closed orbits or cycle graphs in $S = 1$ as $\chi \longrightarrow \infty$.*

- *to* INF^- *or closed orbits or cycle graphs in $S = 1$ as $\chi \longrightarrow -\infty$.*

Proof. The proof is identical to the proofs of Theorem 4.3.4 and Theorem 4.3.5, except that now the boundary ($S = 1$) of the positive and negative invariant sets Z_+ and Z_- contain closed curves as well as equilibrium points. □

In Chapter 6, we prove that the perfect fluid models that tend to INF^+ or INF^- correspond to $\Omega \longrightarrow \infty$ and $\mu \longrightarrow \infty$.

Figure 4.11: The surfaces described by $G = \beta$ in the phase space with $Y_2 > 0$. The phase portraits consist of closed curves and a cycle graph on the vacuum boundary which asymptotically tends to LK^+ and LK^- equilibrium points as illustrated in [23, p.1320] and in the diagram below. The blue surface represents a larger value of β compared to the gray surfaces.

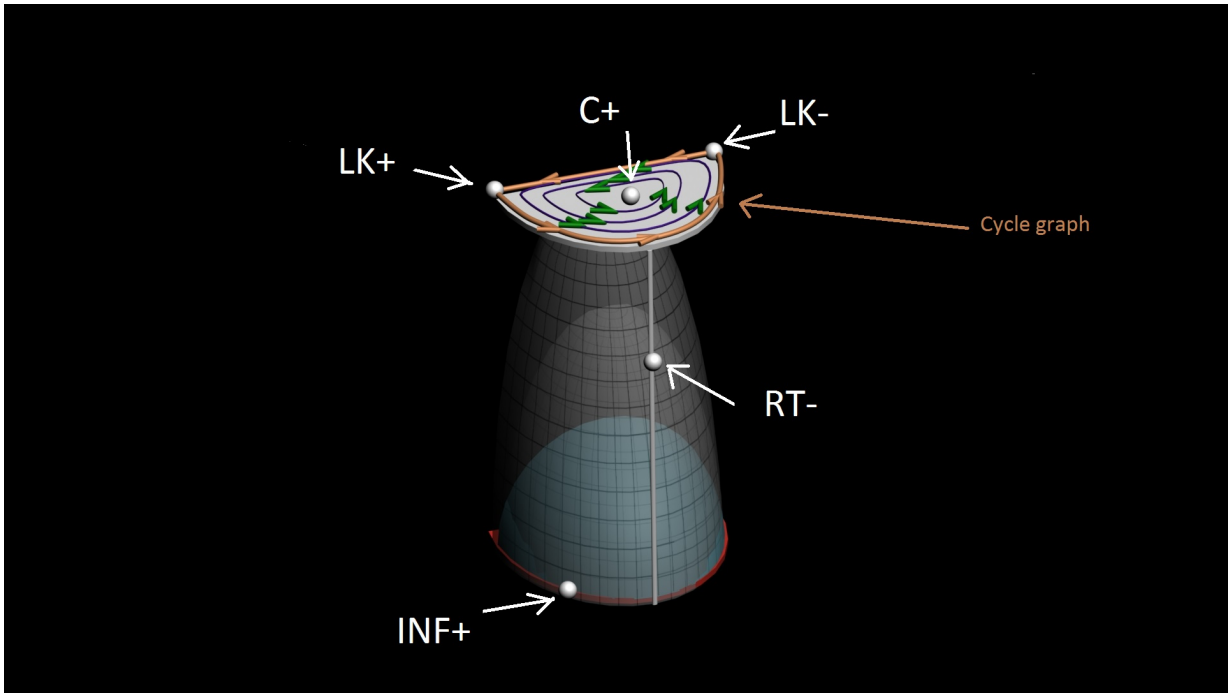

Chapter 5

The case $\gamma = \frac{10}{9}$

When $\gamma = \frac{10}{9}$, the ODEs admit a one parameter family of equilibrium points, which we refer to as *Wainwright equilibrium points*, given by

$$Y_2 = -\frac{20}{9}Y_1, \ S^2 = \frac{7}{3} - 8Y_1^2. \tag{5.1}$$

Due to the fact that we are only interested in models with $Y_4 \geq 0$ and $S \leq 1$, we have the restriction $\frac{1}{6} \leq Y_1^2 \leq \frac{7}{32}$. We have the two arcs of equilibrium points with each arc terminating at a Collins equilibrium point($S = 1$) and RT equilibrium point($Y_4 = 0$). The diagram below represents the two arcs of equilibrium points.

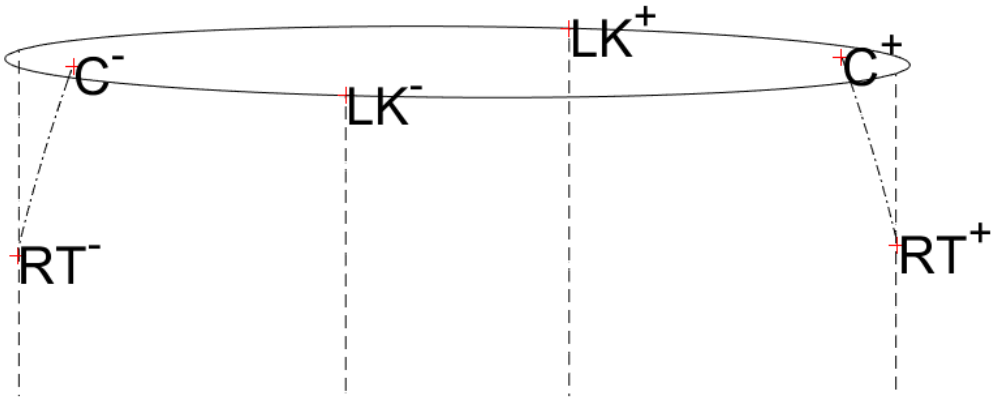

5.1 The Invariant 2-Space

In this case, the ODEs admit a first integral and the phase space is foliated by a one parameter family of 2-spaces. Due to the structure of the ODE, S, $1-S^2$, and Y_4, give rise to the invariant sets, $S=0$, $S=1$, and $Y_4=0$. When $\gamma=\frac{10}{9}$, we have

$$G=\frac{Y_4^3(1-S^2)^4}{S^{14}}. \tag{5.2}$$

From Eq.(4.15) we have

$$\frac{dG}{d\chi}\propto(10\gamma-9). \tag{5.3}$$

Thus, at $\gamma=\frac{10}{9}$, we have $\frac{dG}{d\chi}=0$, which means that G is constant along the flow of the ODEs, and hence the solutions are constrained to the surfaces

$$G=\frac{Y_4^3(1-S^2)^4}{S^{14}}=\alpha. \tag{5.4}$$

for a constant α. On a surface $G=\alpha$, for a constant value of S, Y_4 must be a constant. From Eq.(3.106), constant Y_4 corresponds to the ellipse with the equation

$$1=\frac{Y_1^2}{\left[1-\frac{Y_4}{3(3-2\gamma)}\right]}+\frac{Y_2^2}{\frac{16}{3}(\gamma-1)\Big[3(3-2\gamma)-Y_4\Big]}. \tag{5.5}$$

From the equation above and Eq.(5.4), the semi-major axis and semi-minor axis of the ellipse are functions of S and α. As S increases, the size of these ellipses decrease. Thus, these surfaces are described in three dimensions by a family of ellipses that get smaller in size as they reach the top of the elliptical cylinder. Eq.(5.4) is undefined when $S=0$. And, in addition, these 2-spaces intersect when $Y_4=0$ and $S=0$.
We are interested in the phase portraits on each 2-space described by $G=\alpha$. There exists a value of α for which these 2-spaces cross the arcs of equilibrium points exactly twice. We refer to this value as $\alpha=G_c$ or the critical value of G. Thus, we divide the problem into steps based on the restrictions on the values of α. Let N be the number of points of intersection between the 2-space described by $G=\alpha$ and the arcs of equilibrium points. Table 5.1 demonstrates these steps as well as the diagrams that are associated with each step. The detailed information about the phase portraits in each step is described in Section 5.3.

Table 5.1: The behaviour of the 2-space described by $G = \alpha$ and the corresponding phase portraits.

Restriction on α	N	Shape of the 2-space and the phase portraits	Restrictions on the values of S and Y_4
$\alpha = 0$	4	Fig 5.4	$S = 1$ or $Y_4 = 0$
$0 < \alpha < G_c$	4	Fig 5.5 and Fig 5.6	$0 < S < 1$, $Y_4 < 0$
$\alpha = G_c$	2	Fig 5.7	$0 < S < 1$, $Y_4 > 0$
$\alpha > G_c$	0	Fig 5.8	$0 < S < 1$, $Y_4 > 0$
$\alpha = \infty$	0	Fig 5.9	$S = 0$, $Y_4 > 0$

By using Eq.(3.106), we write G as a function of Y_1, Y_2, and S. In addition, by using Eq.(5.1), we parameterize the arcs of equilibrium points by Y_1. We then parameterize G by Y_1. Along the arcs, we have

$$G(Y_1) = \frac{256(32{Y_1}^2 - 7)^3(1 - 6{Y_1}^2)^4}{(24{Y_1}^2 - 7)^7}. \tag{5.6}$$

As it is revealed from Table 5.1, the values of α increase as the surface tends to the bottom of the elliptical cylinder. The critical value of G is obtained by maximizing the function G along the arcs of equilibrium points. The result is

$$Y_1 = \pm\frac{\sqrt{966}}{69} \approx \pm 0.45,$$
$$G(Y_1 = \pm\frac{\sqrt{966}}{69}) = G_c \approx 3.74 \times 10^{-4}.$$

Since we are interested in drawing the solutions on this 2-space described by the surface $G = \alpha$, these values of Y_1 at G_c are of importance when analyzing the stability of Wainwright equilibrium points.

5.2 The Stability of Wainwright Equilibrium Points

From Table 4.2, for the case labeled as Wainwright, the eigenvalues are functions of Y_1 and S. By substituting Eq.(5.1) into the eigenvalues, considering Sign$(Y_1) = \mp$ (corresponding to Wainwright equilibrium points $\mathrm{W}^{\mp}$), we obtain

$$\lambda_1 = 0, \tag{5.7}$$

$$\lambda_2 = \frac{16}{81}\, Y_1 \mp \frac{16}{81}\sqrt{533Y_1^2 - 112}, \tag{5.8}$$

$$\lambda_3 = \frac{16}{81}\, Y_1 \pm \frac{16}{81}\sqrt{533Y_1^2 - 112}. \tag{5.9}$$

The eigenvalues are complex when the expression $533Y_1^2 - 112$ is negative. This occurs in the interval $Y_1 \in [-\frac{4}{\sqrt{79}}, \frac{4}{\sqrt{79}}]$. Within this interval, in the invariant 2-space, one of the W^- equilibrium points is a stable focus and one of the W^+ equilibrium points is an unstable focus. The stability of Wainwright equilibrium points change because the eigenvalues change sign. The zeros of the eigenvalues are important because they indicate when the change of sign takes place. The eigenvalues are zero when

$$Y_1 = \pm\frac{\sqrt{966}}{69},$$

exactly at the critical point for G along the arc. It is clear that a change of stability takes place when $Y_1 = \pm\frac{\sqrt{966}}{69}$. The Y_1 components of the coordinates for the Robinson–Trautmann equilibrium points are $\frac{\sqrt{14}}{8}$ and $-\frac{\sqrt{14}}{8}$. From the eigenvalues represented in Eq.(5.7)-(5.9), we summarize the stability of the Wainwright equilibrium points in Tables 5.2-5.3.

Table 5.2: The stability of the Wainwright equilibrium points for $Y_1 < 0$.

Restrictions on Y_1	$-\frac{\sqrt{14}}{8} < Y_1 < -\frac{\sqrt{966}}{69}$	$-\frac{\sqrt{966}}{69} < Y_1 < -\frac{4}{\sqrt{79}}$	$-\frac{4}{\sqrt{79}} < Y_1 < -\frac{1}{\sqrt{6}}$
Stability of the Wainwright equilibrium points W^-	Saddle	Stable Node	Stable Focus (Spiral Sink)

Table 5.3: The stability of the Wainwright equilibrium points for $Y_1 > 0$.

Restrictions on Y_1	$\frac{1}{\sqrt{6}} < Y_1 < \frac{4}{\sqrt{79}}$	$\frac{4}{\sqrt{79}} < Y_1 < \frac{\sqrt{966}}{69}$	$\frac{\sqrt{966}}{69} < Y_1 < \frac{\sqrt{14}}{8}$
Stability of the Wainwright equilibrium points W^+	Unstable Focus (Spiral Source)	Unstable Node	Saddle

5.3 Phase Portraits

The surface $G = 0$ corresponds to the union of the two invariant sets $S = 1$ and $Y_4 = 0$. The separatrices and all other types of solutions are identified on this 2-space by folding the top of the elliptical cylinder according to the diagram in Fig 5.1.

Typical solutions, with important highlighted separatrices are drawn on analogous two

Figure 5.1: $G = 0$, joint invariant sets $S = 1$ and $Y_4 = 0$ folded into a cone.

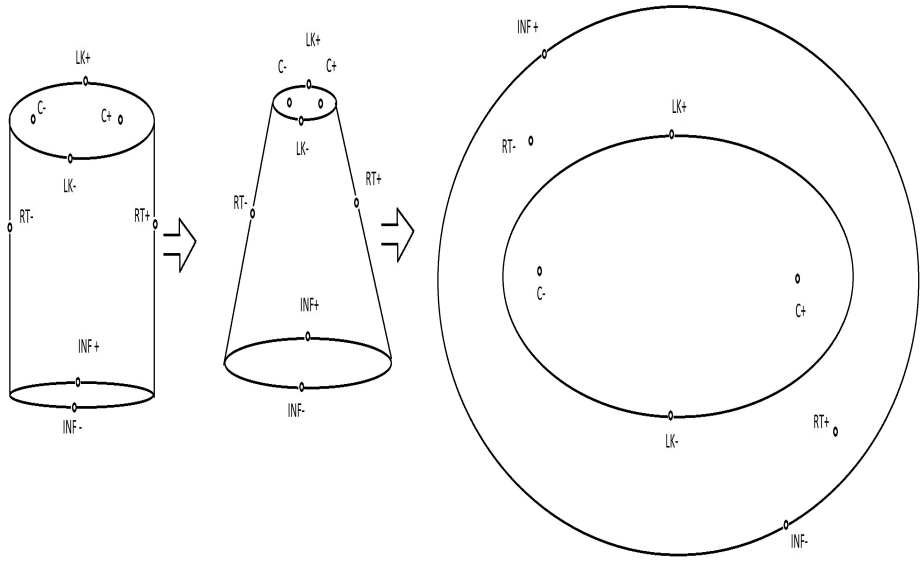

dimensional spaces in each step described by $G = \alpha$ in Figures 5.4-5.9. These 2-dimensional phase portraits are the projections of the solutions in the invariant 2-space onto the $S = 0$ plane.

In the diagrams that follow, well-behaved cosmological models are green, badly-behaved models are red, and the separatrices are in blue. We indicate Wainwright equilibrium points for $Y_1 < 0$ as W^- and for $Y_1 > 0$ as W^+. In addition, in each phase portrait, the well-behaved solutions are trapped in a region between two separatrices. In these particular regions in the phase space, an initial condition leads to a well-behaved cosmological model for $0 < \alpha < G_c$. Moreover, we can not rule out the possibility of the existence of limit cycles. However, the phase portraits are modeled assuming that there exist no limit cycles.

Lemma 5.3.1. *For $\gamma = \frac{10}{9}$, there exists an open set of well-behaved perfect fluid cosmological models that tend to W^+ as $\chi \longrightarrow -\infty$ and to W^- as $\chi \longrightarrow \infty$.*

Proof. The proof is identical to the proof of Theorem 4.3.2. □

Fig 5.4 represents the phase portraits when $G = 0$.
As the value of the constant α increases, the 2-space described by $G = \alpha$ moves away from the vacuum boundary and the top of the elliptical cylinder. The LK and the RT equilibrium points are replaced by the Wainwright equilibrium points. Fig 5.5 illustrates the separatrices, well-behaved cosmological models, as well as badly-behaved cosmological models on the 2-space when α is small but non-zero. As an example for this particular case, a numerically obtained well-behaved cosmological model, in three dimensions, is represented in Fig 5.2. The plot of the dimensionless energy density Ω vs. χ for the typical solutions in these figures is represented by Fig 5.3.
As α increases, and its value approximately reaches the critical value G_c, the distance between the Wainwright equilibrium points decreases and the former stable and unstable focus, W^+ and W^-, equilibrium points become stable and unstable nodes respectively. This is illustrated by Fig 5.6.
At $\alpha = G_c$, the two Wainwright equilibrium points, namely W^+ node and W^+ saddle, coincide. Also, the equilibrium points, W^- node and W^- saddle, coincide. The phase portraits in this case are given by Fig 5.7 where a saddle-node bifurcation takes place [24, p.177].
And finally, when $\alpha > G_c$ or $\alpha = \infty$, the surface $G = \alpha$ has no intersection with the arcs of equilibrium points and the phase portraits contain badly-behaved cosmological models because there exists only INF^+ and INF^- equilibrium points in the 2-space. Fig 5.8-5.9 represents the phase portraits for these cases.

Figure 5.2: Three dimensional phase portraits for $0 < \alpha < G_c$

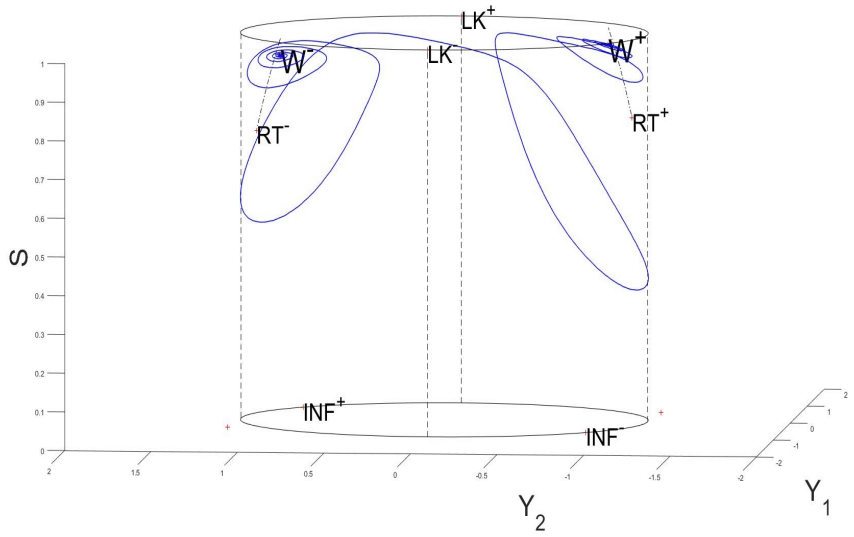

Figure 5.3: Ω vs. χ, for the solution in Fig. 5.2

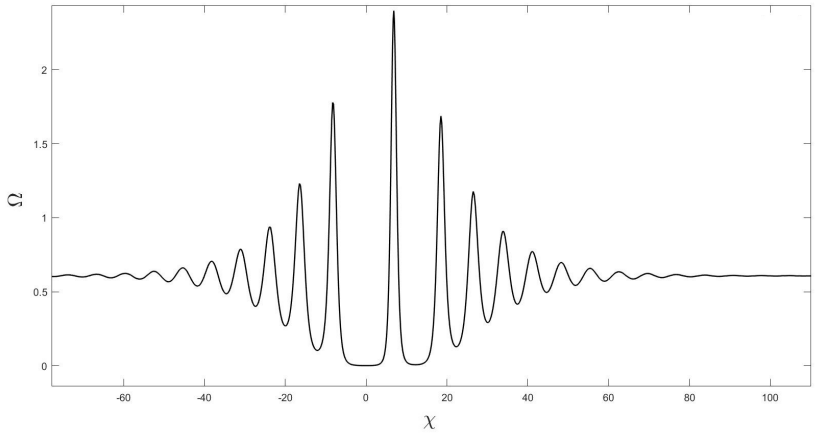

Figure 5.4: $G = 0$, joint invariant sets of $S = 1$ and $Y_4 = 0$.

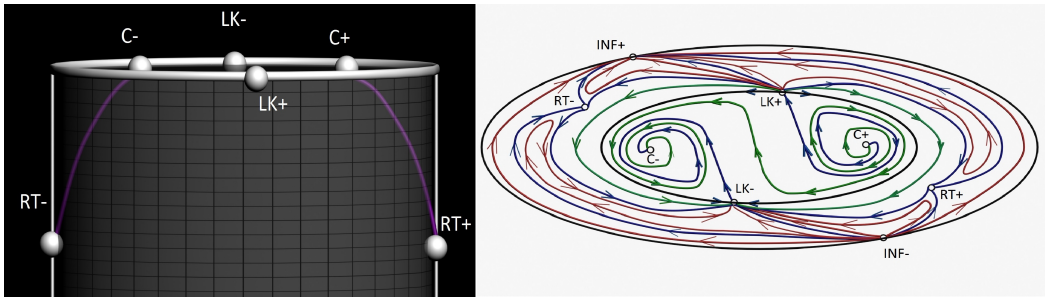

Figure 5.5: $0 < G < G_c$, the surface intersects with four Wainwright equilibrium points.

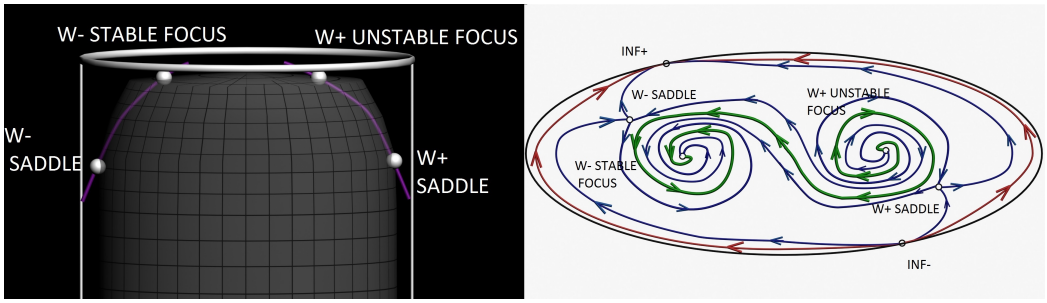

Figure 5.6: $0 < G < G_c$, the surface intersects with four Wainwright equilibrium points.

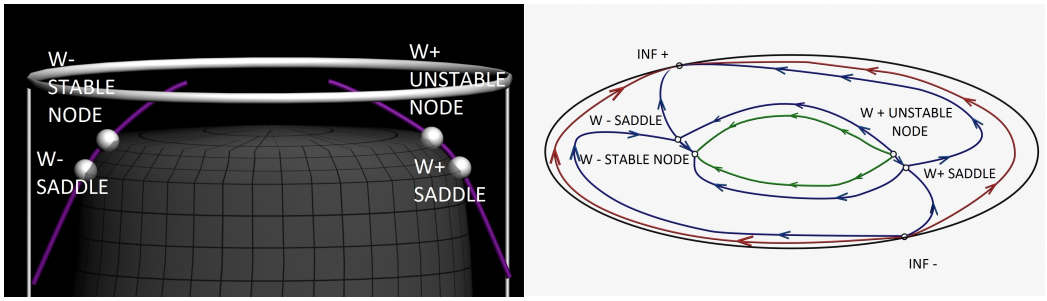

Figure 5.7: The invariant 2-space $G = G_c$.

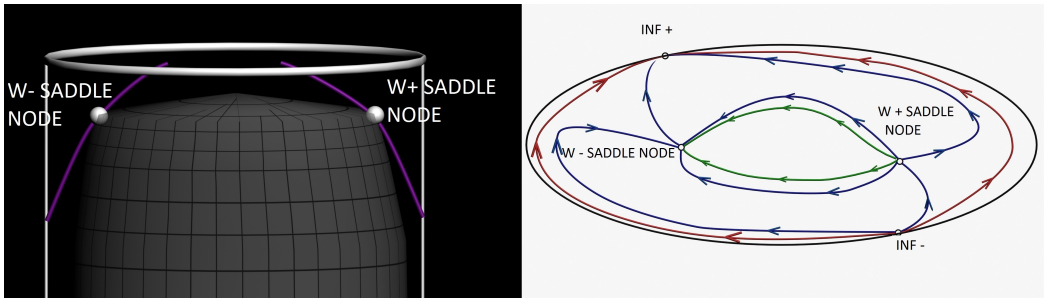

Figure 5.8: The invariant 2-space $G > G_c$.

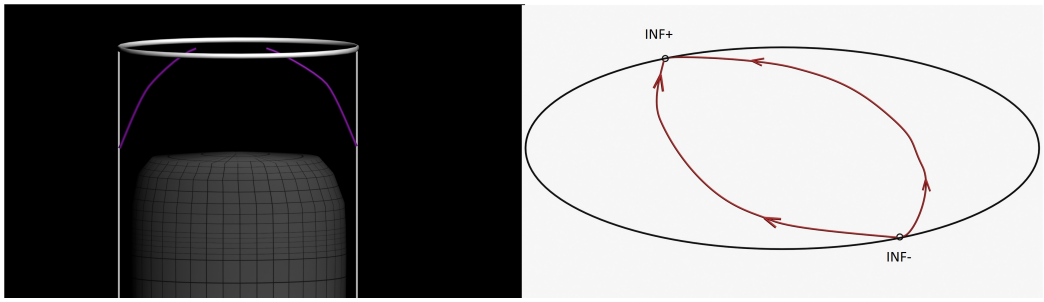

Figure 5.9: The invariant 2-space $G = \infty$.

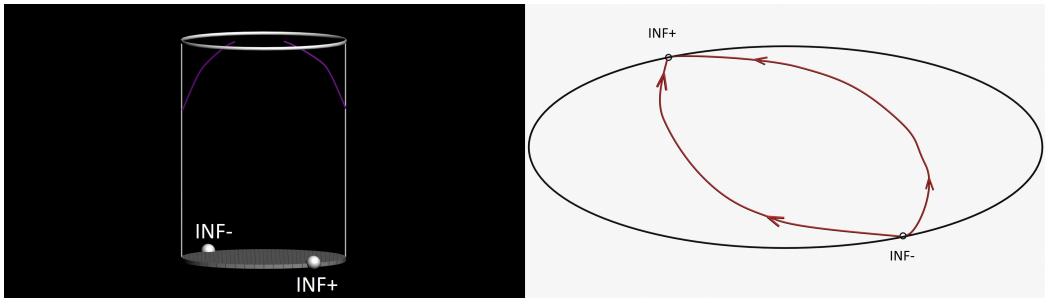

Chapter 6

Asymptotic Analysis of The Kinematical Quantities of The Fluid Near INF^+ Equilibrium Point

In order to analyze the behaviour of the cosmological models with $\Omega > 0$ that tend to the bottom of the elliptical cylinder, we look at the linearization solution near the INF^+ equilibrium point and demonstrate the behaviour of geometrically invariant quantities μ and $\dot{u}_1$, as $\chi \longrightarrow \infty$. Recall from Chapter 3 that badly-behaved cosmological models are the models in which both θ and the energy density μ, or the acceleration $\dot{u}_1$ diverge on a slice $t =$ constant.
We consider the eigenvalues $\lambda_1, \lambda_2, \lambda_3$ of the linearization matrix at the equilibrium point INF^+. The coordinates $(Y_1, Y_2, S) = (c_1, c_2, c_3)$ of INF^+ are

$$\begin{aligned} c_1 &= \frac{2\sqrt{(3-2\gamma)(\gamma-1)}}{\gamma-2}, \\ c_2 &= \frac{4\sqrt{(\gamma-1)(3-2\gamma)}(4-3\gamma)}{\gamma-2}, \\ c_3 &= 0. \end{aligned}$$

Let $\beta_1 = 4-3\gamma$, $\alpha_1 = 8(2\gamma-3)(\gamma-1)$, and $\alpha_2 = \gamma^2+2\gamma-4$, the corresponding eigenvectors are

$$V_{\lambda_1} = \begin{bmatrix} \beta_1 \\ \alpha_1 \\ 0 \end{bmatrix}, V_{\lambda_2} = \begin{bmatrix} 0 \\ 0 \\ 1 \end{bmatrix}, V_{\lambda_3} = \begin{bmatrix} -1 \\ \alpha_2 \\ 0 \end{bmatrix}. \tag{6.1}$$

Let $a, b, c \in \mathbb{R}$ and $C = \sqrt{-8\alpha_1}$, close to INF^+, solutions are approximately given by

$$\mathbf{x}(\chi) = \begin{bmatrix} c_1 \\ c_2 \\ 0 \end{bmatrix} + aV_{\lambda_1} e^{\lambda_1 \chi} + bV_{\lambda_2} e^{\lambda_2 \chi} + cV_{\lambda_3} e^{\lambda_3 \chi}. \tag{6.2}$$

where the eigenvalues are

$$\begin{aligned} \lambda_1 &= -2(\gamma - 1)C, \\ \lambda_2 &= -3(\gamma - 1)C, \\ \lambda_3 &= -(5\gamma - 4)C. \end{aligned}$$

Hence for $Y_1 > 0$, and the range $1 < \gamma < \frac{3}{2}$, we have that $\lambda_3 < \lambda_2 < \lambda_1$. The linearization solution is

$$\mathbf{x}(\chi) = \begin{bmatrix} c_1 \\ c_2 \\ 0 \end{bmatrix} + \begin{bmatrix} \beta_1 e^{\lambda_1 \chi} - e^{\lambda_3 \chi} \\ \alpha_1 e^{\lambda_1 \chi} + \alpha_2 e^{\lambda_3 \chi} \\ e^{\lambda_2 \chi} \end{bmatrix}. \tag{6.3}$$

So

$$Y_1(\chi) = c_1 + \beta_1 e^{\lambda_1 \chi} - e^{\lambda_3 \chi}, \tag{6.4}$$

$$Y_2(\chi) = c_2 + \alpha_1 e^{\lambda_1 \chi} + \alpha_2 e^{\lambda_3 \chi}, \tag{6.5}$$

$$S(\chi) = e^{\lambda_2 \chi}. \tag{6.6}$$

Since

$$\frac{dY_4}{d\chi} = 2Y_4 \Big[(5\gamma - 6)Y_2 + 4(7\gamma - 10)(\gamma - 1)Y_1 - \frac{4(1 - S^2)(\gamma - 1)L}{(2 - \gamma)} \Big]. \tag{6.7}$$

We approximate the R.H.S. using Eq.(6.4)-(6.6) to write

$$\frac{dY_4}{d\chi} \approx 2Y_4 [100\sqrt{(3 - 2\gamma)(\gamma - 1)}(5\gamma - 4)]. \tag{6.8}$$

And so

$$Y_4 \approx K_1 e^{200\sqrt{(3-2\gamma)(\gamma-1)}(5\gamma-4)\chi}. \tag{6.9}$$

where K_1 is a constant of integration. We also have that

$$\Omega(\chi) = \frac{Y_4(\chi)}{S^2(\chi)}. \tag{6.10}$$

So

$$\begin{aligned}\Omega(\chi) &\approx \frac{K_1 e^{200\sqrt{(3-2\gamma)(\gamma-1)}(5\gamma-4)\chi}}{e^{2\lambda_2\chi}},\\ &= \frac{K_1 e^{200\sqrt{(3-2\gamma)(\gamma-1)}(5\gamma-4)\chi}}{e^{2\lambda_2\chi}},\\ &= K_1 e^{8\sqrt{(3-2\gamma)(\gamma-1)}(129\gamma-104)\chi}.\end{aligned}$$

Since $8\sqrt{(3-2\gamma)(\gamma-1)}(129\gamma-104) > 0$, we have

$$\lim_{\chi\to\infty}\Omega(\chi) = \infty. \tag{6.11}$$

We substitute Eq.(3.74) into Eq.(3.60) to get

$$\boldsymbol{\partial}_1(\Omega) = 3\Omega[2+\frac{\gamma}{1-\gamma}]\dot{U},$$

and Eq.(3.62), to get

$$\boldsymbol{\partial}_1(\theta) = -3\dot{U}\theta.$$

Dividing the two equations above yields

$$\frac{\boldsymbol{\partial}_1\Omega}{\boldsymbol{\partial}_1\theta} = -\frac{\Omega[2+\frac{\gamma}{1-\gamma}]}{\theta}. \tag{6.12}$$

Solving the differential equation above gives

$$\Omega = \theta^{\frac{2-\gamma}{\gamma-1}}. \tag{6.13}$$

For $1 < \gamma < \frac{3}{2}$, the exponent $\frac{2-\gamma}{\gamma-1}$ is positive. Since $\Omega \longrightarrow \infty$, as $\chi \longrightarrow \infty$, we have that $\theta \longrightarrow \infty$. We also know that

$$\Omega = \frac{3\mu}{\theta^2}. \tag{6.14}$$

So

$$\mu = \frac{1}{3}\Omega^{\frac{\gamma}{2-\gamma}}. \tag{6.15}$$

Since $\frac{\gamma}{2-\gamma} > 0$, from Eq.(6.15) we conclude that as $\chi \longrightarrow \infty$, the matter-energy density of the fluid diverges.

In addition, we consider the asymptotic behaviour of the expression corresponding to the acceleration of the cosmological fluid $\dot{u}$. We have that the expansion normalized acceleration satisfies

$$\lim_{\chi\to\infty} \dot{U}(\chi) = \infty. \tag{6.16}$$

Proof. We consider the linear term

$$\dot{U} = \frac{1}{3(2-\gamma)}\Big[(3\gamma-2)A - 3(6-5\gamma)N_{\times}\Big]. \tag{6.17}$$

In order to express $\dot{U}$ in terms of variables Y_1 and Y_2, we have

$$A = \frac{3(2-\gamma)}{4}U,\ N_{\times} = -\frac{1}{4}V + \frac{(6-5\gamma)}{3(2-\gamma)}A. \tag{6.18}$$

By substituting the equations above into the equation for $\dot{U}$ we obtain

$$\dot{U} = \frac{1}{3(2-\gamma)}\Big[\Big(\frac{3(3\gamma-2)(2-\gamma)}{4} - \frac{3}{4}(6-5\gamma)^2\Big)U + \frac{3}{4}(6-5\gamma)V\Big]. \tag{6.19}$$

We know that

$$U = \frac{Y_1}{S},\ V = \frac{Y_2}{S}. \tag{6.20}$$

So

$$\dot{U}(\chi) = \frac{1}{3(2-\gamma)S(\chi)}\Big[\Big(\frac{3(3\gamma-2)(2-\gamma)}{4} - \frac{3}{4}(6-5\gamma)^2\Big)Y_1(\chi) + \frac{3}{4}(6-5\gamma)Y_2(\chi)\Big]. \tag{6.21}$$

Let $\gamma_1 = \frac{3(3\gamma-2)(2-\gamma)}{4} - \frac{3}{4}(6-5\gamma)^2$ and $\gamma_2 = \frac{3}{4}(6-5\gamma)$. By substituting the linearization solution, Eq.(6.4)-(6.6), into the equation of $\dot{U}$, we have

$$\dot{U}(\chi) = \frac{1}{3(2-\gamma)e^{\lambda_2\chi}}\Big[\gamma_1\Big(\beta_1 e^{\lambda_1\chi} - e^{\lambda_3\chi} + c_1\Big) + \gamma_2\Big(\alpha_1 e^{\lambda_1\ \chi} + \alpha_2 e^{\lambda_3\chi} + c_2\Big)\Big]. \tag{6.22}$$

We then have

$$\lim_{\chi\to\infty} \dot{U}(\chi) = \lim_{\chi\to\infty} \frac{1}{3(2-\gamma)}\Big[\gamma_1\Big(\beta_1\frac{e^{\lambda_1\chi}}{e^{\lambda_2\chi}} - \frac{e^{\lambda_3\chi}}{e^{\lambda_2\chi}} + \frac{c_1}{e^{\lambda_2\chi}}\Big) + \gamma_2\Big(\alpha_1\frac{e^{\lambda_1\ \chi}}{e^{\lambda_2\chi}} + \alpha_2\frac{e^{\lambda_3\chi}}{e^{\lambda_2\chi}} + \frac{c_2}{e^{\lambda_2\chi}}\Big)\Big]. \tag{6.23}$$

Since we have $\lambda_3 < \lambda_2 < \lambda_1$,

$$\lim_{\chi\to\infty} \dot{U}(\chi) = \lim_{\chi\to\infty} \frac{1}{3(2-\gamma)}\Big[\gamma_1\Big(\beta_1\frac{e^{\lambda_1\chi}}{e^{\lambda_2\chi}} - \mathcal{O}(\frac{e^{\lambda_3\chi}}{e^{\lambda_2\chi}}) + \frac{c_1}{e^{\lambda_2\chi}}\Big) + \gamma_2\Big(\alpha_1\frac{e^{\lambda_1\ \chi}}{e^{\lambda_2\chi}} + \mathcal{O}(\frac{e^{\lambda_3\chi}}{e^{\lambda_2\chi}}) + \frac{c_2}{e^{\lambda_2\chi}}\Big)\Big]. \tag{6.24}$$

So

$$\lim_{\chi\to\infty} \dot{U}(\chi) = \infty. \tag{6.25}$$

□

We know that $\dot{U} = \frac{\dot{u}_1}{\theta}$. From Eq.(6.13), we have that $\theta \longrightarrow \infty$ as $\chi \longrightarrow \infty$, so using Eq.(6.16) we have that

$$\lim_{\chi\to\infty} \dot{u}_1 = \infty. \tag{6.26}$$

This implies that the acceleration of the cosmological fluid diverges as the independent parameter of the ODEs, χ, tends to ∞. Hence, the cosmological models, with $\Omega > 0$ (perfect fluid), that tend to INF^+ equilibrium point are badly-behaved. By the same procedure, one may use the linearization solution near the INF^- equilibrium point to show that the perfect fluid models that tend to INF^- as $\chi \longrightarrow -\infty$ are also badly-behaved.

Conclusion

First, we demonstrated that the spatially inhomogeneous dynamical equilibrium states of exceptional G_2 cosmologies correspond to self-similar spacetimes. One should note that these models possess evolution and thus are cosmological models. Second, we showed that the spatial structure of these models is governed by a 1-parameter, three dimensional system of ODEs. The equilibrium points of this system of ODEs are transitively self-similar cosmologies and the corresponding exact solutions are due to Lifshitz–Khalatnikov, Collins, Robinson–Trautmann, and Wainwright and they are the asymptotic states of the generic self-similar exceptional G_2 inhomogeneous models. The scalar invariant shear of the models considered in this thesis have the minimum value of $\frac{1}{7} \approx 0.1428$ and this value occurs when the equation of state parameter is $\frac{8}{7}$ and $\Sigma_{13} = 0$. This value is much larger than the currently observed value which is approximately of order $\sim 10^{-9}$ (see for example [29, 27]).

The main results of this thesis are:

- For $1 < \gamma < \frac{10}{9}$ and $\frac{4}{3} < \gamma < \frac{10}{7}$, there is an open set of perfect fluid, self-similar, exceptional G_2 inhomogeneous models that are well-behaved, and they are asymptotic to the homogeneous Collins model at large spatial distance. Typical matter-energy density profile of such models is given in Fig 4.7. In addition, using the existence of a monotone function, we showed that there are only the following possibilities: such models are either well-behaved and asymptotically tend to the homogeneous Collins model or they are badly-behaved meaning that their basic physical variables, corresponding to the cosmological fluid, diverge. There are no other possibilities.

- For $\frac{10}{7} < \gamma < \frac{3}{2}$ there is an open set of perfect fluid, self-similar, exceptional G_2 inhomogeneous models that are well-behaved, and they are asymptotic to the homogeneous Lifshiftz–Khalatnikov model at large spatial distance. Typical matter-energy density profile of such models is given in Fig 4.9. In addition, using the same monotone function, we showed that there are only the following

possibilities: such models are either well-behaved and asymptotically tend to the homogeneous Lifshiftz–Khalatnikov model or they are badly-behaved. There are no other possibilities.

- For all values of γ in $(1, \frac{3}{2})$, there exists an open set of well-behaved vacuum, self-similar, exceptional G_2 inhomogeneous cosmological models that are asymptotic to the Lifshiftz–Khalatnikov model at large spatial distance.

Some analysis is provided for the models with $\gamma = \frac{10}{9}$ and $\gamma = \frac{6}{5}$. In the former case the system of ODEs has a first-integral and if we assume that there are no limit cycles, there exists an open set of perfect fluid, self-similar, exceptional G_2 inhomogeneous cosmological models that are asymptotic to the homogeneous Wainwright model at large spatial distance. In the latter case, using the same monotone function, we showed that the trajectories are either badly behaved or asymptotic to closed curves that correspond to the models with two HO KVFs in [23].

References

[1] PAR Ade, N Aghanim, et al. Planck 2015 results-XIII. cosmological parameters. *Astronomy & Astrophysics*, 594:A13, 2016.

[2] C Clarkson. Establishing homogeneity of the universe in the shadow of dark energy. *Comptes Rendus Physique*, 13(6-7):682–718, 2012.

[3] C Clarkson, B Bassett, and Hui-Ching Lu. A general test of the copernican principle. *Physical Review Letters*, 101(1):011301, 2008.

[4] A Clocchiatti, BP Schmidt, AV Filippenko, P Challis, AL Coil, R Covarrubias, A Diercks, P Garnavich, L Germany, R Gilliland, et al. Hubble space telescope and ground-based observations of type ia supernovae at redshift 0.5: cosmological implications. *The Astrophysical Journal*, 642(1):1, 2006.

[5] RH Dicke. The measurement of thermal radiation at microwave frequencies. In *Classics in Radio Astronomy*, pages 106–113. Springer, 1946.

[6] RH Dicke, PJE Peebles, PG Roll, and DT Wilkinson. Cosmic black-body radiation. *The Astrophysical Journal*, 142:414–419, 1965.

[7] GFR Ellis. Inhomogeneity effects in cosmology. *Classical and Quantum Gravity*, 28(16):164001, 2011.

[8] GFR Ellis and H Van Elst. Cosmological models. *Cargese Lectures, Cosmology Group, Department of Mathematics and Applied Mathematics, University of Cape Town, South Africa*, 1998.

[9] GFR Ellis and MAH MacCallum. A class of homogeneous cosmological models. *Communications in Mathematical Physics*, 12(2):108–141, 1969.

[10] GFR Ellis and H Van Elst. Cosmological models. In *Theoretical and Observational Cosmology*, pages 1–116. Springer, 1999.

[11] DJ Fixsen. The temperature of the cosmic microwave background. *The Astrophysical Journal*, 707(2):916, 2009.

[12] A Friedmann. On the curvature of space. *General Relativity and Gravitation*, 31(12):1991–2000, 1999.

[13] A Friedmann. On the possibility of a world with constant negative curvature of space. *General Relativity and Gravitation*, 31(12):2001–2008, 1999.

[14] JR Gott III et al. A map of the universe. *The Astrophysical Journal*, 624(2):463, 2005.

[15] D Hanson and A Lewis. Estimators for CMB statistical anisotropy. *Physical Review D*, 80(6):063004, 2009.

[16] D Harnett. Master's thesis. *University of Waterloo*, 1996.

[17] CG Hewitt. Phd thesis. *University of Waterloo*, 1989.

[18] CG Hewitt. An investigation of the dynamical evolution of a class of bianchi VI-1/9 cosmological models. *General Relativity and Gravitation*, 23(6):691–712, 1991.

[19] CG Hewitt, JT Horwood, and J Wainwright. Asymptotic dynamics of the exceptional Bianchi cosmologies. *Classical and Quantum Gravity*, 20(9):1743, 2003.

[20] CG Hewitt and J Wainwright. Orthogonally transitive G2 cosmologies. *Classical and Quantum Gravity*, 7(12):2295, 1990.

[21] CG Hewitt and J Wainwright. A dynamical systems approach to Bianchi cosmologies: orthogonal models of class B. *Classical and Quantum Gravity*, 10(1):99, 1993.

[22] CG Hewitt, J Wainwright, and M Glaum. Qualitative analysis of a class of inhomogeneous self-similar cosmological models. II. *Classical and Quantum Gravity*, 8(8):1505, 1991.

[23] CG Hewitt, J Wainwright, and SW Goode. Qualitative analysis of a class of inhomogeneous self-similar cosmological models I. *Classical and Quantum Gravity*, 5(10):1313, 1988.

[24] MW Hirsch, S Smale, and RL Devaney. *Differential equations, dynamical systems, and an introduction to chaos*. Academic press, 2012.

[25] L Hsu and J Wainwright. Self-similar spatially homogeneous cosmologies: orthogonal perfect fluid and vacuum solutions. *Classical and Quantum Gravity*, 3(6):1105, 1986.

[26] E Hubble. A relation between distance and radial velocity among extra-galactic nebulae. *Proceedings of the National Academy of Sciences*, 15(3):168–173, 1929.

[27] TR Jaffe, AJ Banday, HK Eriksen, KM Górski, and FK Hansen. Evidence of vorticity and shear at large angular scales in the wmap data: a violation of cosmological isotropy? *The Astrophysical Journal Letters*, 629(1):L1, 2005.

[28] RA Knop et al. New constraints on ωm, $\omega\lambda$, and w from an independent set of 11 high-redshift supernovae observed with the hubble space telescope. *The Astrophysical Journal*, 598(1):102, 2003.

[29] A Kogut, G Hinshaw, and AJ Banday. Limits to global rotation and shear from the cobe dmr four-year sky maps. *Physical Review D*, 55(4):1901, 1997.

[30] D Kramer, H Stephani, M MacCallum, and E Herlt. Exact solutions of einstein's field equations. *Berlin*, 1980.

[31] VG LeBlanc, D Kerr, and J Wainwright. Asymptotic states of magnetic Bianchi vi cosmologies. *Classical and Quantum Gravity*, 12(2):513, 1995.

[32] G Lemaître. Evolution of the expanding universe. *Proceedings of the National Academy of Sciences*, 20(1):12–17, 1934.

[33] MAH MacCallum. Cosmological models from a geometric point of view. In *Cargese lectures in physics. Vol. 6*. 1973.

[34] CW Misner, KS Thorne, and JA Wheeler. *Gravitation*. Princeton University Press, 2017.

[35] AA Penzias and RW Wilson. A measurement of excess antenna temperature at 4080 mc/s. *The Astrophysical Journal*, 142:419–421, 1965.

[36] S Perlmutter, G Aldering, G Goldhaber, RA Knop, P Nugent, PG Castro, S Deustua, S Fabbro, A Goobar, DE Groom, et al. Measurements of ω and λ from 42 high-redshift supernovae. *The Astrophysical Journal*, 517(2):565, 1999.

[37] HP Robertson. Kinematics and world-structure. *The Astrophysical Journal*, 82:284, 1935.

[38] HP Robertson. Kinematics and world-structure II. *The Astrophysical Journal*, 83:187, 1936.

[39] HP Robertson. Kinematics and world-structure III. *The Astrophysical Journal*, 83:257, 1936.

[40] KS Sibirskiĭ. *Introduction to topological dynamics*. Noordhoff International Pub, 1975.

[41] N Van den Bergh. A class of inhomogeneous cosmological models with separable metrics. *Classical and Quantum Gravity*, 5(1):167, 1988.

[42] N Van den Bergh. A qualitative discussion of the wils inhomogeneous stiff fluid cosmologies. *Classical and Quantum Gravity*, 9(10):2297, 1992.

[43] J Wainwright. A classification scheme for non-rotating inhomogeneous cosmologies. *Journal of Physics A: Mathematical and General*, 12(11):2015, 1979.

[44] J Wainwright. Exact spatially inhomogeneous cosmologies. *Journal of Physics A: Mathematical and General*, 14(5):1131, 1981.

[45] J Wainwright. A dynamical systems approach to Bianchi cosmologies: orthogonal models of class a. *Classical and Quantum Gravity*, 6(10):1409, 1989.

[46] J Wainwright and GFR Ellis. *Dynamical systems in cosmology*. Cambridge University Press, 2005.

[47] AG Walker. On milne's theory of world-structure. *Proceedings of the London Mathematical Society*, 2(1):90–127, 1937.

[48] P Wils. Inhomogeneous perfect fluid cosmologies with a nonorthogonally transitive symmetry group. *Classical and Quantum Gravity*, 8(2):361, 1991.

Appendix A

Orthonormal vs. Coordinate Frames

Let (M, g) be a pseudo-Riemannian manifold of any signature. Let ∇ be the Levi-Civita connection. Fix a frame $\mathbf{v}_1, .., \mathbf{v}_n$. The Christoffel symbols $\Gamma^n{}_{ij}$ are defined by

$$\nabla_{\mathbf{v}_i}\mathbf{v}_j = \Gamma^k{}_{ij}\mathbf{v}_k. \tag{A.1}$$

The commutation functions $\gamma^k{}_{ij}$ are defined by

$$[\mathbf{v}_i, \mathbf{v}_j] = \gamma^k{}_{ij}\mathbf{v}_k, \tag{A.2}$$

Let η_{ij} be the standard flat diagonal metric with that signature (in our case $\eta_{ij} = \text{diag}(-1, 1, 1, 1)$). We say the frame is *orthonormal* if

$$g(\mathbf{v}_i, \mathbf{v}_j) = \eta_{ij}. \tag{A.3}$$

Given that ∇ is metric compatible, if the frame is orthonormal then

$$\begin{aligned} 0 &= \nabla_{\mathbf{v}_k} g(\mathbf{v}_i, \mathbf{v}_j) \\ &= g(\nabla_{\mathbf{v}_k}\mathbf{v}_i, \mathbf{v}_j) + g(\mathbf{v}_i, \nabla_{\mathbf{v}_k}\mathbf{v}_j) \\ &= \Gamma^a{}_{ki} g(\mathbf{v}_a, \mathbf{v}_j) + \Gamma^b{}_{kj} g(\mathbf{v}_i, \mathbf{v}_b) \\ &= \Gamma^a{}_{ki}\eta_{aj} + \Gamma^b{}_{kj}\eta_{ib} \\ &= \Gamma^j{}_{ki}\eta_{jj} + \Gamma^i{}_{kj}\eta_{ii} \quad \text{(no-sum)}. \end{aligned}$$

Thus,

$$\Gamma^j{}_{ki} = -\Gamma^i{}_{kj}(\frac{\eta_{ii}}{\eta_{jj}}) \quad \text{(no-sum)}. \tag{A.4}$$

However, given that ∇ is torsion-free, if the frame is commutative,

$$\begin{aligned} 0 &= [\mathbf{v}_i, \mathbf{v}_j] \\ &= \nabla_{\mathbf{v}_i}\mathbf{v}_j - \nabla_{\mathbf{v}_j}\mathbf{v}_i \\ &= \Gamma^k{}_{ij}\mathbf{v}_k - \Gamma^k{}_{ji}\mathbf{v}_k \\ &= (\Gamma^k{}_{ij} - \Gamma^k{}_{ji})\mathbf{v}_k. \end{aligned}$$

Thus,

$$\Gamma^k{}_{ij} = \Gamma^k{}_{ji}. \tag{A.5}$$

Eq.(A.4) and Eq.(A.5) reveal that geometric quantities possess different symmetries depending on the properties of the frame.
To help with the derivation of Christoffel symbols, we use Koszul's formula

$$\begin{aligned} 2g(\nabla_{\mathbf{X}}\mathbf{Y}, \mathbf{Z}) = \mathbf{X}g(\mathbf{Y}, \mathbf{Z}) + \mathbf{Y}g(\mathbf{Z}, \mathbf{X}) - \mathbf{Z}g(\mathbf{X}, \mathbf{Y}) \\ - g(\mathbf{Y}, [\mathbf{X}, \mathbf{Z}]) - g(\mathbf{X}, [\mathbf{Y}, \mathbf{Z}]) + g(\mathbf{Z}, [\mathbf{X}, \mathbf{Y}]). \end{aligned}$$

The curvature of the connection is defined by

$$R(\mathbf{X}, \mathbf{Y})\mathbf{Z} := \nabla_{\mathbf{X}}\nabla_{\mathbf{Y}}\mathbf{Z} - \nabla_{\mathbf{Y}}\nabla_{\mathbf{X}}\mathbf{Z} - \nabla_{[\mathbf{X},\mathbf{Y}]}\mathbf{Z},$$

and gives rise to the Riemann curvature tensor

$$R(\mathbf{X}, \mathbf{Y}, \mathbf{Z}, \mathbf{W}) := g(R(\mathbf{X}, \mathbf{Y})\mathbf{Z}, \mathbf{W}).$$

From Koszul's formula, we have

$$\begin{aligned} 2g(\nabla_{\mathbf{v}_i}\mathbf{v}_j, \mathbf{v}_k) = \mathbf{v}_i g(\mathbf{v}_j, \mathbf{v}_k) + \mathbf{v}_j g(\mathbf{v}_k, \mathbf{v}_i) - \mathbf{v}_k g(\mathbf{v}_i, \mathbf{v}_j) \\ - g(\mathbf{v}_j, [\mathbf{v}_i, \mathbf{v}_k]) - g([\mathbf{v}_j, \mathbf{v}_k], \mathbf{v}_i) + g(\mathbf{v}_k, [\mathbf{v}_i, \mathbf{v}_j]) \end{aligned}$$

The L.H.S. of the equation is

$$\begin{aligned} 2g(\nabla_{\mathbf{v}_i}\mathbf{v}_j, \mathbf{v}_k) &= 2g(\Gamma^a{}_{ij}\mathbf{v}_a, \mathbf{v}_k) \\ &= 2\Gamma^a{}_{ij}g(\mathbf{v}_a, \mathbf{v}_k). \end{aligned}$$

So Kozul's formula is expressed as

$$\begin{aligned} 2\Gamma^a{}_{ij}g(\mathbf{v}_a, \mathbf{v}_k) &= \mathbf{v}_i g(\mathbf{v}_j, \mathbf{v}_k) + \mathbf{v}_j g(\mathbf{v}_k, \mathbf{v}_i) - \mathbf{v}_k g(\mathbf{v}_{i,j}) \\ &\quad - g(\mathbf{v}_j, [\mathbf{v}_i, \mathbf{v}_k]) - g([\mathbf{v}_j, \mathbf{v}_k], \mathbf{v}_i) + g(\mathbf{v}_k, [\mathbf{v}_i, \mathbf{v}_j]) \\ &= \mathbf{v}_i g(\mathbf{v}_j, \mathbf{v}_k) + \mathbf{v}_j g(\mathbf{v}_k, \mathbf{v}_i) - \mathbf{v}_k g(\mathbf{v}_i, \mathbf{v}_j) \\ &\quad - \gamma^b{}_{ik}g(\mathbf{v}_j, \mathbf{v}_b) - \gamma^n{}_{jk}g(\mathbf{v}_n, \mathbf{v}_i) + \gamma^m{}_{ij}g(\mathbf{v}_k, \mathbf{v}_m). \end{aligned}$$

Since,

$$\Gamma^{a}_{\ ij}\ g(\mathbf{v}_a, \mathbf{v}_k) = \Gamma^{a}_{\ ij}\ g_{ak},$$

we have,

$$\begin{aligned}\Gamma^{a}_{\ ij} g_{ak} = \frac{1}{2}\Big[&\mathbf{v}_i g(\mathbf{v}_j, \mathbf{v}_k) + \mathbf{v}_j g(\mathbf{v}_k, \mathbf{v}_i) - \mathbf{v}_k g(\mathbf{v}_i, \mathbf{v}_j) \\ &- \gamma^{b}_{\ ik} g(\mathbf{v}_j, \mathbf{v}_b) - \gamma^{n}_{\ jk} g(\mathbf{v}_n, \mathbf{v}_i) + \gamma^{m}_{\ ij} g(\mathbf{v}_k, \mathbf{v}_m)\Big].\end{aligned} \tag{A.6}$$

Therefore, we conclude that

$$\Gamma^{a}_{\ ij} = \frac{1}{2} g^{ak}\Big[\mathbf{v_i} g_{jk} + \mathbf{v}_j g_{ki} - \mathbf{v}_k g_{ij} - \gamma^{b}_{\ ik} g_{jb} - \gamma^{n}_{\ jk} g_{ni} + \gamma^{m}_{\ ij} g_{km}\Big].$$

In addition, we derive

$$\begin{aligned} R_{ijkl} &= R(\mathbf{v}_i, \mathbf{v}_j, \mathbf{v}_k, \mathbf{v}_l) \\ &= g(R(\mathbf{v}_i, \mathbf{v}_j)\mathbf{v}_k, \mathbf{v}_l) \\ &= g(\nabla_{\mathbf{v}_i}\nabla_{\mathbf{v}_j}\mathbf{v}_k - \nabla_{\mathbf{v}_j}\nabla_{\mathbf{v}_i}\mathbf{v}_k - \nabla_{[\mathbf{v}_i,\mathbf{v}_j]}\mathbf{v}_k, \mathbf{v}_l) \\ &= g(\nabla_{\mathbf{v}_i}\nabla_{\mathbf{v}_j}\mathbf{v}_k, \mathbf{v}_l) - g(\nabla_{\mathbf{v}_j}\nabla_{\mathbf{v}_i}\mathbf{v}_k, \mathbf{v}_l) - g(\nabla_{[\mathbf{v}_i,\mathbf{v}_j]}\mathbf{v}_k, \mathbf{v}_l) \\ &= g(\nabla_{\mathbf{v}_i}(\Gamma^{n}_{\ jk}\mathbf{v}_n), \mathbf{v}_l) - g(\nabla_{\mathbf{v}_j}(\Gamma^{m}_{\ ik}\mathbf{v}_m), \mathbf{v}_l) - g(\nabla_{[\mathbf{v}_i,\mathbf{v}_j]}\mathbf{v}_k, \mathbf{v}_l) \\ &= \mathbf{v}_i(\Gamma^{n}_{\ jk}) g_{nl} + \Gamma^{n}_{\ jk}\Gamma^{a}_{\ in} g_{al} - \mathbf{v}_j(\Gamma^{m}_{\ ik}) g_{ml} - \Gamma^{m}_{\ ik}\Gamma^{b}_{\ jm} g_{bl} - \gamma^{r}_{\ ij}\Gamma^{s}_{\ rk} g_{sl}. \end{aligned} \tag{A.7}$$

We relabel some of the indices and get

$$R_{ijkl} = g_{nl}\Big[\mathbf{v}_i(\Gamma^{n}_{\ jk}) + \Gamma^{s}_{\ jk}\Gamma^{n}_{\ is} - \mathbf{v}_j(\Gamma^{n}_{\ ik}) - \Gamma^{m}_{\ ik}\Gamma^{n}_{\ jm} - \gamma^{r}_{\ ij}\Gamma^{n}_{\ rk}\Big]. \tag{A.8}$$

We have $R_{ijkl} = g_{nl} R_{ijk}^{\ \ n}$. So

$$R_{ijk}^{\ \ n} = \mathbf{v}_i(\Gamma^{n}_{\ jk}) - \mathbf{v}_j(\Gamma^{n}_{\ ik}) - \Gamma^{m}_{\ ik}\Gamma^{n}_{\ jm} + \Gamma^{s}_{\ jk}\Gamma^{n}_{\ is} - \gamma^{r}_{\ ij}\Gamma^{n}_{\ rk}.$$

The Ricci curvature tensor is then

$$R_{ik} = \mathbf{v}_i(\Gamma^{n}_{\ nk}) - \mathbf{v}_n(\Gamma^{n}_{\ ik}) - \Gamma^{m}_{\ ik}\Gamma^{n}_{\ nm} + \Gamma^{s}_{\ nk}\Gamma^{n}_{\ is} - \gamma^{r}_{\ in}\Gamma^{n}_{\ rk}.$$

From all of the above, we illustrate the differences between the quantities of interest in the coordinate and orthonormal frame in Table A.1.

Table A.1: Geometric quantities in coordinate and orthonormal frame

Coordinate frame	Orthonormal frame
$\frac{\partial}{\partial x_0}, ..., \frac{\partial}{\partial x_3}$	$\mathbf{e}_0, ..., \mathbf{e}_3$
$[\frac{\partial}{\partial x_i}, \frac{\partial}{\partial x_j}] = 0$	$[\mathbf{e}_i, \mathbf{e}_j] = \gamma^k{}_{ij}\mathbf{e}_k$
$g = g_{ij}dx^i dx^j$	$g = -(\mathbf{e}^0)^2 + (\mathbf{e}^1)^2 + (\mathbf{e}^2)^2 + (\mathbf{e}^3)^2$
$\Gamma^a{}_{ij} = \frac{1}{2}g^{ak}\left[g_{jk,i} + g_{ki,j} - g_{ij,k}\right]$	$\Gamma^a{}_{ij} = \frac{1}{2}g^{ak}\left[\gamma^b{}_{ki}g_{jb} + \gamma^n{}_{kj}g_{ni} - \gamma^m{}_{ji}g_{km}\right]$
$\Gamma^a{}_{ji} = \Gamma^a{}_{ij}$	$\Gamma^j{}_{ki} = -\Gamma^i{}_{kj}(\frac{\eta_{ii}}{\eta_{jj}})$ (no-sum)
$R_{ijk}{}^n = \Gamma^n{}_{jk,i} - \Gamma^n{}_{ik,j}$ $- \Gamma^m{}_{ik}\Gamma^n{}_{jm} + \Gamma^s{}_{jk}\Gamma^n{}_{is}$	$R_{ijk}{}^n = \mathbf{e}_i(\Gamma^n{}_{jk}) - \mathbf{e}_j(\Gamma^n{}_{ik})$ $- \Gamma^m{}_{ik}\Gamma^n{}_{jm} + \Gamma^s{}_{jk}\Gamma^n{}_{is} - \gamma^r{}_{ij}\Gamma^n{}_{rk}$
$R_{ik} = \Gamma^n{}_{nk,i} - \Gamma^n{}_{ik,n}$ $- \Gamma^m{}_{ik}\Gamma^n{}_{nm} + \Gamma^s{}_{nk}\Gamma^n{}_{is}$	$R_{ik} = \mathbf{e}_i(\Gamma^n{}_{nk}) - \mathbf{e}_n(\Gamma^n{}_{ik})$ $- \Gamma^m{}_{ik}\Gamma^n{}_{nm} + \Gamma^s{}_{nk}\Gamma^n{}_{is} - \gamma^r{}_{in}\Gamma^n{}_{rk}$

We now provide alternative proofs for specializations of equation Eq.(A.6) in two different scenarios. First we assume that the frame $\mathbf{v}_i = \mathbf{e}_i$ is orthonormal.
Since $g(\mathbf{e}_a, \mathbf{e}_b) = \eta_{ab}$ is constant,

$$\begin{aligned} 0 &= \nabla_{\mathbf{e}_c} g(\mathbf{e}_a, \mathbf{e}_b) \\ &= g(\nabla_{\mathbf{e}_c}\mathbf{e}_a, \mathbf{e}_b) + g(\mathbf{e}_a, \nabla_{\mathbf{e}_c}\mathbf{e}_b) \\ &= \Gamma_{cab} + \Gamma_{cba}. \end{aligned} \tag{A.9}$$

And since

$$\gamma^r{}_{ab}\mathbf{e}_r = [\mathbf{e}_a, \mathbf{e}_b] = \nabla_{\mathbf{e}_a}\mathbf{e}_b - \nabla_{\mathbf{e}_b}\mathbf{e}_a = (\Gamma^r{}_{ab} - \Gamma^r{}_{ba})\mathbf{e}_r, \tag{A.10}$$

we have that

$$\gamma^r{}_{ab} = \Gamma^r{}_{ab} - \Gamma^r{}_{ba}. \tag{A.11}$$

By using Eq.(A.9) and Eq.(A.11), we raise and lower the indices via $g_{ab} = \eta_{ab} = \eta^{ab}$ to obtain

$$\Gamma_{abc} = \frac{1}{2}(\gamma_{abc} + \gamma_{cab} - \gamma_{bca}).$$

One should always remember that this formula is only valid in an orthonormal frame.

Suppose now that we are using a coordinate frame. Since spacetime is a smooth pseudo-Riemannian manifold with a Levi-Civita connection, the covariant derivative admits the torsion free and the metric compatibility conditions. The metric compatibility condition in the coordinate frame is

$$g^{ab}{}_{;r} \;=\; 0. \tag{A.12}$$

By permuting the indices one can obtain three equations $g_{ab;r} = 0$, $g_{rb;a} = 0$, $g_{ar;b} = 0$, from which the following relation can be derived

$$\Gamma^{r}{}_{ab} = \frac{1}{2} g^{rs}[g_{sa,b} + g_{sb,a} - g_{ab,s}]. \tag{A.13}$$

Appendix B

Existence of Orthonormal Frame

This appendix provides an explicit construction of an orthonormal frame for any Lorentzian metric. The existence of such a frame is clear from Sylvester's law of inertia. However, a constructive proof is useful.

Lemma B.0.1. *Let g be a Lorentzian metric. Then there exists locally an orthonormal frame.*

Proof. We construct this frame from a coordinate frame $\frac{\partial}{\partial x^0}, ..., \frac{\partial}{\partial x^3}$, using its metric tensor g_{ij}. Since the metric tensor $[g_{ij}]$ is symmetric, it is diagonalizable. Let $\lambda_0 < 0$ and $\lambda_0, ..., \lambda_3 > 0$ be the eigenvalues of $[g_{ij}]$. Then, there exists an orthogonal matrix A and a diagonal matrix D such that

$$g = ADA^T = A \begin{bmatrix} \lambda_0 & 0 & 0 & 0 \\ 0 & \lambda_1 & 0 & 0 \\ 0 & 0 & \lambda_2 & 0 \\ 0 & 0 & 0 & \lambda_3 \end{bmatrix} A^T. \tag{B.1}$$

We choose a matrix h such that for

$$D' := \begin{bmatrix} \frac{1}{\sqrt{|\lambda_0|}} & 0 & 0 & 0 \\ 0 & \frac{1}{\sqrt{|\lambda_1|}} & 0 & 0 \\ 0 & 0 & \frac{1}{\sqrt{|\lambda_2|}} & 0 \\ 0 & 0 & 0 & \frac{1}{\sqrt{|\lambda_3|}} \end{bmatrix}, \tag{B.2}$$

$$[h_i{}^j] := D'A^T. \tag{B.3}$$

Let

$$\mathbf{e}_i := h_i{}^j \frac{\partial}{\partial x^j}. \tag{B.4}$$

Then

$$\begin{aligned} g(\mathbf{e}_i, \mathbf{e}_j) &= g(h_{ik}\frac{\partial}{\partial x^k}, h_{jl}\frac{\partial}{\partial x^l}) \\ &= h_{ik} g_{kl} h_{lj} \\ &= [hgh^T]_{ij} \\ &= [D'A^T g[D'A^T]^T]_{ij} \\ &= [D'A^T(ADA^T)AD'^{\,T}]_{ij} \\ &= [D'(A^TA)D(A^TA)D']_{ij} \\ &= [D'DD']_{ij} \\ &= \eta_{ij}. \end{aligned}$$

□

Appendix C

Proof Of The Conservation Equation

In this appendix, we provide, for completeness, a proof for the result

$$T^{ab}{}_{;b} = 0 \implies \dot{\mu} = -u^a{}_{;a}\gamma\mu. \tag{C.1}$$

The result is often stated without proof, for instance in [9, 10, p.108, p.10].

Proof. Using the fact that the stress energy tensor is divergent free, we have

$$0 = T^{ab}{}_{;b} = p_{,b}\, g^{ab} + p g^{ab}{}_{;b} + \Big[(p+\mu)u^a u^b\Big]_{;b}.$$

Since the covariant derivative of the metric tensor is zero, we have that

$$0 = T^{ab}{}_{;b} = p_{,b}\, g^{ab} + \Big[(p_{,b}+\mu_{,b})u^a u^b + (u^a{}_{;b}u^b + u^a u^b{}_{;b})(p+\mu)\Big].$$

We contract the above with u_a, and using the fact that $u^a u_a = -1$ which implies $2u^a u_{a;b} = 0$, we have

$$\begin{aligned} 0 = u_a T^{ab}{}_{;b} &= p_{,b}\, u_a g^{ab} + \Big[-p_{,b}u^b - \mu_{,b}u^b + (u_a u^a{}_{;b}u^b - u^b{}_{;b})(p+\mu)\Big], \\ &= -u^b\mu_{,b} + (u_a u^a{}_{;b}u^b - u^b{}_{;b})(p+\mu), \\ &= -u^b\mu_{,b} + (-u^b{}_{;b})(p+\mu). \end{aligned}$$

So we have

$$\dot{\mu} = -u^a{}_{;a}(p+\mu).$$

By substituting the equation of state in Eq.(1.10) in the equation above, we get

$$\dot{\mu} = -u^a{}_{;a}\gamma\mu. \tag{C.2}$$

□

Appendix D

Derivation Of The PDEs From The EFEs

In this appendix, we illustrate the derivation of the EFEs under the assumptions and choices of Chapters 1 and 2. The equations Eq.(2.29) and Eq.(2.30) in the EFEs, are

$$\begin{aligned}
\mathbf{e}_0\theta &= -\frac{1}{3}\theta^2 - \Big((\sigma_{11})^2 + (\sigma_{22})^2 + (\sigma_{33})^2 + 2(\sigma_{13})^2\Big) \\
&\quad + (\mathbf{e}_1 + \dot{u}_1 - 2a_1)\dot{u}^1 - \frac{1}{2}(\mu + 3p), \qquad \text{(D.1)} \\
\mathbf{e}_0\sigma_{11} &= -3H\sigma_{11} + 2(\varepsilon^{12}{}_1\sigma_{11}\Omega_2 + \varepsilon^{32}{}_1\sigma_{13}\Omega_2) \\
&\quad + (\mathbf{e}_1 + \dot{u}_1 + a_1)\dot{u}_1 - \frac{1}{3}(\mathbf{e}^1 + \dot{u}^1 + a^1)\dot{u}_1 \\
&\quad - \mathbf{e}_1 a_1 + \frac{1}{3}\mathbf{e}_1 a^1 + \frac{4}{3}(n_2^3 n_3^2), \qquad \text{(D.2)} \\
\mathbf{e}_0\sigma_{22} &= -3H\sigma_{22} + \varepsilon^{22}{}_2\sigma_{22}\Omega_2 + \varepsilon^{22}{}_2\sigma_{22}\Omega_2 \\
&\quad - \frac{1}{3}(\mathbf{e}^1 + \dot{u}^1 + a^1)\dot{u}_1 - \varepsilon^{31}{}_2 n_{23}\dot{u}_1 \\
&\quad + \frac{1}{3}\mathbf{e}_1 a^1 + (\mathbf{e}_\mu n_{32}\varepsilon_2{}^{\mu 3} - 2n_{32}\varepsilon_2{}^{13}a_1) - (\ \ 2n_2^3 n_{32}\ \ ) + \frac{4}{3}(n_2^3 n_3^2), \qquad \text{(D.3)} \\
\mathbf{e}_0\sigma_{33} &= -3H\sigma_{33} + 2\Omega_2(\varepsilon^{12}{}_3\sigma_{31} + \varepsilon^{32}{}_3\sigma_{33}) - \frac{1}{3}(\mathbf{e}^1 + \dot{u}^1 + a^1)\dot{u}_1 \\
&\quad - \varepsilon^{21}{}_3 n_{32}\dot{u}_1 \ + \ \frac{1}{3}\mathbf{e}_1 a^1 + (\mathbf{e}_\mu n_{23}\varepsilon_3{}^{\mu 2} - 2a_1 n_{23}\varepsilon_3{}^{12}) \\
&\quad - (2n_3^\mu n_{\mu 3}) + \frac{4}{3}(n_2^3 n_3^2), \qquad \text{(D.4)}
\end{aligned}$$

$$\begin{aligned}\mathbf{e}_0\sigma_{13} &= -3H\sigma_{13} + \varepsilon^{12}{}_1\sigma_{31}\Omega_2 + \varepsilon^{32}{}_1\sigma_{33}\Omega_2 + \varepsilon^{32}{}_3\sigma_{13}\Omega_2 + \varepsilon^{12}{}_3\sigma_{11}\Omega_2 \\ &+ \frac{1}{2}\mathbf{e}_3\dot{u}_1 - \frac{1}{2}\varepsilon^{21}{}_1 n_{32}\dot{u}_1 - \frac{1}{2}(\mathbf{e}_3 a_1) \\ &+ \frac{1}{2}(\mathbf{e}_1 n_{23}\varepsilon_1{}^{12} + \mathbf{e}_2 n_{23}\varepsilon_1{}^{22} + \mathbf{e}_3 n_{23}\varepsilon_1{}^{32} - 2a_1\varepsilon_1{}^{12}n_{23}). \end{aligned} \tag{D.5}$$

The equation for the density μ in the EFEs, namely Eq.(2.31), is

$$\begin{aligned}\mu &= 3H^2 - \sigma^2 + \omega^2 - 2\,\omega_\alpha\Omega^\alpha + \frac{1}{2}R, \\ &= \frac{1}{3}\theta^2 - \frac{1}{2}\Big((\sigma_{11})^2 + (\sigma_{22})^2 + (\sigma_{33})^2 + 2(\sigma_{13})^2\Big) + 2\mathbf{e}_1 a_1 - 3\,(a_1)^2 - \,(n_{23})^2. \end{aligned} \tag{D.6}$$

Due to the perfect fluid, the equation for the momentum density $q_\alpha = 0$, Eq.(2.32), yields

$$\begin{aligned}q_\alpha = 0 = \frac{2}{3}\mathbf{e}_\alpha\theta &- (\mathbf{e}_1\sigma^1_\alpha + \mathbf{e}_2\sigma^2_\alpha + \mathbf{e}_3\sigma^3_\alpha - 3a_1\sigma^1_\alpha) \\ &- \varepsilon_\alpha{}^{12}\sigma_{13}n_{23} - \varepsilon_\alpha{}^{23}\sigma^2_2 n_{23} - \varepsilon_\alpha{}^{32}\sigma_{33}n_{23}. \end{aligned} \tag{D.7}$$

The equation above yields the three equations below

$$0 = \frac{2}{3}\mathbf{e}_1\theta - (\mathbf{e}_1\sigma^1_1 + \mathbf{e}_3\sigma^3_1 - 3a_1\sigma^1_1) - \varepsilon_1{}^{12}\sigma_{13}n_{23} - \varepsilon_1{}^{23}\sigma^2_2 n_{23} - \varepsilon_1{}^{32}\sigma_{33}n_{23}, \tag{D.8}$$

$$0 = \frac{2}{3}\mathbf{e}_2\theta - (\mathbf{e}_2\sigma^2_2) - \varepsilon_2{}^{12}\sigma_{13}n_{23} - \varepsilon_2{}^{23}\sigma^2_2 n_{23} - \varepsilon_2{}^{32}\sigma_{33}n_{23}, \tag{D.9}$$

$$0 = \frac{2}{3}\mathbf{e}_3\theta - (\mathbf{e}_1\sigma^1_3 + \mathbf{e}_3\sigma^3_3 - 3a_1\sigma^1_3) - \varepsilon_3{}^{12}\sigma_{13}n_{23} - \varepsilon_3{}^{23}\sigma^2_2 n_{23} - \varepsilon_3{}^{32}\sigma_{33}n_{23}. \tag{D.10}$$

The Jacobi Identities are

$$\begin{aligned}\mathbf{e}_0 n_{23} = -\frac{1}{3}\theta n_{23} + \sigma^2_2 n_{32} + \sigma^3_3 n_{23} + \Big(\varepsilon^{22}{}_2 n_{32} + \varepsilon^{32}{}_3 n_{23}\Big)\Omega_2 \\ - \frac{1}{2}\mathbf{e}_3\Omega_2 - \Big(\,\dot{u}_1\frac{1}{2}[\sigma_{22}\varepsilon_3{}^{12} + \sigma_{13}\varepsilon_2{}^{11} + \sigma_{33}\varepsilon_2{}^{13}] \\ + \frac{1}{2}\mathbf{e}_1[\sigma_{22}\varepsilon_3{}^{12} + \sigma_{13}\varepsilon_2{}^{11} + \sigma_{33}\varepsilon_2{}^{13}] \\ + \frac{1}{2}\mathbf{e}_2[\sigma_{22}\varepsilon_3{}^{22} + \sigma_{13}\varepsilon_2{}^{21} + \sigma_{33}\varepsilon_2{}^{23}] \\ + \frac{1}{2}\mathbf{e}_3[\sigma_{22}\varepsilon_3{}^{32} + \sigma_{13}\varepsilon_2{}^{31} + \sigma_{33}\varepsilon_2{}^{33}]\ \Big). \end{aligned} \tag{D.11}$$

The evolution of the curvature variable a_1 is described by

$$\begin{aligned}\mathbf{e}_0 a_1 = &-\frac{1}{3}\theta a_1 - \sigma_1^1 a_1 - (\mathbf{e}_1 + \dot{u}_1)\frac{1}{3}\theta + \frac{1}{2}(\mathbf{e}_1\sigma_1^1 + \mathbf{e}_3\sigma_1^3) + \frac{1}{2}\dot{u}_1\sigma_{11} \\ &- \frac{1}{2}(\varepsilon_1{}^{12}\mathbf{e}_1\Omega_2 + \varepsilon_1{}^{22}\mathbf{e}_2\Omega_2 + \varepsilon_1{}^{32}\mathbf{e}_3\Omega_2 + \varepsilon_1{}^{12}\dot{u}_1\Omega_2 - 2\varepsilon_1{}^{12}a_1\Omega_2).\end{aligned} \tag{D.12}$$

And we also have to compute

$$0 = \mathbf{e}_0\omega_\alpha = \frac{1}{2}[-\varepsilon_\alpha{}^{11}\mathbf{e}_1\dot{u}_1 - \varepsilon_\alpha{}^{21}\mathbf{e}_2\dot{u}_1 - \varepsilon_\alpha{}^{31}\mathbf{e}_3\dot{u}_1 + \varepsilon_\alpha{}^{11}a_1\dot{u}_1]. \tag{D.13}$$

The equation above gives

$$0 = [-\varepsilon_1{}^{11}\mathbf{e}_1\dot{u}_1 - \varepsilon_1{}^{21}\mathbf{e}_2\dot{u}_1 - \varepsilon_1{}^{31}\mathbf{e}_3\dot{u}_1 + \varepsilon_1{}^{11}a_1\dot{u}_1], \tag{D.14}$$

$$0 = [-\varepsilon_2{}^{11}\mathbf{e}_1\dot{u}_1 - \varepsilon_2{}^{21}\mathbf{e}_2\dot{u}_1 - \varepsilon_2{}^{31}\mathbf{e}_3\dot{u}_1 + \varepsilon_2{}^{11}a_1\dot{u}_1], \tag{D.15}$$

$$0 = [-\varepsilon_3{}^{11}\mathbf{e}_1\dot{u}_1 - \varepsilon_3{}^{21}\mathbf{e}_2\dot{u}_1 - \varepsilon_3{}^{31}\mathbf{e}_3\dot{u}_1 + \varepsilon_3{}^{11}a_1\dot{u}_1]. \tag{D.16}$$

In addition, we compute

$$\begin{aligned}0 &= (\mathbf{e}_\beta - 2a_\beta)n_\alpha^\beta + \varepsilon_\alpha{}^{\mu\nu}\mathbf{e}_\mu a_\nu, \\ &= (\mathbf{e}_2 n_\alpha^2 + \mathbf{e}_3 n_\alpha^3) + \varepsilon_\alpha{}^{11}\mathbf{e}_1 a_1 + \varepsilon_\alpha{}^{21}\mathbf{e}_2 a_1 + \varepsilon_\alpha{}^{31}\mathbf{e}_3 a_1.\end{aligned} \tag{D.17}$$

And the contracted Bianchi identities are

$$\begin{aligned}\mathbf{e}_0\mu &= -3H(\mu + p) - \sigma_\alpha^\beta\pi_\beta^\alpha - (\mathbf{e}_\alpha + 2\dot{u}_\alpha - 2a_\alpha)q^\alpha, \\ &= -\theta(\mu + p),\end{aligned} \tag{D.18}$$

$$\mathbf{e}_0 q_\alpha = 0 = -\mathbf{e}_\alpha p - (\mu + p)\dot{u}_\alpha. \tag{D.19}$$

We now use the definition of $\varepsilon_{\alpha\beta\nu}$ in Eq.(2.6), and get

$$\begin{aligned}
\mathbf{e}_0\theta &= -\frac{1}{3}\theta^2 - \Big((\sigma_{11})^2 + (\sigma_{22})^2 + (\sigma_{33})^2 + 2(\sigma_{13})^2\Big) \\
&\quad + (\mathbf{e}_1 + \dot{u}_1 - 2a_1)\dot{u}_1 - \frac{1}{2}(\mu + 3p), && \text{(D.20)}\\
\mathbf{e}_0\sigma_{11} &= -\theta\sigma_{11} + \frac{2}{3}\Big(\mathbf{e}_1(\dot{u}_1) + (\dot{u}_1)^2 + a_1\dot{u}_1\Big) - \frac{2}{3}\mathbf{e}_1(a_1) + \frac{4}{3}(n_{23})^2, && \text{(D.21)}\\
\mathbf{e}_0\sigma_{22} &= -\theta\sigma_{22} - \frac{1}{3}(\mathbf{e}_1\dot{u}_1 + (\dot{u}_1)^2 + a_1\dot{u}_1) - n_{23}\dot{u}_1 + \frac{1}{3}\mathbf{e}_1 a_1 \\
&\quad - (\mathbf{e}_1(n_{32}) - 2n_{32}a_1) - \frac{2}{3}(n_{23})^2, && \text{(D.22)}\\
\mathbf{e}_0\sigma_{33} &= -\theta\sigma_{33} + 2\Omega_2(\sigma_{31}) - \frac{1}{3}\Big(\mathbf{e}_1\dot{u}_1 + (\dot{u}_1)^2 + a_1\dot{u}_1\Big) \\
&\quad + n_{23}\dot{u}_1 \ + \ \frac{1}{3}\mathbf{e}_1 a_1 + (\mathbf{e}_1 n_{23} - 2a_1 n_{23}) - \frac{2}{3}(n_{23})^2, && \text{(D.23)}\\
\mathbf{e}_0\sigma_{13} &= -\theta\sigma_{13} - \sigma_{33}\Omega_2 + \sigma_{11}\Omega_2 + \frac{1}{2}\mathbf{e}_3\dot{u}_1 - \frac{1}{2}\mathbf{e}_3 a_1 - \frac{1}{2}\mathbf{e}_3 n_{23}. && \text{(D.24)}
\end{aligned}$$

The three equations that resulted from zero energy flux, Eq.(2.32), reduce to

$$\begin{aligned}
0 &= \frac{2}{3}\mathbf{e}_1\theta - (\mathbf{e}_1\sigma_{11} + \mathbf{e}_3\sigma_{13} - 3a_1\sigma_{11}) + -\sigma_{22}n_{23}, && \text{(D.25)}\\
0 &= \frac{2}{3}\mathbf{e}_2\theta - (\mathbf{e}_2\sigma_{22}), && \text{(D.26)}\\
0 &= \frac{2}{3}\mathbf{e}_3\theta - (\mathbf{e}_1\sigma_{13} + \mathbf{e}_3\sigma_{23} - 3a_1\sigma_{13}). && \text{(D.27)}
\end{aligned}$$

The Jacobi Identities are

$$\begin{aligned}
\mathbf{e}_0 n_{23} &= -\frac{1}{3}\theta n_{23} + \sigma_{22}n_{23} + \sigma_{33}n_{23} \\
&\quad - \frac{1}{2}\mathbf{e}_3\Omega_2 - (\ \dot{u}_1\frac{1}{2}\sigma_{22} - \frac{1}{2}\sigma_{33}\dot{u}_1 + \frac{1}{2}\mathbf{e}_1\sigma_{22} - \frac{1}{2}\mathbf{e}_1\sigma_{33} + \frac{1}{2}\mathbf{e}_3\sigma_{13}\ \ ), && \text{(D.28)}\\
\mathbf{e}_0 a_1 &= -\frac{1}{3}\theta a_1 - \sigma_{11}a_1 - \frac{1}{3}\mathbf{e}_1\theta - \frac{1}{3}\dot{u}_1\theta + \frac{1}{2}\mathbf{e}_1\sigma_{11} + \frac{1}{2}\mathbf{e}_3\sigma_{13} + \frac{1}{2}\mathbf{e}_3\Omega_2 + \frac{1}{2}\dot{u}_1\sigma_{11}, && \text{(D.29)}\\
0 &= \mathbf{e}_0\omega_\alpha, \\
&= \frac{1}{2}\Big(-\varepsilon_\alpha{}^{11}\mathbf{e}_1\dot{u}_1 - \varepsilon_\alpha{}^{21}\mathbf{e}_2\dot{u}_1 - \varepsilon_\alpha{}^{31}\mathbf{e}_3\dot{u}_1 + \varepsilon_\alpha{}^{11}a_1\dot{u}_1\Big) \Longrightarrow\ 0 = \mathbf{e}_3\dot{u}_1\ 0 = \mathbf{e}_2\dot{u}_1. && \text{(D.30)}
\end{aligned}$$

And the contracted Bianchi identities are

$$\mathbf{e}_0\mu = -\theta(\mu + p), \tag{D.31}$$
$$\mathbf{e}_0 q_\alpha = 0 = -\mathbf{e}_\alpha p - (\mu + p)\dot{u}_\alpha. \tag{D.32}$$

By substituting the equation of state Eq.(1.10) into the conservation equation Eq.(1.12) we obtain

$$\mathbf{e}_0\mu = -\gamma\mu\theta. \tag{D.33}$$

We substitute σ_{13} for Ω_2. The EFEs, the Jacobi identities, and the contracted Bianchi identities are reduced to the following system of PDEs

$$\begin{aligned}\mathbf{e}_0\theta = &-\frac{1}{3}\theta^2 - \Big((\sigma_{11})^2 + (\sigma_{22})^2 + (\sigma_{33})^2 + 2(\sigma_{13})^2\Big) \\ &+ (\mathbf{e}_1 + \dot{u}_1 - 2a_1)\dot{u}_1 - \frac{1}{2}(\mu + 3p),\end{aligned} \tag{D.34}$$
$$\mathbf{e}_0\sigma_{11} = -\theta\sigma_{11} - 2(\sigma_{13})^2 + \frac{2}{3}\Big(\mathbf{e}_1(\dot{u}_1) + (\dot{u}_1)^2 + a_1\dot{u}_1\Big) - \frac{2}{3}\mathbf{e}_1(a_1) + \frac{4}{3}(n_{23})^2, \tag{D.35}$$
$$\begin{aligned}\mathbf{e}_0\sigma_{22} = &-\theta\sigma_{22} - \frac{1}{3}\Big(\mathbf{e}_1\dot{u}_1 + (\dot{u}_1)^2 + a_1\dot{u}_1\Big) - n_{23}\dot{u}_1 + \frac{1}{3}\mathbf{e}_1 a_1 \\ &- \Big(\mathbf{e}_1(n_{32}) - 2n_{32}a_1\Big) - \frac{2}{3}(n_{23})^2,\end{aligned} \tag{D.36}$$
$$\begin{aligned}\mathbf{e}_0\sigma_{33} = &-\theta\sigma_{33} + 2(\sigma_{13})^2 - \frac{1}{3}\Big(\mathbf{e}_1\dot{u}_1 + (\dot{u}_1)^2 + a_1\dot{u}_1\Big) \\ &+ n_{23}\dot{u}_1 \; + \; \frac{1}{3}\mathbf{e}_1 a_1 + \Big(\mathbf{e}_1(n_{23}) - 2a_1 n_{23}\Big) - \frac{2}{3}(n_{23})^2,\end{aligned} \tag{D.37}$$
$$\mathbf{e}_0\sigma_{13} = -\theta\sigma_{13} - \sigma_{33}\sigma_{13} + \sigma_{11}\sigma_{13} + \frac{1}{2}\mathbf{e}_3\dot{u}_1 - \frac{1}{2}\mathbf{e}_3 a_1 - \frac{1}{2}\mathbf{e}_3 n_{23}, \tag{D.38}$$

$$\mu = \frac{1}{3}\theta^2 - \frac{1}{2}\Big((\sigma_{11})^2 + (\sigma_{22})^2 + (\sigma_{33})^2 + 2(\sigma_{13})^2\Big) + 2\mathbf{e}_1 a_1 - 3\ (a_1)^2 - \ (n_{23})^2, \quad \text{(D.39)}$$

$$0 = q_1 = \frac{2}{3}\mathbf{e}_1(\theta) - \Big(\mathbf{e}_1\sigma_{11} + \mathbf{e}_3\sigma_{13} - 3a_1\sigma_{11}\Big) + \sigma_{33}n_{23} - \sigma_{22}n_{23}, \quad \text{(D.40)}$$

$$0 = q_2 = \frac{2}{3}\mathbf{e}_2(\theta) - (\mathbf{e}_2\sigma_{22}), \quad \text{(D.41)}$$

$$0 = q_3 = \frac{2}{3}\mathbf{e}_3(\theta) - \Big(\mathbf{e}_1\sigma_{13} + \mathbf{e}_3\sigma_{23} - 3a_1\sigma_{13}\Big) - \sigma_{13}n_{23}, \quad \text{(D.42)}$$

$$\begin{aligned}\mathbf{e}_0 n_{23} = &-\frac{1}{3}\theta n_{23} + \sigma_{22}n_{23} + \sigma_{33}n_{23} \\ &- \frac{1}{2}\mathbf{e}_3\sigma_{13} - \Big(\ \dot{u}_1\frac{1}{2}\sigma_{22} - \frac{1}{2}\sigma_{33}\dot{u}_1 + \frac{1}{2}\mathbf{e}_1\sigma_{22} - \frac{1}{2}\mathbf{e}_1\sigma_{33} + \frac{1}{2}\mathbf{e}_3\sigma_{13}\ \Big),\end{aligned} \quad \text{(D.43)}$$

$$\mathbf{e}_0 a_1 = -\frac{1}{3}\theta a_1 - \sigma_{11}a_1 - \frac{1}{3}\mathbf{e}_1\theta - \frac{1}{3}\dot{u}_1\theta + \frac{1}{2}\mathbf{e}_1\sigma_{11} + \frac{1}{2}\mathbf{e}_3\sigma_{13} + \frac{1}{2}\mathbf{e}_3\sigma_{13} + \frac{1}{2}\dot{u}_1\sigma_{11}, \quad \text{(D.44)}$$

$$0 = \mathbf{e}_3\dot{u}_1, \quad \text{(D.45)}$$

$$0 = \mathbf{e}_2\dot{u}_1, \quad \text{(D.46)}$$

$$\mathbf{e}_0\mu = -\gamma\mu\theta, \quad \text{(D.47)}$$

$$\mathbf{e}_0 q_\alpha = 0 = -\mathbf{e}_\alpha p - \gamma\mu\dot{u}_\alpha. \quad \text{(D.48)}$$

Since both $\mathbf{e}_2$ and $\mathbf{e}_3$ have been aligned with the orbits of the isometry group, the system of PDEs in Eq.(D.34)-(D.48) reduce to

$$\begin{aligned}
\mathbf{e}_0\theta &= -\frac{1}{3}\theta^2 - \Big((\sigma_{11})^2 + (\sigma_{22})^2 + (\sigma_{33})^2 + 2(\sigma_{13})^2\Big) \\
&\quad + (\mathbf{e}_1 + \dot{u}_1 - 2a_1)\dot{u}_1 - \frac{1}{2}(3\gamma - 2)\mu, && \text{(D.49)} \\
\mathbf{e}_0\sigma_{11} &= -\theta\sigma_{11} - 2(\sigma_{13})^2 + \frac{2}{3}\Big(\mathbf{e}_1\dot{u}_1 + (\dot{u}_1)^2 + a_1\dot{u}_1\Big) - \frac{2}{3}\mathbf{e}_1 a_1 + \frac{4}{3}(n_{23})^2, && \text{(D.50)} \\
\mathbf{e}_0\sigma_{22} &= -\theta\sigma_{22} - \frac{1}{3}\Big(\mathbf{e}_1\dot{u}_1 + (\dot{u}_1)^2 + a_1\dot{u}_1\Big) - n_{23}\dot{u}_1 + \frac{1}{3}\mathbf{e}_1 a_1 \\
&\quad - (\mathbf{e}_1 n_{32} - 2n_{32}a_1) - \frac{2}{3}(n_{23})^2, && \text{(D.51)} \\
\mathbf{e}_0\sigma_{33} &= -\theta\sigma_{33} + 2(\sigma_{13})^2 - \frac{1}{3}\Big(\mathbf{e}_1\dot{u}_1 + (\dot{u}_1)^2 + a_1\dot{u}_1\Big) \\
&\quad + n_{23}\dot{u}_1 \; + \; \frac{1}{3}\mathbf{e}_1 a_1 + (\mathbf{e}_1 n_{23} - 2a_1 n_{23}) - \frac{2}{3}(n_{23})^2, && \text{(D.52)} \\
\mathbf{e}_0\sigma_{13} &= -\theta\sigma_{13} - \sigma_{33}\sigma_{13} + \sigma_{11}\sigma_{13}, && \text{(D.53)} \\
\mu &= \frac{1}{3}\theta^2 - \frac{1}{2}\Big((\sigma_{11})^2 + (\sigma_{22})^2 + (\sigma_{33})^2 + 2(\sigma_{13})^2\Big) + 2\mathbf{e}_1 a_1 - 3\,(a_1)^2 - \;(n_{23})^2, && \text{(D.54)} \\
0 = q_1 &= \frac{2}{3}\mathbf{e}_1\theta - \Big(\mathbf{e}_1\sigma_{11} - 3a_1\sigma_{11}\Big) + \sigma_{33}n_{23} - \sigma_{22}n_{23}, && \text{(D.55)} \\
0 = q_3 &= -\mathbf{e}_1\sigma_{13} + 3a_1\sigma_{13} - \sigma_{13}n_{23}, && \text{(D.56)} \\
\mathbf{e}_0 n_{23} &= -\frac{1}{3}\theta n_{23} + \sigma_{22}n_{23} + \sigma_{33}n_{23} \\
&\quad - (\;\dot{u}_1\frac{1}{2}\sigma_{22} - \frac{1}{2}\sigma_{33}\dot{u}_1 + \frac{1}{2}\mathbf{e}_1\sigma_{22} - \frac{1}{2}\mathbf{e}_1\sigma_{33}\;), && \text{(D.57)} \\
\mathbf{e}_0 a_1 &= -\frac{1}{3}\theta a_1 - \sigma_{11}a_1 - \frac{1}{3}\mathbf{e}_1\theta - \frac{1}{3}\dot{u}_1\theta + \frac{1}{2}\mathbf{e}_1\sigma_{11} + \frac{1}{2}\dot{u}_1\sigma_{11}, && \text{(D.58)} \\
\mathbf{e}_0\mu &= -\gamma\mu\theta, && \text{(D.59)} \\
0 &= -(\gamma - 1)\mathbf{e}_1\mu - \gamma\mu\dot{u}_1. && \text{(D.60)}
\end{aligned}$$

This concludes the derivation of the EFEs under our assumptions and choices.